ANALYTICAL DEVELOPMENTS BASED ON MASS SPECTROMETRY TO DETECT AND QUANTIFY DNA MUTATIONS

Dissertation

zur

Erlangung der naturwissenschaftlichen Doktorwürde

(Dr. sc. nat.)

vorgelegt der

Mathematisch-naturwissenschaftlichen Fakultät

der

Universität Zürich

von

Jean-Christophe Prost

von

Corcelles-Cormondrèche NE

Promotionskomitee

Prof. Dr. Stefan Bienz (Vorsitz)

PD. Dr Laurent Bigler

Prof. Dr Roland Sigel

Zürich, 2013

Die vorliegende Arbeit wurde von der Mathematisch-naturwissenschaftlichen Fakultät der Universität Zürich im Frühlingsemester 2013 als Dissertation angenommen

Promotionskomitee: Prof. Dr. Stefan Bienz (Vorsitzt), PD Dr. Laurent Bigler, Prof. Dr. Roland Sigel

A Joëlle et Wanda

TABLE OF CONTENTS

CHAPTER 1

INTRODUCTION

1.1 DNA

1.1.1 Generalities

All living organisms have a genome containing their complete genetic code. In eukaryotic cells, this genetic code is distributed among chromosomes consisting of double strand helical DNA molecules. DNA encloses coding and non-coding sequences. The coding sequences correspond to genes, which specify the type of proteins that are made by the cells. The first step consists of the transcription of the DNA to build the messenger RNA (mRNA, Figure 1). Proteins are then synthesized from mRNA in a second step called translation [1].

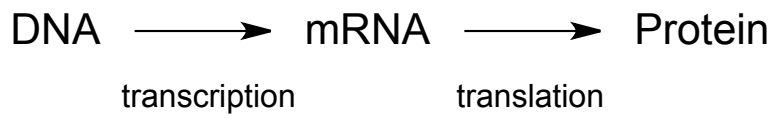

Figure 1: Flow of genetic information in normal cells [1]

As mentioned above, DNA is the center of the complete genetic information for all life forms. It consists of a long polymer composed of two twisted polynucleotide chains forming a double helix. Each chain is made of repeating units called deoxynucleotides or bases. The backbone of each strand is composed of alternated phosphate on the 3' position and sugar moieties on the 5' position of the 2-deoxyribose. The bases are located on the 1' position of 2-deoxyribose. Two different classes of bases containing respectively two purine and two pyrimidine derivatives build up these chains. The purines are adenine (A) and guanine (G), and the

pyrimidines are cytosine (C) and thymine (T, Figure 2). The sequence of bases corresponds therefore to the primary structure of DNA.

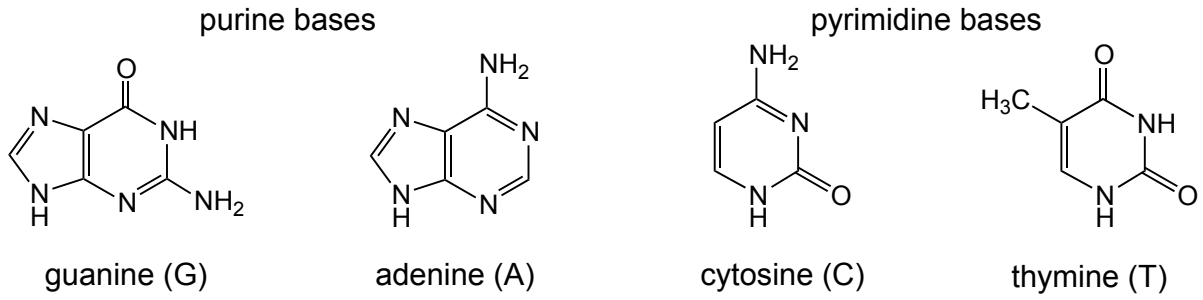

Figure 2: Purine and pyrimidine bases (abbreviations are shown in brackets)

In the early 50s Watson and Crick have proposed a model for the structure of DNA still in use to date showing four major features:

- DNA is constituted of two polynucleotide strands forming a double helix and held together by hydrogen bonds. Each base has its complementary base (Figure 3). Adenine always pairs with thymine (A:T) and guanine with cytosine (G:C). This corresponds to the secondary structure of DNA.

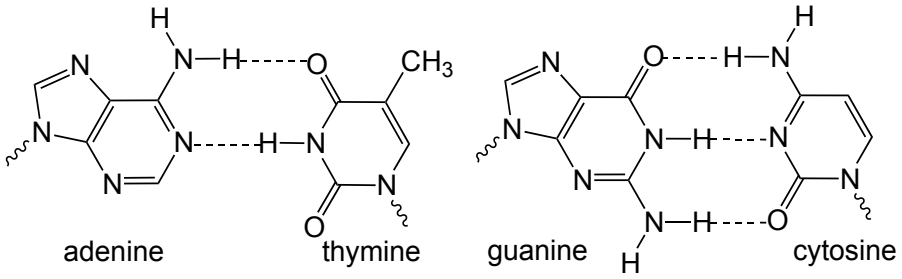

Figure 3: On the left, A:T base pairing with two hydrogen bonds and on the right, G:C base pairing with three hydrogen bonds. The non-covalent interactions are shown as dashed lines.

- Double helix DNA has different conformations called tertiary structures. They show a specific right-handed direction as the most common B-type and as A-type. Only Z-type DNA is left-handed (Figure 4). DNA is also found in other conformations as hairpins, triplexes or guanine quadruplexes [2].

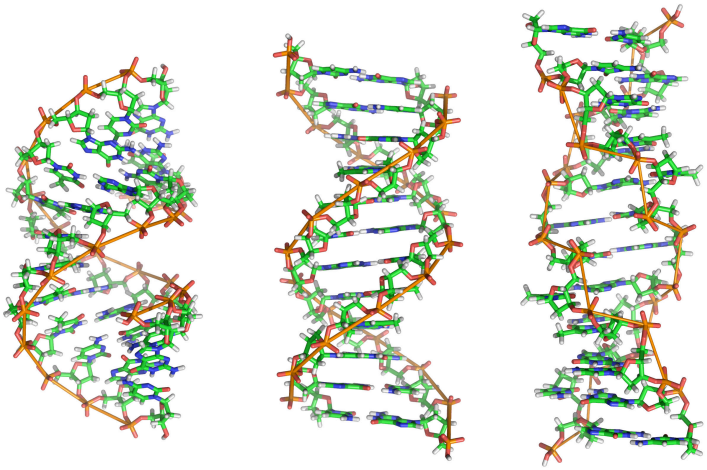

Figure 4: Tertiary structures of A-DNA (right), B-DNA (middle) and Z-DNA (left) [3].

- The ends of each strand are called 5’ and 3’, which correspond to the position of the OH groups on the deoxyribose units forming the DNA backbone (Figure 5). DNA double helixes are anti-parallel and the 5’ end of one strand is paired with the 3’ end of its complementary strand. DNA helix is constituted of one minor and one major groove. One helical turn is about 34 Å and corresponds to about 10.5 base pairs [4]. The main forces stabilizing the double helix are π-π interactions between aromatic rings of the bases [5].

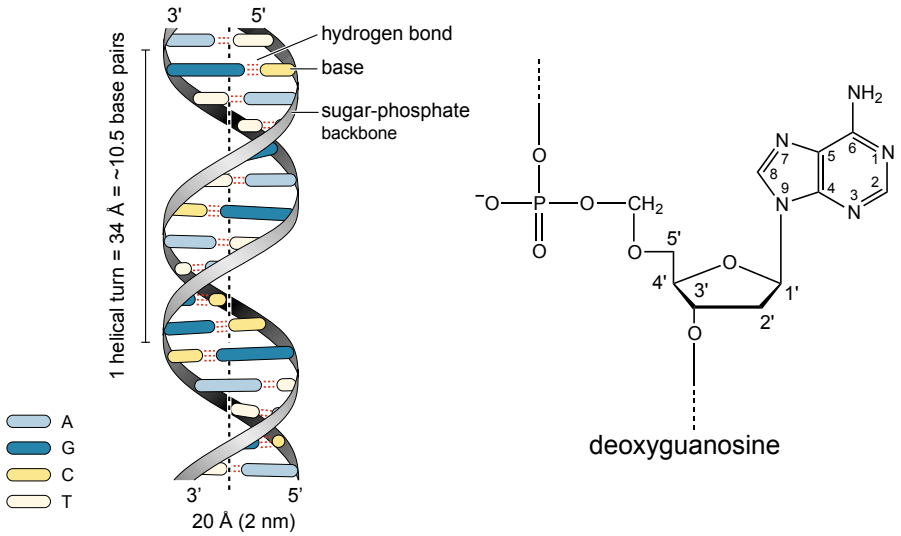

Figure 5: Representation of a DNA helix and a deoxyguanosine moiety (phosphate + 2-deoxyribose + guanosine) (reproduced after [4])

- N-atoms from the bases are still partially accessible to form potential hydrogen bonding. These hydrogen bonds provide access to other molecules, like drugs or proteins that play essential roles in the replication and transcription of DNA [6].

In humans, the complete extended DNA contained in one cell is about 2 m long. To fit in the nucleus DNA has to be compressed having a diameter of 5 to 10 μm [7]. This packaging is obtained by an interaction of DNA with small basic proteins, the histones. DNA wrapped around 8 histones forms the basic unit of chromatin called nucleosome (Figure 6). These aggregates have the primary function to reduce the volume of DNA and to fortify DNA during the different cell division processes, preventing damage, as well as controlling gene expression and DNA replication [1].

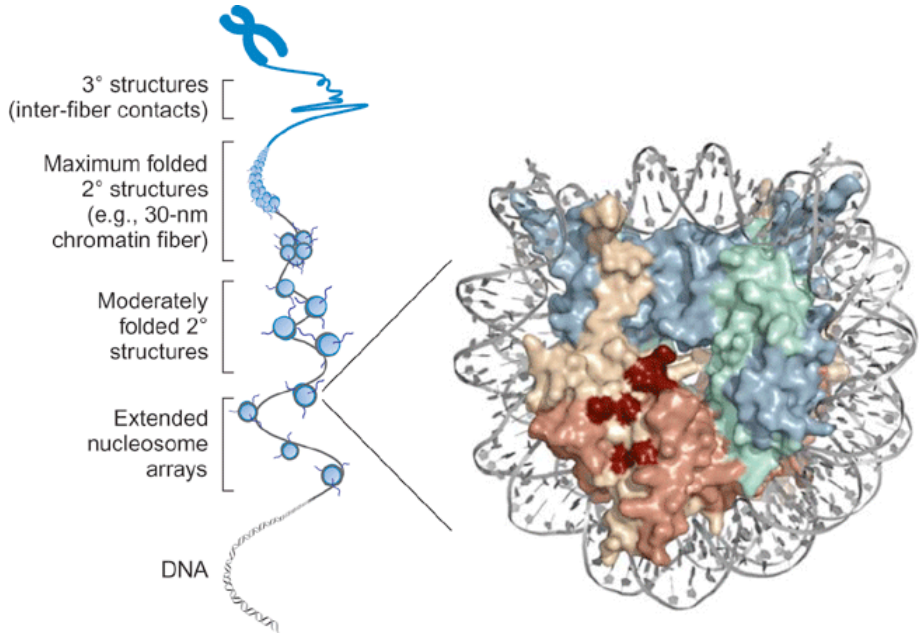

Figure 6: Multiple levels of chromatin compaction (left) with one nucleosome (right). (reproduced after [8]).

Modifications of histones by acetylation, methylation or phosphorylation modulate the chromatin structure and mediate the epigenetic regulation of gene expression. This mediation is essential for cellular differentiation and morphogenesis, and will induce the creation of different cell types possessing different gene expressions but keeping exactly the same genome sequence [1].

1.1.2 Epigenetics

From a historical point of view, the word “epigenetics” described all phenomena that were impossible to explain by genetic principles. Conrad Waddington defined 1942 epigenetics as “the branch of biology which studies the causal interactions between genes and their products, which bring the phenotype into being” [9]. A modern definition of epigenetics is “the study of mitotically and/or meiotically heritable changes in gene function that cannot be explained by changes in DNA

sequence” [10]. In concrete terms, the term “epigenetic” is used to explain the study of stable chemical modifications in gene expression that happen during the different cell division processes [11], resulting for example in physical changes between parents and offspring, as eye or hair color, but maintaining the exact genome sequence. The two major molecular mechanisms influencing gene expression are histone modification and DNA methylation.

Epigenetics became recently one of the most expanding fields in biology because of important discoveries as the CpG islands, or the finding of new histone variants and modifications. Specially recent technological breakthroughs made large-scale studies on complete sets of epigenetic modifications on the genetic material of the cell possible, and allow nowadays the mapping of epigenetic marks that are critical for regulating gene or RNA expression as e.g. histone modification, DNA methylation, or nucleosome positioning [12]. Misregulation of these epigenetic marks and mutations in the epigenetic development are associated to e.g. cancer, neurological disorders, and autoimmune diseases [12]. Exhaustive comprehension of epigenetic mechanisms, their interaction and alteration in health and diseases, has become a priority in biomedical research [12].

1.1.3 DNA mutations

Mutations are basically changes in the genomic sequence and the most important cause of diversity between organisms. All organisms undergo mutations that are divided in advantageous, neutral and lethal classes [13]. Advantageous mutations can contribute to evolutionary changes due to environmental influences. Lethal mutations in cellular processes have been associated with damages in the genomic sequence that often result in cancers. These damages can arise from endogenous changes like DNA methylation, replication errors, DNA base instability, or free radical attack generated during metabolism. They can also result from exogenous factors like ionizing and UV radiations, or chemical carcinogens [14].

a) DNA methylation

DNA methylation is a very important epigenetic process. It is essential for human development, maintaining the organism working normally. DNA methylation is used as a powerful mechanism in gene expression and silencing, maintaining genome stability. An increasing number of human diseases with many different syndromes as e.g. lupus and muscular dystrophy have been associated with aberrant methylation [15].

The mechanism of DNA methylation is based on the covalent addition of a methyl group on the 5 position of a cytosine that is preceded by a guanosine in the DNA sequence (CpG nucleotide). This methylation, also called CpG methylation, depends on the methyl donor cofactor S-adenosyl methionine (SAM) and the enzyme DNA methyl-transferase, whereby SAM is transformed in S-adenosyl homocysteine (SAH) as shown in Figure 7. The SAM/SAH ratio has often been used as an indicator of cellular methylation potential with cases of hypomethylation (decrease of methylation) or hypermethylation (increase of methylation). This ratio is determined using stable isotope dilution tandem mass spectrometry [16].

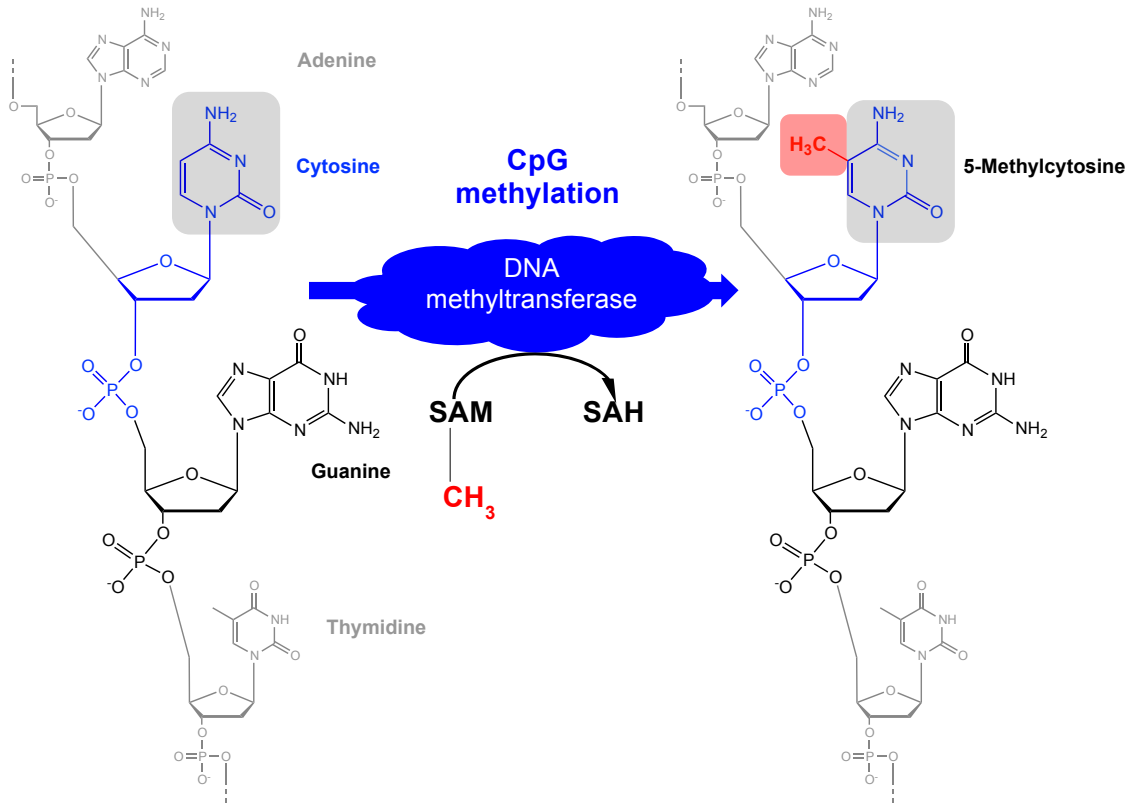

Figure 7: DNA methylation mechanism (reproduced after [17])

b) UV induced mutations

UV solar radiation is known to induce DNA mutations and to be directly involved in human skin cancer. UV light is classified in three categories, UVA (400-315 nm), UVB (315-280 nm), and UVC (<280 nm). Only radiations in the range of UVA and about 10% of UVB reach the earth surface, the rest of UVB and UVC is absorbed by the ozone protecting layer in the atmosphere [18]. Decrease of the ozone layer due to human activities became recently a problem on earth. The resulting increase of UVB radiations, the most energetic, mutagenic and carcinogenic part of solar radiation, is directly absorbed by cellular DNA and associated to skin cancer [19].

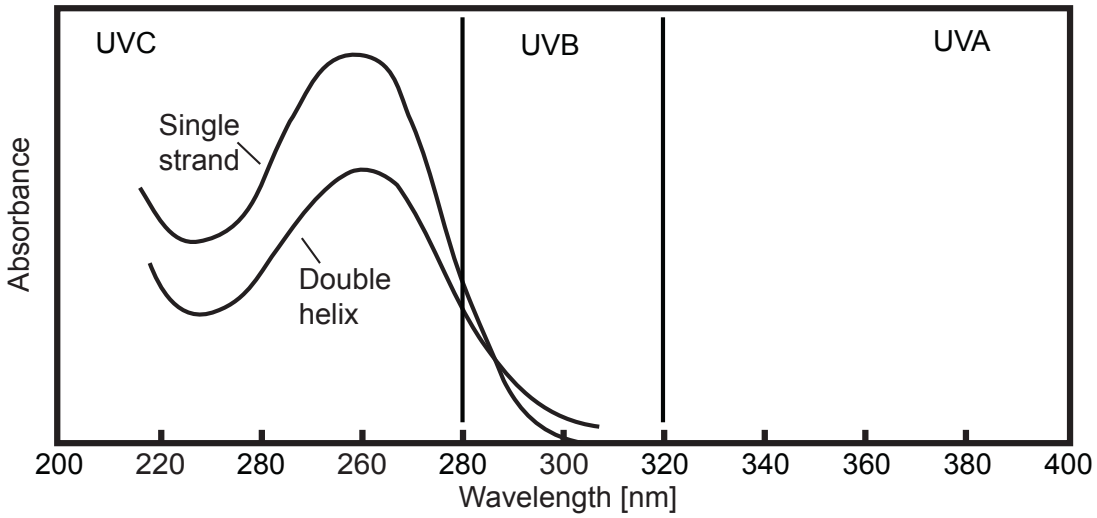

Figure 8: Wavelength domains of UV radiations and absorption spectra of single and double strand DNA

DNA absorbs UV light between 220 and 300 nm (Figure 8), leading to the formation of mainly cyclobutane pyrimidine dimers (CPD) and pyrimidine pyrimidone photoproducts (6-4 PP). CPDs are formed in a [2+2] photocycloaddition reaction, whereby the C5-C6 double bonds of adjacent bases are fused in a cyclobutane ring. 6-4 PPs also undergo [2+2] photocycloadditions, involving the C5-C6 double bond and the C4 carbonyl group of two adjacent pyrimidines [20].

Formation of other photoproducts has been observed to a lesser extent, e.g., reaction between two adjacent adenine bases or between adenine and vicinal thymine, oxidation of adenosine in 8-oxo-7,8-dihydro-2'-deoxyguanosine (Figure 9), and photohydration of cytosine [21]. Cross-linked reactions have also been reported in G-quadruplex between two non-adjacent thymidines [19].

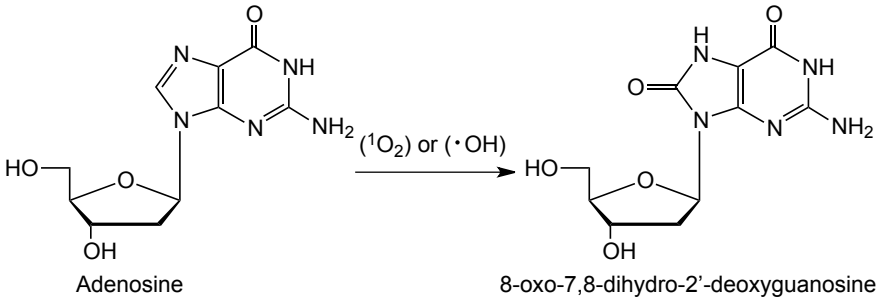

Figure 9: Photooxidation of adenosine generated by either UVB or UVA light

The most intensively investigated UV induced DNA modifications are cyclobutane pyrimidine dimers and pyrimidone photoproducts [21]. These mutations occur between adjacent purine bases TpT, TpC, CpT and CpC under UVB and A radiations. The dimerization yields are variable and correspond to about 1-18 lesions per 10^9 bases [21]. TpT is described as most reactive pair. Figure 10 represents all cyclobutane pyrimidine dimers (*c-s* T<>T and *t*-s T<>T) and pyrimidone photoproducts (6-4 TT and Dewar TT) formed under UVC and B radiations. The yields of photoisomerisation of 6-4 TT in Dewar TT are significantly increased at 312 nm.

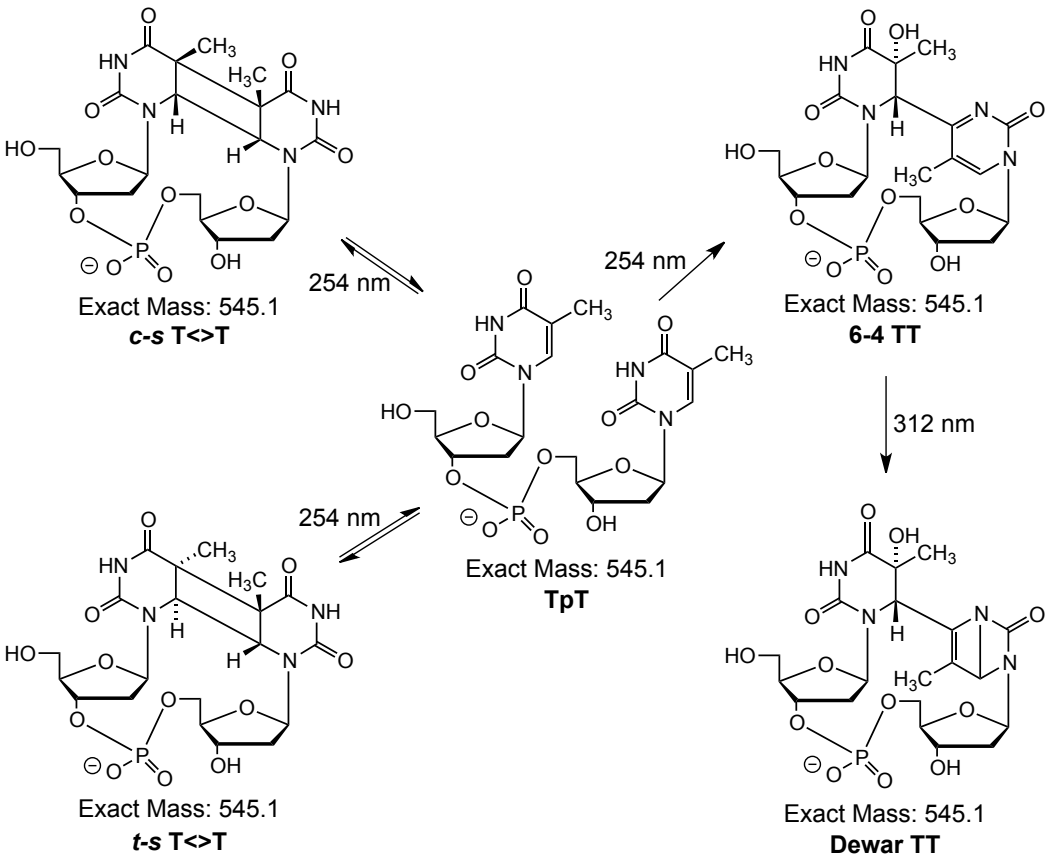

Figure 10: Structure of thymine dimeric photoproducts induced by UV-light

Many DNA mutations are triggered by UVB radiation because of the low energy absorbance of DNA at wavelengths above 315 nm. Nevertheless, UVB and UVA radiations can lead to photooxidative reactions. The reaction mechanism is still unclear but deoxyguanosine is probably transformed to 8-oxo-7,8-dihydro-2'-deoxyguanosine, induced either by $^{\bullet}OH$ radical or by a reaction between a singlet oxygen and a triplet excited purine base [18, 22].

Non-covalent interactions of small molecules with DNA may have an influence on DNA mutations. They will therefore be discussed more in detail in the next chapter.

1.1.4 Non-covalent interactions with DNA

a) Generalities

Non-covalent interactions with DNA play an essential role in biological processes because they are the molecular basis of many anti-tumor, anti-bacterial and anti-viral drugs [23]. DNA is a long polymer chain made of two strands held together through non-covalent H-bonding between complementary bases and stabilized by π -π interactions. The wrapping of both strands forms a right-handed helix with a major groove and a minor groove. These grooves and the anionic 5'-phosphate 2-deoxyribose backbone lead DNA to form non-covalent complexes with various substrates, as e.g. small molecules, metal ions, and proteins.

Different interactions have been observed including major- and minor-groove, intercalation between bases, ion pairing with the sugar-phosphate backbone, covalent binding or metal–coordination with the bases [24].

Compounds with a high affinity to DNA can influence gene expression and at the same time affect cell proliferation and cell differentiation [25]. The structure of drugs with a broad domain of activity as e.g. antiviral, antibiotic, and anticancer that interact non-covalently with DNA are shown in Figure 11 [23, 25, 26].

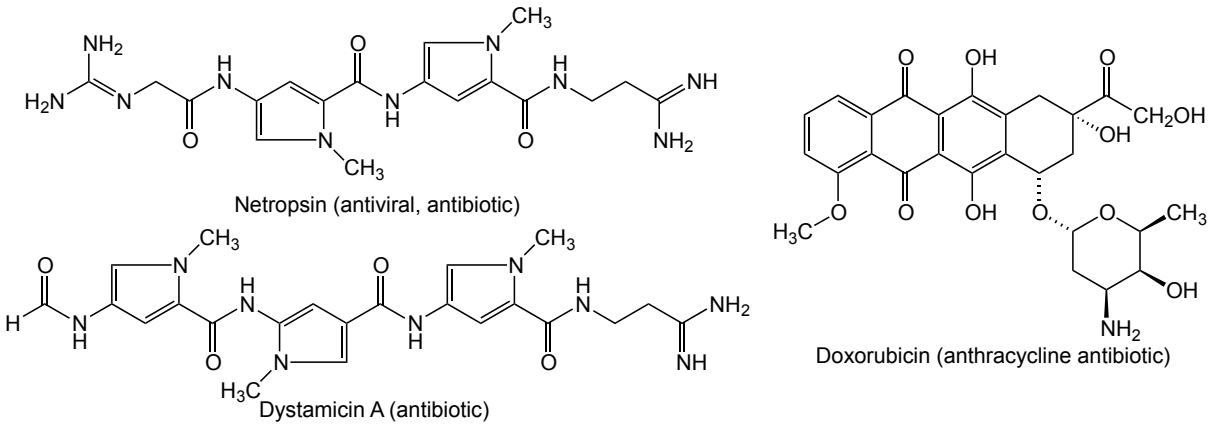

Figure 11: Drugs forming non-covalent interactions with DNA.

Chemical bonds are classified in covalent, ionic, metallic, and intra-molecular or non-covalent bonds. They have a different energy, varying roughly from 100 kcal/mol for carbon-hydrogen bonds down to 2-20 kcal/mol for non-covalent interactions. Weak reversible bindings due to e.g. electrostatic forces (Van der Waals, Coulomb, Debye, Keesom, or London, several kcal/mol), π -π interactions (2-10 kcal/mol), and hydrogen bonding (5-18 kcal/mol) are playing a key role in the majority of relevant biological processes [27].

b) Non-covalent interactions between oligonucleotides and ligands

Five types of non-covalent binding between ligands and oligonucleotides have been described: 1) electrostatic attraction with the negatively charged DNA backbone, 2) major groove interactions, 3) minor groove interactions, 4) intercalation between base pairs in the major groove, and 5) intercalation between base pairs in the minor groove [28].

Considering the two most important binding modes, intercalation and minor groove interactions, intercalation was recognized first because tertiary structure and chemical properties of DNA are affected. Rapidly, this change of DNA shape showed a high mutagenic potential and inspired DNA-targeted chemotherapy [29].

The driving forces of intercalation interactions are coming essentially from π-stacking and stabilizing electrostatic interactions, where the ligand, mostly small organic molecules with an aromatic system, needs maximum overlap with the DNA base pair (Figure 12). Interactions occur with a slight preference in regions of alternating pyrimidine-purine bases, with a weak selectivity for 5'-CG compared to 5'-TA [29].

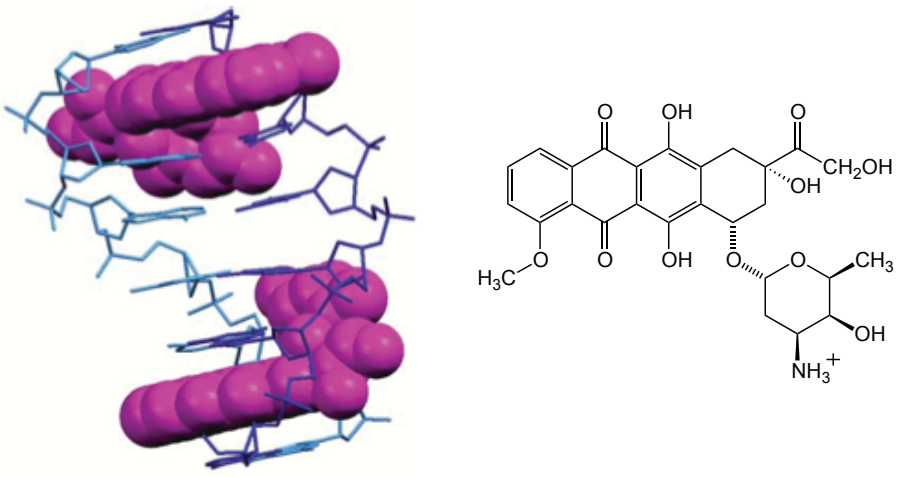

Figure 12: Intercalation complex between two doxorubicin drugs (pink) and DNA [24]

The concept of groove binding by small molecules is more recent. Despite the fact that minor groove binding drugs are under-represented in clinical use, they are presented as the most promising targets for de novo design [29]. The minor groove of DNA is reported as an AT-rich region, and a majority of minor-groove ligands bind certainly to the minor-groove in B-DNA [25]. Stability is obtained via strong van der Waals interactions between negative electrostatic potential of the DNA backbone and mainly positively charged ligands at physiological pH (Figure 13).

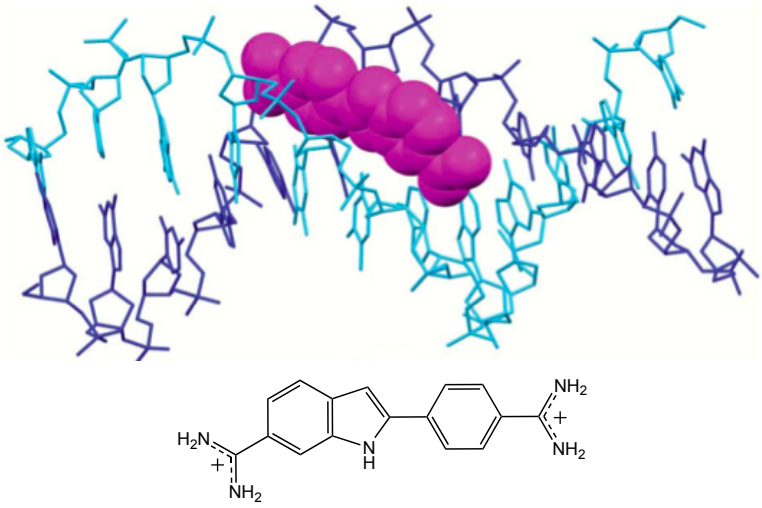

Figure 13: Minor-groove interactions between DAPI (pink) and DNA [24]

Groove width, groove depth, and electrostatic potential are critical DNA features for the recognition of small molecules. Width of the minor groove varies with the sequence [29]. GC-rich grooves (8 Å) are twice as large as AT-rich ones (3-4 Å). The depth of GC-rich grooves is less pronounced than that of AT due to the exocyclic amine. On the other hand, this amine has a nucleophilic character, increasing the

recognition through formation of H-bond bridges. Compared to intercalation, minor groove binding induces little or no conformation changes in DNA [29]. Interactions along minor grooves occur simultaneously with individual base pairs and the sugar wall and provide cooperative binding contacts, leading to an increase of recognition specificity and also to a high degree of target selectivity [29].

c) Examination of non-covalent interactions using mass spectrometry

It is normally impractical to study interactions between the huge genomic DNA and small ligands. Therefore, short sequences of single or double DNA strands with around 4-20 oligomers have been chosen. They can on one hand mimic important DNA active sites and on the other hand allow collection as well as interpretation of analytical data. Various methods are known for investigating non-covalent interactions between substrates and DNA. Analytical procedures based on NMR or IR spectroscopy, circular dichroism, gel footprinting or X-ray crystallography have been described to determine binding stoichiometry, specificity and affinity of such complexes.

The possibility to measure and analyze large and fragile biomolecules raised with the development of electrospray ionization mass spectrometry (ESI-MS) by Fen et al. in the 80's [30]. ESI is a soft ionization technique, which allows the direct transfer of numerous samples from solution to gas phase at room temperature and atmospheric pressure. This method is so soft that non-covalent interactions can be investigated with mass spectrometry. Furthermore, Mc Lafferty mentioned 1981 that MS merges the three "S" benefits, sensitivity, specificity and speed, leading to one of the most powerful analytical technique available [31].

ESI-MS has the major advantage of requiring only very small amounts of sample in the low-picomole range [25]. The selectivity of the method leads to a decrease of chemical noise arising from complicated matrices by tuning the MS parameters in order to favor transmission of large ions. Depending on their molecular mass and polarity, (bio)molecules are detected as single or multiple charged particles. Figure 14 shows for example the ESI-MS of a 14mer double strand (ds) DNA acquired in the negative ionization mode under formation of 4– and 5– charged ions.

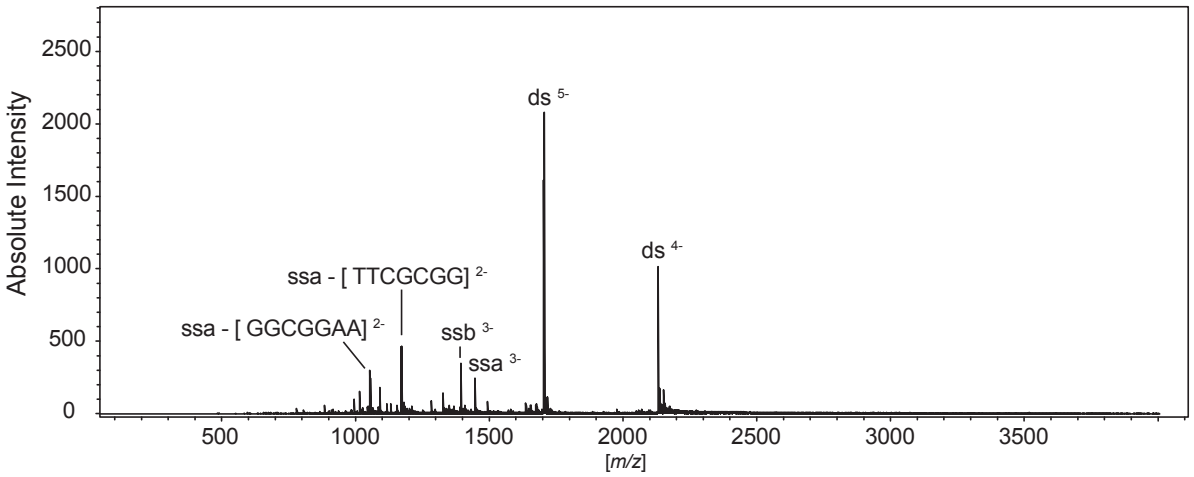

Figure 14: ESI-MS spectrum of ds DNA, d(GGCGGAATTCGCGG/CCGCCTTAAGCGCC) (ssa/ssb; M_R 8525.5 Da), 1 pmol/µL in propan-2-ol/(2.5mM piperidine+imidazole *v/v*) 1:1

Many different types of non-covalent interactions as e.g. protein-protein [32], protein-ligands [32], DNA-protein [32, 33], DNA-RNA [34], DNA-DNA [34], and DNA/RNA-small molecules [23, 25, 34] have been investigated by MS. Two important aspects have to be considered in such analyses: 1) how do the complexes behave during the transfer from solution to gas phase and 2) do the observed ion signals really correspond to ionized species present in sample solution? Joseph Loo summarized in 2000 the experimental principles of the MS method used for studying non-covalent complexes. At the same time, he tried to correlate the problematic of transfer between solution and gas phase. He pointed out important experimental variables as solution conditions for efficient and effective desolvation, insisting on buffer pH and ionic strength, which are critical for the targeted non-covalent complex stability.

By now it is broadly accepted that stoichiometry of complexes in solution and their relative signal intensities show good correlations in ESI-MS. It has been demonstrated that the types of interactions in the complexes influence MS results and can be differentiated by ESI-MS considering the gas phase ions [35]. Of course, results obtained by ESI-MS should be confirmed by other analytical methods, in particular by those based on dissolved samples such as NMR, IR spectroscopy, or circular dichroism. To smaller extent also other methods such as X-ray crystallography can be used to support MS results.

Stoichiometry

MS can be used for qualitative and quantitative studies of non-covalent interactions. Figure 15 shows two ESI-MS spectra of a 14-mer ds DNA sequence mixed with vitexin, a common flavonoid, at two different ratios of 1:10 and 1:80.

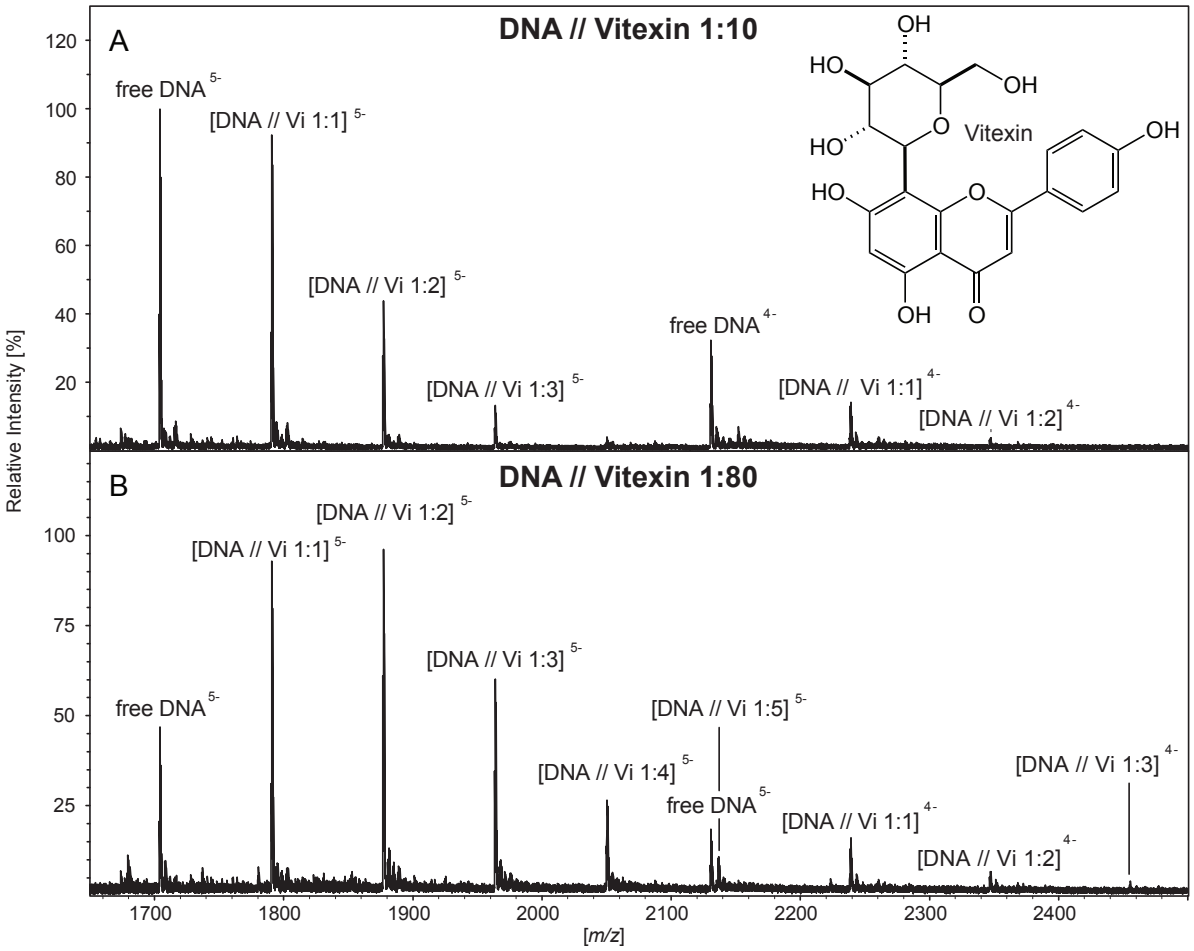

Figure 15: Complex of 14-mer ds DNA, d(AACTCCCGGCACAC/GTGTGCCGGGAGTT, 1 pmol/µL in propan-2-ol/(2.5mM piperidine + imidazole v/v) 1:1, with vitexin at a DNA/vitexin ratio of (A) 1:10 and (B) 1:80, respectively

In a first step the charge state of the ions detected has to be assigned and the most abundant ionic species characterized. Considering the 5– ions, the base peak signal at 10-fold excess of vitexin was corresponding to free ds DNA. However, at 80-fold excess, the base peak was shifted to the 1:2 ds DNA // vitexin complex.

Selectivity

The affinity of a ligand to specific DNA sequences, e.g. with GC rich or AT rich regions, can also be investigated using ESI-MS. After measuring different sequences with one ligand, it is possible to determine if this ligand has more affinity with AT or with GC rich regions. In a further step, such results can be extrapolated to interaction

properties of this substrate with DNA [25]. This type of studies, where different ligands have been mixed to different DNA sequences, will be presented in Chapter 2.

Estimation of interaction forces

ESI-MS can also be used to estimate relative forces of interactions. Competitive experiments can be performed using for example one sequence of single or double stranded DNA mixed with different ligands. The sequence is chosen in order to mimic the DNA active site or to show some specific properties as e.g basicity or shape. Comparing the signal intensities of the complexes detected by ESI-MS allowed the determination of the ligand showing the highest affinity to a given sequence [25].

In Figure 16 self-complementary single strand ATAT has been used to screen the four ligands Hoechst 33342, 4',6-Diamidino-2-phenylindole (DAPI), Netropsin, and Berenil. Comparing signal intensities in all ESI-MS spectra, one can conclude that Hoechst 33342 shows the strongest interactions with ATAT, with almost disappearance of ATAT signals [36].

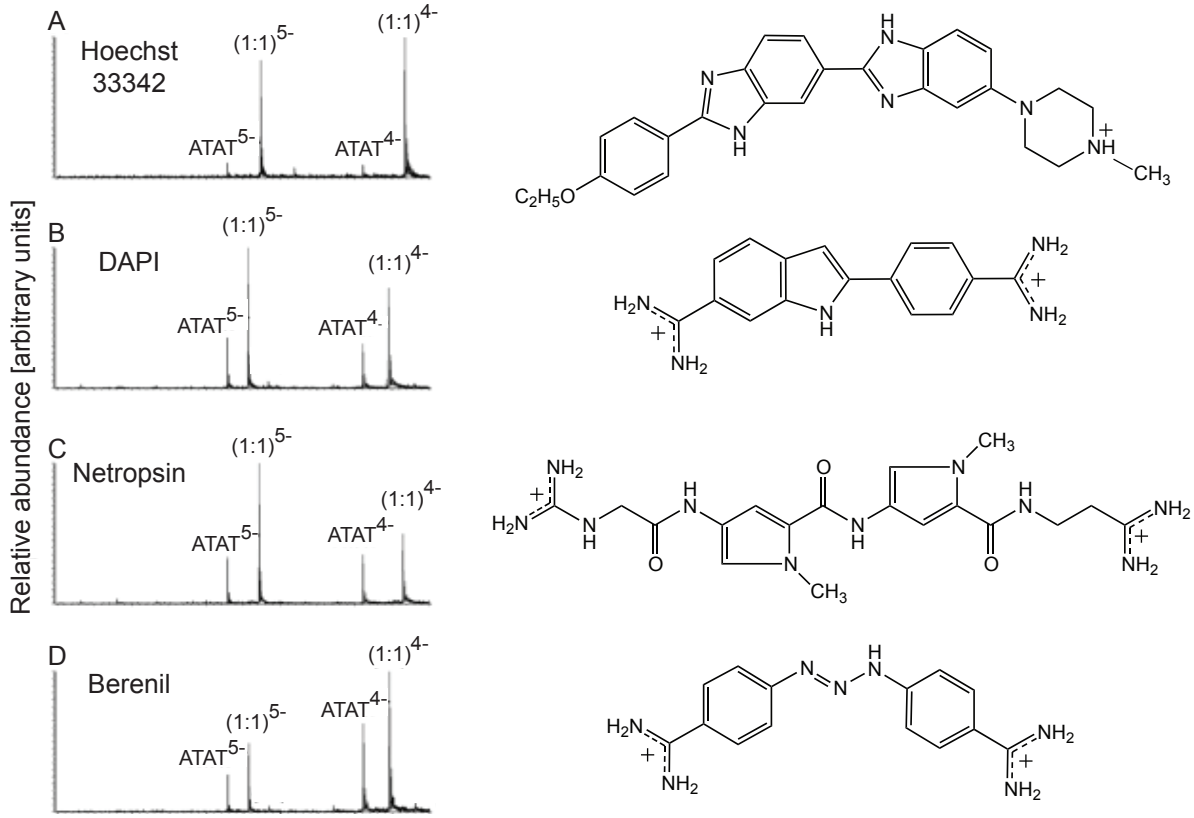

Figure 16: Comparison of four different drugs interacting with the single strand sequence ATAT (10 pmol/µL in NH_4OAc aq. with 20 % MeOH) (reproduced after [36]).

Another way to estimate le relative force of interaction is to use ESI-MS/MS, as for example between ds DNA and flavonoid aglycones or glycosides [37]. Aglycone flavonoids were shown to interact less strong with DNA than glycosylated flavonoids, because the neutral loss of the ligand was found to be more prominent in the MS/MS. On the other hand, the higher affinity of glycoside flavonoids to DNA was confirmed with the loss of base fragments. Figure 17 shows the MS/MS spectra of a given DNA sequence with four different flavonoids obtained by fragmenting the 5– precursor ions of the ds DNA // flavonoid complexes [38]. The four spectra show rather different fragmentation patterns. At most complete loss of ligand is observed in spectrum A), indicating a rather low force of interaction between the aglycone flavonoid quercetin and ds DNA. In the case of the isoflavone glycoside genistin (spectrum C), the loss of a few bases losses is observed in the ESI-MS/MS. However, in the case of the ds DNA complexes of glycosylated flavonol and flavanone vitexin and rutin, almost exclusively loss of nucleobases and no loss of the ligands was observed (spectra B and D), indicating strong interactions between ligands and ds DNA.

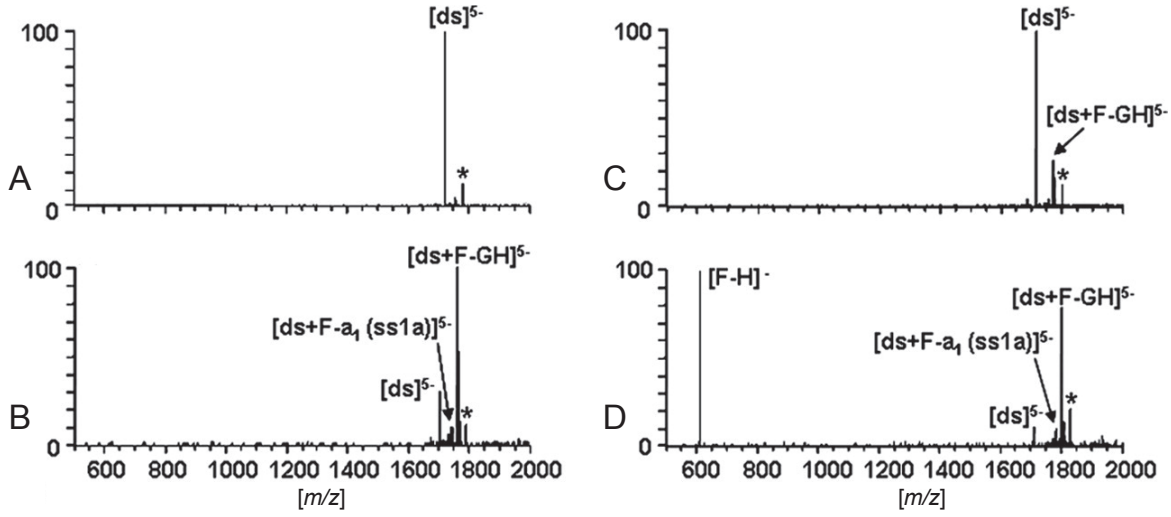

Figure 17: (–)-ESI-MS/MS spectra showing the 5– charged complexes of dsDNA with A) quercetin; B) vitexin; C) genistin; and D) rutin. Precursor ions are labeled with an asterisk [39].

1.2 Quantification

1.2.1 Introduction

Quantitative determinations are demanded in various domains as, e.g. discovery, development and manufacturing of new pharmaceutical drugs, food contaminants, environmental pollutants, forensics, and proteomics. Many analytical methods have been developed for this purpose, principally based on high-performance liquid and capillary gas chromatography combined with detection systems as e.g. mass spectrometry, UV, fluorescence, or flame ionization.

Two approaches of quantitative determination can principally be followed:

- Qualitative: consists in calculating the relative quantity of one or more substances in comparison to each other. This is presented in Chapter 2, where, the relative intensities of complexes between secondary metabolites and short DNA sequences are used to quantify the fraction of bound DNA.

- Quantitative: leads to determine absolute amount or concentrations of one or more substances, as showed in Chapter 4, where the absolute amount of methylation grade is quantified in patients DNA.

These procedures do not depend on the analytical method used. Qualitative quantifications are usually easier to perform whereby quantitative are more accurate. Considering the application domains mentioned above, quantitative methods are prevalent.

Since all quantitative experiments are subject to various errors and uncertainties, it is essential to consider and to estimate these errors in order to be able to interpret correctly the results obtained and to draw the right conclusions. For this purpose, a model based on a theoretical error distribution has been designed with a mathematical equation in order to evaluate the “precision” of the measurement. Typically, repeated analyses follow a Gaussian or normal distribution that can be represented by equation (1) and the curve shown in Figure 18 [40].

$$(1) \qquad f(x) = \frac{1}{\sigma\sqrt{2\pi}} \exp\left[\frac{-(x-\mu)^2}{2\sigma^2}\right] \qquad -\infty < x < +\infty$$

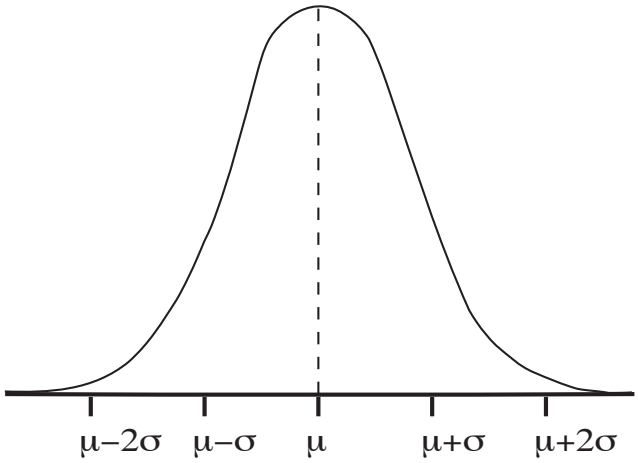

Figure 18: Gaussian curve with μ mean and σ^2 variance

In a normal distribution, μ represents the mean corresponding to the real value of the quantity that is measured (Figure 18). The spread of the curve σ, also known as standard deviation, indicates the random error of the measurement.

The mean $\bar{x}$, average value of a few replicate measurements (see equation 2), and its standard deviation *s* (3) can be used to evaluate μ and σ, which are the characteristics of hypothetical and infinite populations of data.

$$(2) \qquad \bar{x} = \frac{\sum_i x_i}{n}$$

and

$$(3) \qquad s = \sqrt{\frac{\sum_i (x_i - \bar{x})}{n-1}}$$

with *n* measurements, x_1, x_2, etc.

The mean $\bar{x}$ and the standard deviation *s* allow calculating the relative standard deviation (RSD) that is more commonly expressed as a percentage and is called coefficient of variation (CV):

$$(4) \qquad CV(\%) = 100\frac{s}{\bar{x}}$$

CV represents the dispersion of the probability distribution of x_1, x_2, etc.

Qualitative quantification approaches can be used, e.g., to follow the completion of chemical reactions by comparing the signal intensity of the reaction product(s) with

that of the starting material(s). Within this thesis, absolute amounts of sample components have been determined and therefore quantitative aspects will be presented in more details.

1.2.2 Quantitative aspects

a) Calibration

Every quantitative measurement needs a specific calibration for each analyte. In this most important step, the detector response of the instrument has to be correlated to the concentration of the analyte.

Different modes of calibration are available and their choice depends on sample complexity, matrix, and accuracy of the results required. “External calibration” and “internal calibration” are the two most familiar methods used. The “area normalization” approach is often used to determine the purity of a sample in the case where no internal standard exists or where the relative concentration of a substance is more significant than the absolute concentration. The technique of “standard addition” is applied if no blank sample is available and the matrix of the sample may influence the retention time and/or the detector response of the analytes.

For complex matrices as e.g. plasma or plant material, it is suggested to prepare the calibration curve in blank matrix, where all elements of the sample are found except the compounds that have to be quantified. Such a matrix-based calibration is not required if the matrix does practically not influence chemical or physical properties of the molecules and therefore their signal response [41].

External calibration

First, a precise amount of reference standard – analyte itself in a pure form or substance with closely related structure – is weighted and diluted in an adequate solvent (aqueous or organic, with or without buffer) to prepare a stock solution. From the stock solution, different dilution steps are performed to obtain several solutions of different concentrations in the range of interest and to have enough data to make a calibration curve. At least five to six points are needed for a suitable calibration curve.

A calibration curve can be built up following a linear or an exponential dilution scheme [41]. Linear calibration points are distributed regularly over the chosen concentration range. However, by an exponential dilution scheme, there is a higher

density of calibration points in the lower concentration range. Then the same volume is injected for each concentration. In both cases a linear plot is usually obtained.

Analyses of highly concentrated standards in the upper range of the calibration curve can lead to sample carry over. It is therefore preferable to perform the measurement for the calibration curve from the lowest to the highest concentration to avoid this problem and measuring a blank sample after the most concentrated standard solution.

When all standard concentrations used for the calibration curve have been measured, the calibration curve can be plotted and the concentration of an unknown analyte calculated using the slope S' of this curve:

$$(5) \qquad ng/mL\ analyte = \frac{area\ analyte}{S'}$$

An external calibration can only be used in cases of simple sample preparation (weighing, dilution, dissolution, pipetting, filtration) and minor matrix effects, which exclude loss of analyte and standard.

An example of the use of external calibration to determine the concentration of cytosine is shown in Figure 19. These data of quantification of the DNA methylation grade were obtained with a method base on UHPLC-MS/MS for the quantification of the methylation in DNA (see Chap. 4 for more details).

A better accuracy can be obtained with the addition of an internal standard (IS) and performing an internal calibration.

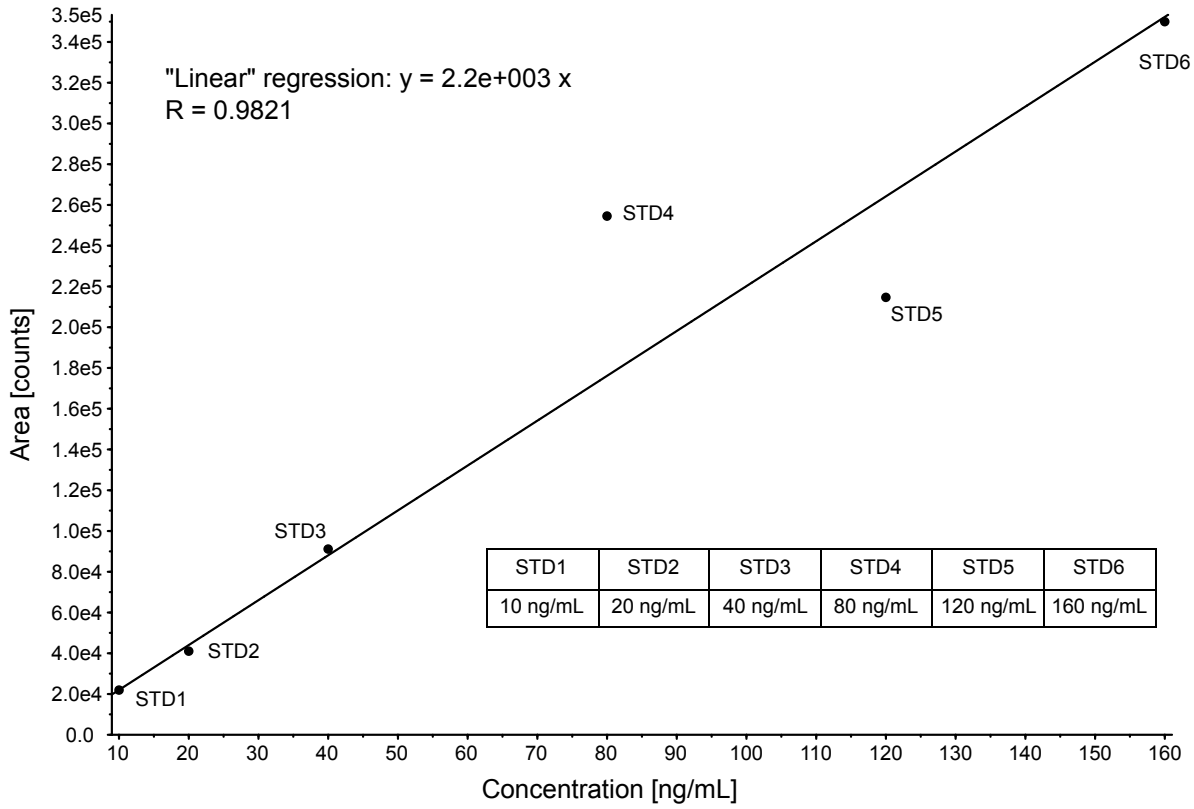

STD1	STD2	STD3	STD4	STD5	STD6
10 ng/mL	20 ng/mL	40 ng/mL	80 ng/mL	120 ng/mL	160 ng/mL

Figure 19: Quantification determination of cytosine with external calibration and linear dilution scheme using UHPLC-ESI-MS/MS

Internal calibration

Internal calibration is often used in cases of critical sample preparation, e.g. low extraction yields and problems of adsorption or evaporation.

Set up of the standard solution and of the calibration curve is similar for internal and for external calibration. In the case of internal calibration, a known amount of IS is added to all samples and to all calibration standards preferentially prepared in blank matrix, prior to any sample preparation step. All samples are then treated with the same sample preparation procedure.

After analyzing all samples in a sequence, analyte concentrations are calculated on the same basis as for external calibration with one modification. Instead of measuring absolute analyte areas, the ratio between areas of analyte and IS as shown in equation (6) are used [41]:

$$ng / mL\ analyte = \frac{area\ analyte / area\ IS}{S'} \qquad (6)$$

In case of external calibration, the quantity is correlated to an absolute value of the signal area. However, the quantity is related to the ratio of IS and analyte signal area

if internal calibration is performed. The use of relative amounts usually significantly improves accuracy of the calibration curve and leads to increased correlation coefficient.

Data quality strongly depends on the choice of the IS. Prerequisites for successful quantification with internal calibration are [41]:

i) Has to be as similar as possible to have the most comparable chemical properties compared to the analyte in order to avoid any discrimination during sample preparation and analysis;
ii) The IS must be chemically stable under work-up conditions;
iii) Whether IS nor any sample compound with the same retention time as the IS have ever been detected in the same sample;
iv) Pure IS or at least IS with known purity is required. Eventual contaminations have to be characterized and may not interfere with the sample;
v) The IS has to be well resolved from all unknown peaks in the chromatogram but still have a preferably similar retention time as the analyte;
vi) Chromatographic resolution higher than 1.5 [1] is recommended between analyte and IS, except in LC-MS methods using stable-isotope-labeled (SIL) internal standards (see Chap. hereafter);

Figure 20 shows a calibration curve with IS calculated from the same data used for external calibration (Figure 19). After internal calibration correction, the coefficient of correlation of the linear regression increased from R = 0.9821 to 0.9997. Such an improvement illustrates the importance of IS for correcting handling and instrumental inaccuracies.

[1] The resolution *Rs* is defined as the distance between the centers of two eluting peaks as measured by retention time or column volume divided by the average width of the respective peaks. Baseline resolution between two well formed peaks indicates 100% purity and requires an *Rs* value above 1.5

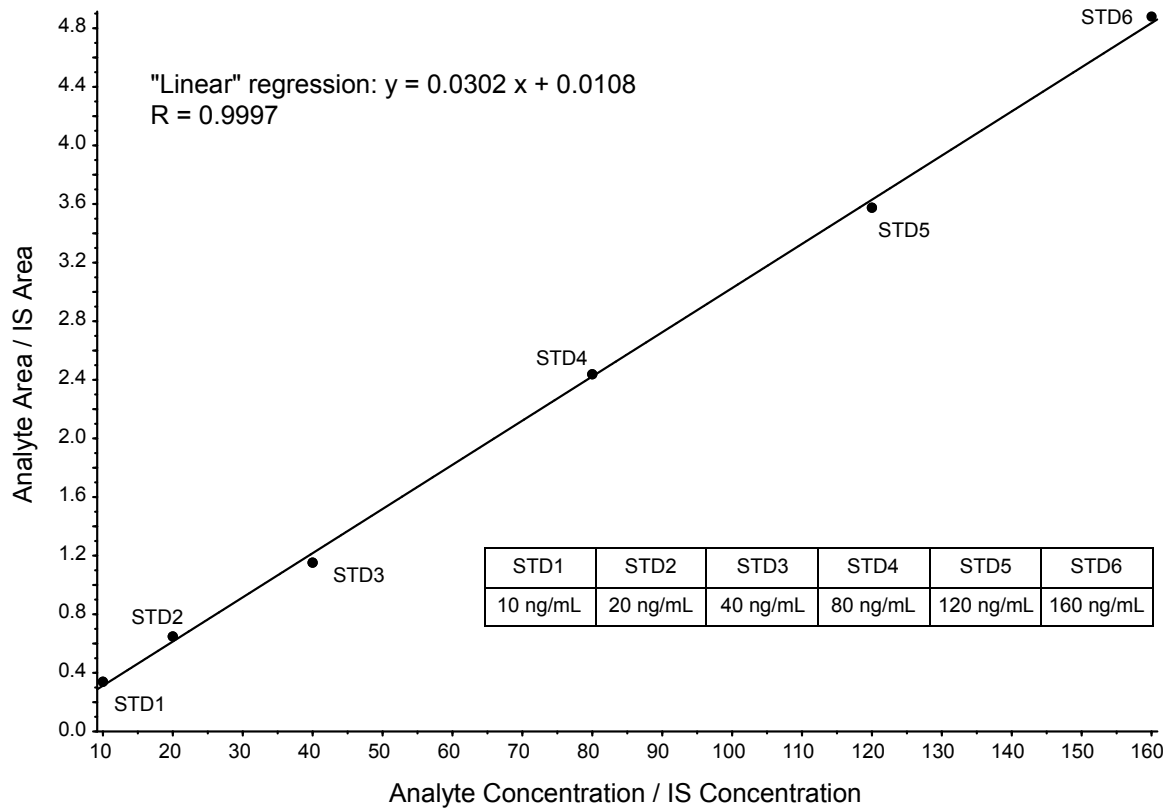

STD1	STD2	STD3	STD4	STD5	STD6
10 ng/mL	20 ng/mL	40 ng/mL	80 ng/mL	120 ng/mL	160 ng/mL

Figure 20: Calibration curve obtained for cytosine quantification after correction with the signal area of labeled cytosine as IS according to equation (6)

Standard addition

The method of standard addition consists of spiking the sample that contains the substance to quantify with this substance in a pure form. This procedure is appropriate if no blank sample is available and if the sample matrix may influence the recovery and the detector response of the analyte.

The method can be used with a single or a multiple-point calibration. In the case of a single point calibration, the sample is split in two similar fractions. The first one is used as it is and to the second a known amount of reference standard is added. Both samples are then prepared and analyzed exactly the same way. The signal areas of the two measurements are then compared, and known this, the concentration of the original sample, without added standard, can be estimated.

More accurate than the single point calibration is the multiple-point calibration. For this, the sample is split into fractions that contain different amounts of standard material in order to obtain a calibration curve. The concentration of the unknown sample corresponds then to the intersection of the regression line with the x-axis [41]

(Figure 21). The accuracy can be improved by using an internal standard (different compound with similar properties (see above)).

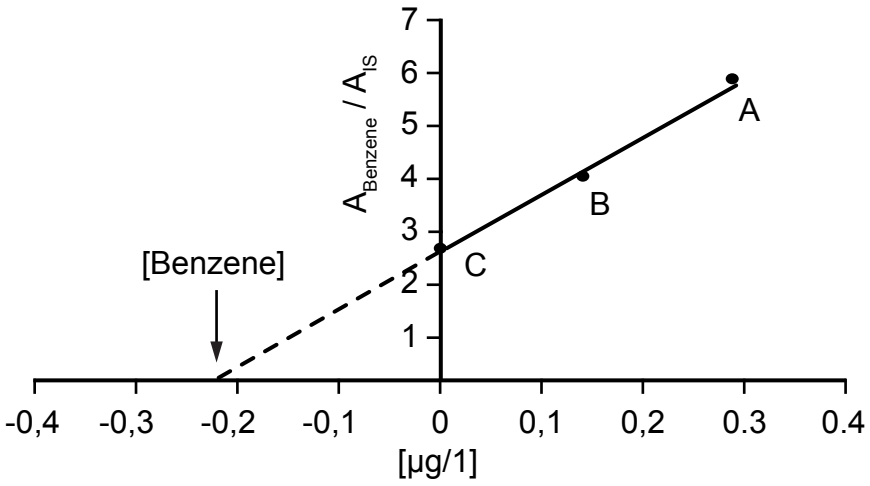

Figure 21: Benzene quantification in urine samples using standard addition. The concentration can be calculated using the equation of the linear regression (y = 10.863x + 2.5748, R^2 = 0.9981). A and B are urine samples spiked with 2.30 and 0.29 μg/L of benzene, respectively. Intersection $y = 0$: $x = –0.237$ and [benzene] = 0.237 μg/L (Reproduced after [42]).

Area normalization

This procedure is often used to follow the completion of a chemical reaction and the purity of the product(s) formed. The results of this qualitative method can be reported as “percentage peak area” or as “area normalization”. In the first case, all signal areas are added and then every peak is described as a percentage of the total.

In the case of results expressed as “area normalization”, all peaks are reported to one chosen reference signal and described as a percentage of this reference.

For both techniques it is presumed that the detector response is the same for unknown and standardized signals. This is often not the case and represents a strong limitation factor that is difficult to avoid [41].

Quality control (QC) samples

QCs analyses during method development and validation are used for several reasons, e.g. to check precision, accuracy, limit of quantification, recovery and robustness and ruggedness of a method. They are required for the validation of new analytical processes (inter- and intra-day, inter- and intra-assay) and for stability studies.

QC samples are preferably prepared from weighed aliquots of blank matrix spiked with known amounts of analytical standard. Stock solutions of analytical standard used for QC samples should be set up independently from those used to obtain the calibration curve in order to check potential weighing errors.

Measurements of QC samples are distributed into the analysis sequence between blanks, calibrators and analytical samples. They are not used in the calculation of the calibration curve but they permit to evaluate the acceptability of the results within the sequence and in a longer-term study, e.g. over weeks or months [43].

b) Systematic and random errors

Analytical instruments produce error-prone data. In order to estimate the individual error of a final result it is necessary to know the type and origin of the contribution errors due to the experimental set-up or the analytics (every single instrument has its own error). Two types, random and systematic errors, have been described.

Random errors, which are unpredictable, describe errors that affect the measurement such as temperature changes or mostly human errors. The term of “random errors” is also associated with the term of “precision” (see Figure 22). The random errors are analyzed with statistical methods, using means, standard deviation and coefficient of variation. Random errors can be reduced by repeating the measurement many times, and obtaining a more precise mean value. Higher precision measurements will lead to smaller standard deviations (fluctuation) of the final result.

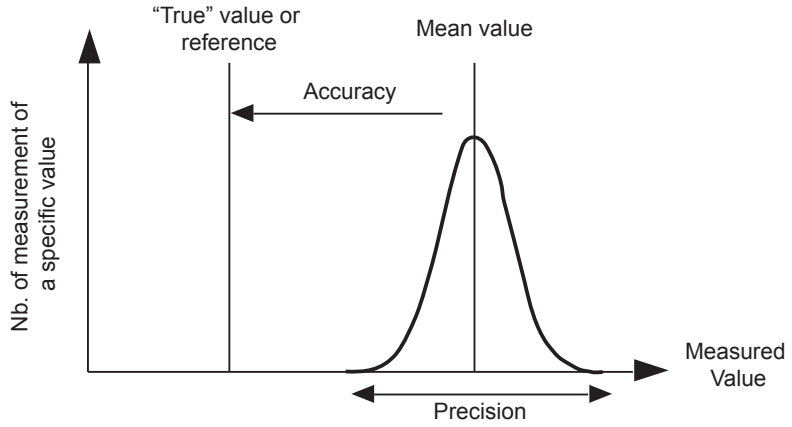

Figure 22. Illustration of “mean value”, “accuracy” and “precision” (Reproduced after *[43]*)

Systematic errors are predictable and are usually due to the analytical instrumentation. They could arise from problems such as poor calibration or imperfection in data processing. Systematic errors represent the deviation of the

mean values obtained from the “true” values. This deviation is also called “accuracy” (Figure 22).

It is important to know the quality of the quantification in terms of precision and accuracy (see Figure 23) and to find out the origin of observed or even suspected systematic errors in order to minimize them. In contrast to random errors, multiplying the number of analyses will not attenuate systematic errors. Only identifying and quantifying systematic errors can improve the accuracy of the results.

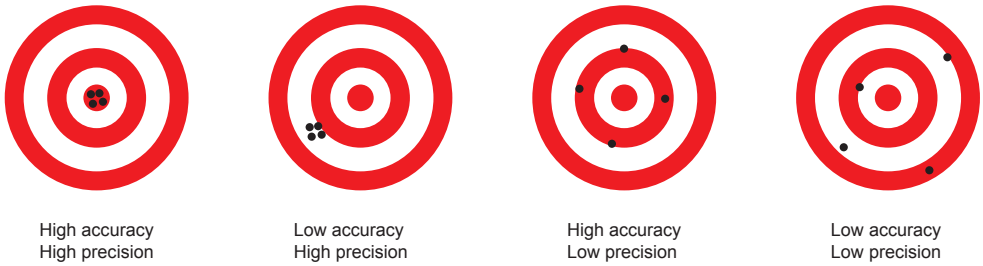

Figure 23: Dartboard visualizing term of precision and accuracy (Reproduced after [43])

c) Limit of detection (LOD) and limit of quantification (LOQ)

The LOD is defined as lowest amount or concentration of an analyte where still a signal-to-noise ratio (S/N) of 2-3 is observed (see Figure 24). At this ratio, the analyte is still detected but the signal intensity is not sufficient to allow quantifications. In chromatographic methods, the signal of the analyte would have two or three times the intensity of the base line (noise).

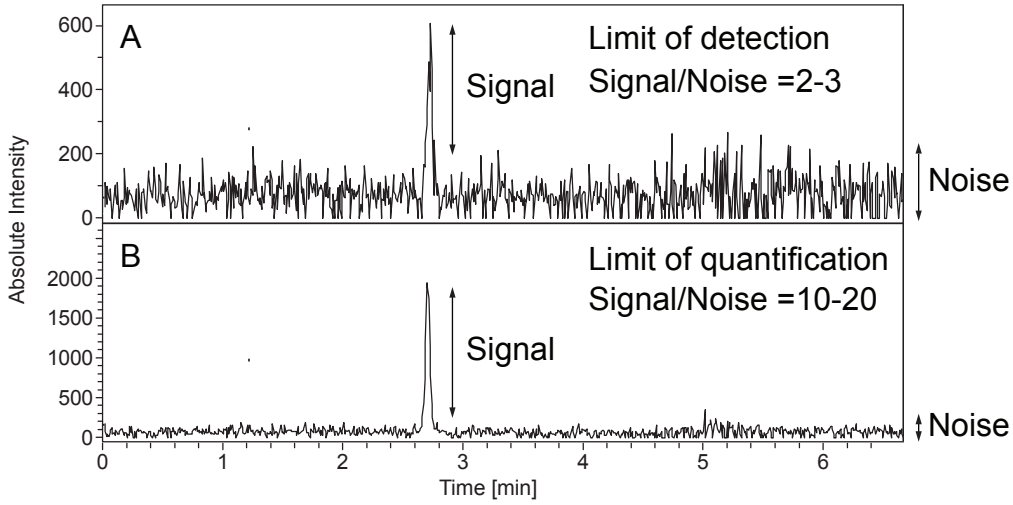

Figure 24: Minimal S/N ratio allowing (A) detection and (B) quantification

The LOQ corresponds, on the other hand, to the minimum amount injected producing a signal that would be within the standard deviation of the calibration curve. Ten to twenty times the intensity of the base line noise obtained for the matrix (blank sample) is usually enough to be used for precise quantifications [44].

d) Dynamic range and linearity

The dynamic range of a detector is defined as upper and lower limit of analyte concentration allowing quantifications with sufficient precision and accuracy.

Analytical methods with a linear dynamic range yield data proportional to the analyte concentration. Usually, this domain corresponds to a linear sensitivity of the detector within a determined value (normally ±5%) [44]. Dynamic ranges are mostly expressed in linear curves, although quadratic or enhanced quadratic curves can also be obtained.

Determination of cytosine using a QTOF mass analyzer in full scan mode, lead to a quadratic regression over the quantification range. The same determination measured with a Qtrap mass analyzer, scanning in triple quadrupole MS/MS mode, leads to a linear regression (Figure 25).

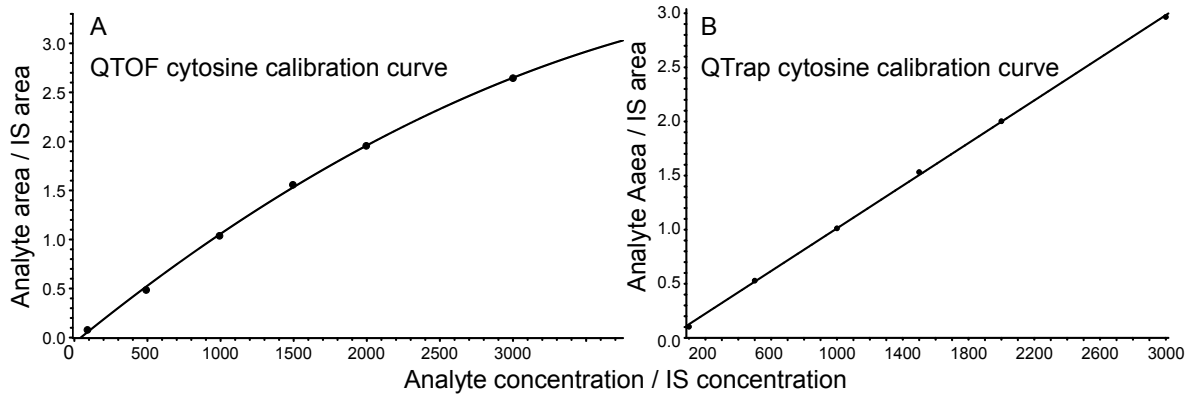

Figure 25: Calibration curve of cytosine obtained from (A) QTOF and (B) QTrap mass analyzer data

1.2.3 Selection of the analytical method

a) Generalities

The choice of the analytical method used for quantification depends extremely on the complexity of the sample. Urine, plasma, blood, plant extracts, spider venom, wastewater, or solid matters are analyzed with different procedures due to different properties of the matrices. It is also important to know how many components have to be quantified in order to choose the adequate method. For instance samples containing only one component do not require the use of hyphenated chromatographic methods. For mixtures, However, a chromatographic separation method is required, e.g. gas chromatography (GC), ultra high performance liquid chromatography (UHPLC) or, to lesser extent, capillary electrophoresis (CE).

Numerous spectroscopic methods can be used for quantification as e.g. nuclear magnetic resonance spectroscopy, Fourier transform infrared spectroscopy, UV/Vis spectroscopy, fluorescence spectroscopy, flame ionization (in combination with GC), diode array (HPLC, CE), or mass spectrometry (GC, HPLC, CE). Hyphenation of chromatography prior to detection leads to the most powerful quantification methods.

b) Chromatography

Chromatography is required in many areas of analytics, like e.g. discovery, development and manufacturing of new pharmaceutical drugs, food contaminants, environmental pollutants, or forensics, because the target compounds are dissolved in complex matrices. The two separation methods most widely used in analytical quantification are GC and HPLC/UHPLC. Both techniques are complementary and will be described in more detail below.

Gas chromatography (GC)

The basic process of GC involves sample evaporation in a heated injector, followed by separation of the mixture components in an appropriate GC column. Only (small) volatile molecules, which do not decompose during injection, are appropriate for GC analysis as e.g. pesticides, flavors, essential oils, hydrocarbon fuels, and many drugs. Analytes as e.g. acids, amino acids, amines, amides, saccharides, and steroids are too polar and require derivatization in order to increase their volatility and/or stability [45]. GC can be used for qualitative analyses like controlling purity of a substance, and for quantitative determinations. The parameters that influence separation on GC

columns are the type of carrier gas, the properties of the stationary phase, the length and diameter of the column, and temperature.

An inert carrier gas, usually helium or nitrogen, allows the analytes to elute. The gas has to be highly pure to avoid constant detection of chemical noise and column degradation. The velocity of the carrier gas plays a role in the separation of the analytes.

A GC column consists of an open fused silica capillary of 10 to 60 m length with an inner diameter between 0.10 – 0.53 mm [45]. The inner capillary walls are uniformly coated with a liquid film of stationary phase as e.g. methylated polysiloxane. The choice of the column and its stationary phase is mainly depending on, the polarity of the compounds and the presence of specific functional groups. The column is heated because the boiling point (or vapor pressure) also influences the separation. Analyses can be performed at constant temperature (isothermic run) or temperature-programmed. In this case, the temperature is increased at a constant rate in order to elute also compounds with stronger retention [45]. A compromise in the temperature gradient has to be found in order to optimize separation efficiency and analysis time.

The critical point in GC injection is the required fast transfer of the mixture into the gas phase and onto the column. The goal is to minimize peak broadening and to maximise the signal-to-noise ratio for each analyte [45]. Many injection systems have been developed, whereby split/splitless is most common. The split mode is used for highly concentrated samples and splitless mode for trace analyses. Programmable-temperature vaporizing (PTV) and cold on-column injectors are used for the analysis of heat-sensitive compounds. These injectors also show optimal recovery for most analytes because the discrimination during the injection process is reduced [45].

Quantitative determinations by GC are usually performed with a mass spectrometer or with flame ionization detector, whereby MS is the most sensitive and selective analyzer (see hereafter).

High performance liquid chromatography (HPLC) and ultra high performance liquid chromatography (UHPLC)

HPLC and UHPLC are used for the separation of various analytes, in particular non-volatile organic compounds. Both techniques need a stationary (column) and a mobile (solvent) phase. In analytical chemistry, columns of 30 to 250 mm length and 1 to 4.5 mm diameter are filled with stationary phase, usually silica based, of 1.7 to

10 μm particle size [41]. Columns are characterized according to retention strength and selectivity, whereby several practical requirements such as sufficient stability, reproducibility, peak shape and column efficiency N[2] play an important role.

Various solid supports exist for separation by reversed-phase (most widespread), normal phase, hydrophilic interaction liquid chromatography (HILIC), ion exchange, and size exclusion.

Reversed-phase chromatography involves alkyl chains like C_{18}, C_8 or C_4 covalently bound via silicon to a solid support and a polar mobile phase containing water. Polar molecules will interact stronger with the polar mobile phase and are retained less on the column, whereas apolar molecules will interact stronger with the hydrophobic column and be retained more. Selection and percentage of the organic solvent (mostly acetonitrile or MeOH) influences the strength of retention. Analyses can be performed with isocratic or gradient elution. The advantage of the gradient elution is to obtain best analyte separation efficiencies at different polarities.

Solvent pumps of HPLC instruments support pressures up to 400 bar. Recently, UHPLC systems have been developed for very fast separations in a few minutes [41]. They can operate with up to 1000 bar pressure and allow the use of special columns with smaller particle sizes, between 1.7 to 2.2 μm. The high backpressure resulting from the small particle size can be partially compensated by increasing the column temperature.

Higher N values and better separation efficiency allow decreasing run time without loss of resolution, as shown in Figure 26 [41].

[2] Column efficiency is influenced by the particle size and characterized as number of theoretical plates N

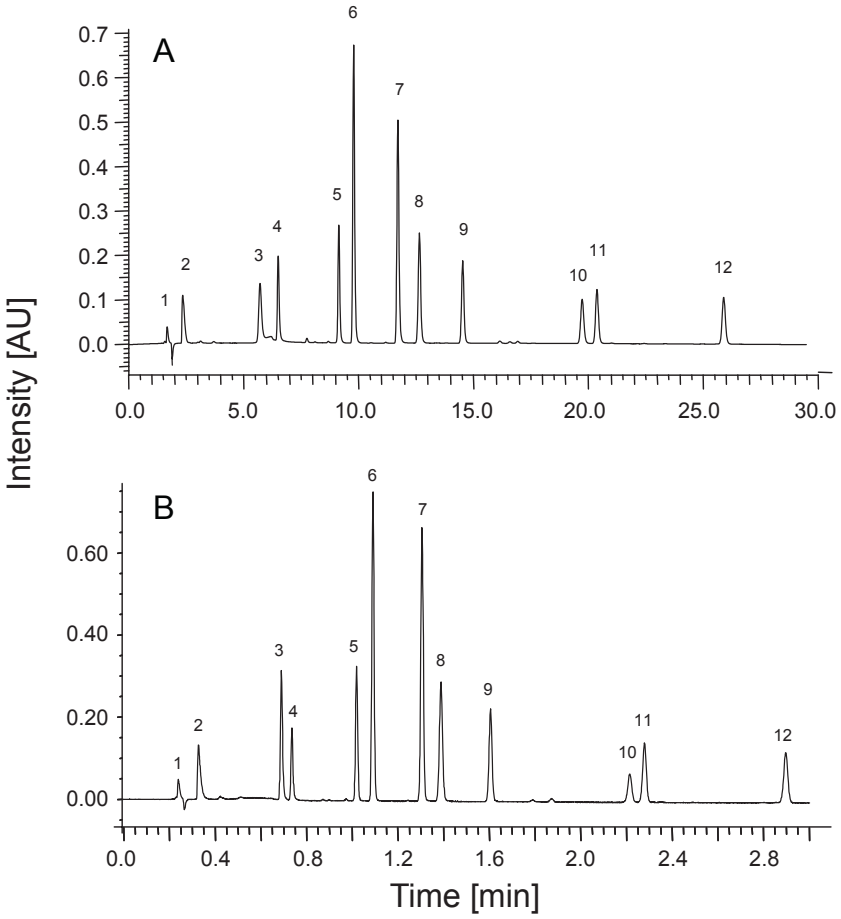

Figure 26: Separation of a standard mixture using (A) HPLC and (B) UHPLC (Reproduced after [46])

c) Mass spectrometry as method of choice

Mass spectrometry (MS) is nowadays one of the most powerful detection methods used in quantitative analytics. Because of unreached specificity and sensitivity, quantitative applications have been developed in a wide range of areas such as environmental and food chemistry [47-50], doping analysis [51-53], pharmacokinetics [54-56] and all “omics” technologies [57-59].

Selection of ionization methods

For mass spectrometry, neutral molecules have to be ionized, in order to be separated according to their mass-to-charge ratio. The most common methods used for ionization are electron ionization (EI), chemical ionization (CI), electrospray ionization (ESI), atmospheric pressure chemical ionization (APCI) and matrix-assisted laser desorption ionization (MALDI). The choice of the ionization mode will

depend on the polarity and molecular weight of the compounds of interest (see Figure 27).

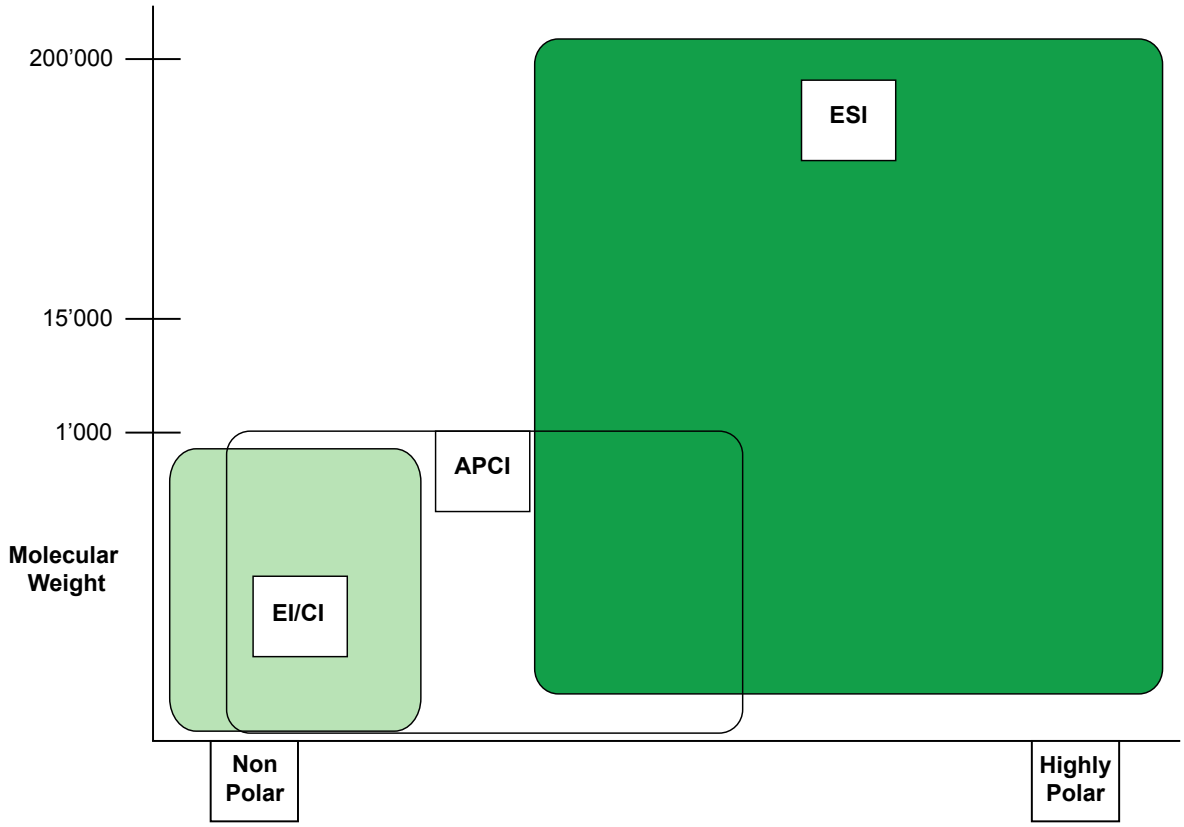

Figure 27: Domains of efficient ionization in relation to polarity and molecular weight of the analytes

i) Electron ionization is the method of choice for thermally stable and volatile compounds with a molecular mass below 1'000 g/mol. Substances are transferred in the ion source of the MS into the gas phase by evaporation. The vaporized molecules collide with a 70 eV energy rich electron beam, are ionized by loss of an electron, and form cationic radicals ($M^{+\bullet}$, molecular ion). These ions possess a residual energy of 10 ± 3 eV that leads to fragmentation reactions [60], whereby the most abundant charged particles are stable fragment ions or products of favored fragmentation reactions. Knowledge about these reactions can be used for structure elucidation. Furthermore each compound shows under EI conditions (70 eV) a specific EI fragmentation pattern that can be used as fingerprint. These analytical data can be collected in databases of EI mass spectra, as e.g. the well-known NIST or Wiley libraries.

ii) Chemical ionization is also used for the thermally stable and volatile molecules. It is softer than EI, and quasi-molecular ions $[M + H]^+$ or $[M - H]^-$ with almost no

fragmentation are produced. Negative chemical ionization is mostly used with compounds containing acidic or highly electronegative (halogen or nitro) groups. The process of chemical ionization starts with the ionization of a reactant gas as e.g. CH_4, *i*-C_4H_{10} or NH_3 by EI. These ionized reactant gases can then act as acids, and the molecules of the analyte are ionized in a second step by proton transfer reactions. CI is principally used for the quantification of pesticides containing nitro-aromatic derivatives.

iii) Electrospray ionization allows the soft transfer of a broad diversity of compounds into the gas phase; compounds with a molecular mass up to several 100 kDa as e.g. inorganic ions, peptides, proteins, nucleic acids, and polymers [61]. Ionization is effected by spraying a sample dissolved in a polar solvent, such as H_2O, CH_3CN, or CH_3OH, and that contains a volatile buffer from a capillary tip into the ion source. The use of N_2 sheath gas and a high electric field (2-5 kV) is required to form charged droplets and to evaporate them, leading to charged molecules [60]. Protonated $[M + H]^+$, deprotonated $[M - H]^-$ quasi-molecular-ions or adducts like $[M + Na]^+$, $[M + K]^+$, $[M + NH_4]^+$, or $[M + CF_3COO]^-$ are formed in ESI-MS. Multiple charged adducts as $[M + nH]^{n+}$ and $[M - nH]^{n-}$ are also very common. An extremely low limit of detection, picomole per analysis, can be obtained but this limit strongly depends on the conditions used (solvent, flow rate, buffer, sample purity).

iv) Atmospheric pressure chemical ionization allows the analysis of polar to relatively non-polar molecules such as esters, steroids, nitro-compounds or alcohols with a mass range of up to 2'000 Da. The sample solution is directly nebulized through a heated capillary at atmospheric pressure. A high-voltage corona needle ionizes the N_2 sheath gas by discharge. $N_2^{+\bullet}$ reacts then with the eluent to form species like H_3O^+, OH^-, or $OH^\bullet$ if H_2O is used as the solvent. Finally, the ionized solvent reacts with analyte molecules to form protonated $[M + H]^+$ or deprotonated $[M - H]^-$ quasi-molecular-ions [60].

In comparison to ESI, APCI does not form metal adducts like e.g. $[M + Na]^+$, $[M + K]^+$, which improves the accuracy of quantitative determinations. Furthermore, APCI sources tolerate higher flow rates and allow the use of analytical HPLC column with 4 mm ID.

Properties and specifications of the most common ion sources used in quantitative determinations are summarized in Table 1.

	EI	CI	ESI	APCI
Sample introduction	Evaporation	Evaporation	Dissolved in polar solvent (e.g. H_2O, CH_3CN, and CH_3OH) and buffered with volatile ions (conc ≤ 0.1%)	Dissolved in polar to mid-polar solvents (e.g. CH_3CN, CH_3OH, $CHCl_3$, or CH_2Cl_2; and buffered with volatile ions (conc ≤0.1%)
Substance class	Alkane, aromatic, halogen, ester, ketone, nitrile, nitro and amine derivative	Alcohol, ketone, ester, amine, lipid (M=1000)	DNA, RNA, protein, peptide, polymer, polar lipid, nucleotide, nucleoside, saccharide, organo metallic compound, non-covalent complex	Nitro, alcohol, ester, amine, and steroid derivatives
Decomposition	Thermic	Thermic	None	Little thermic
Mass range *m*/*z*	1-1000	18-1000	18-200'000 (Formation of M^{n+} ions)	18-2000
Common molecular or quasi-molecular-ion	$M^{+\bullet}$	$[M + H]^+$, $[M + C_4H_9]^+$, $[M + NH_4]^+$, $[M - H]^-$	$[M + H]^+$, $[M + Na]^+$, $[M + K]^+$, $[M + nH]^{n+}$, $[M - H]^-$, $[M - nH]^{n-}$	$[M + H]^+$, $[M - H]^-$, $M^{-\bullet}$ $[M + \text{solvent} + H]^+$
Coupling to Chromatographic methods	GC	GC	HPLC/UHPLC/CE	HPLC/UHPLC & GC

Table 1: Overview of ionization methods and their characteristics [60] according to literature

There is an increasing need for analyzing complex biological matrix like urine, blood or plasma. MS is often the detector of choice for quantitative determinations because the ionization methods that have been implemented allow hyphenation with GC for the analysis of volatile and non-polar compounds and with HPLC for the analysis of non-volatile and more polar analytes. On-line coupling to chromatographic techniques also allows automation and higher throughput of samples. Separation of analytes from matrix molecules also increases selectivity and sensitivity. Discrimination of detection due to variable ionization efficiencies can be reduced for compounds with different functionalities. This phenomenon, called ion suppression, is principally observed in ESI-MS and can be partially compensated by using internal standards (see below)

Selection of mass analyzer

Ionized molecules are separated in mass analyzers according to their mass to charge ratio (*m*/*z*). Mass analyzers have been categorized according to physical principles used for ion separation [62]:

- Ion beam (e.g. sector field, quadrupole or triple quadrupole instruments)

- Ion trap (quadrupole ion trap, Orbitrap, Fourier-transform ion cyclotron resonance)

- Time-of-flight (TOF)

Principally, all mass analyzers can be used for quantitative determinations, but technical characteristics will often limit their application. The most important properties are scan rate, sensitivity, resolution power, mass accuracy and mass range. For example, the number of MS scans in one chromatographic signal is related to the peak width and to the scan rate of the mass analyzer. Increase of scan rate can lead to better chromatographic resolution but decreases sensitivity.

Mass analyzers characteristics will be presented shortly in order to facilitate the development of the most appropriate method in quantitative determination.

i) Ion beam

- Double focusing sector field instruments are the oldest mass spectrometers still in use. They are made of electric and/or magnetic field sectors. After acceleration, ions are deflected in function of their kinetic energy and velocity [60]. These instruments are usually equipped with electron or chemical ionization sources and are easily coupled with GC. They have a mass range of up to *m*/*z* 6'000. Sector field instruments provide high resolving power (RP) up to 100'000, but at the cost of transmission efficiency and therefore sensitivity [43]. In quantitative analysis, high RP is used to increase the selectivity by decreasing the chemical background noise. In combination with GC, sector field instruments are often used in quantification of e.g. dioxins (LOD below 20 fg) .

- Quadrupole mass analyzers are widely used because of their ease of operation and maintenance, robustness, low price and compactness. They consist of four parallel rods whereby beams of ions with a unique *m/z* value have a stable trajectory at a given potential. At the same time, all other ions entering the quadrupole will be lost. These analyzers provide a mass range until ca. 4'000 *m/z* at low resolution (ca. 0.6 Da) [62]. Two operating modes are usually used. The full scan (FS) mode is used to transmit one *m/z* value after another over a mass range. The selected ion monitoring (SIM) mode is chosen to filter a specific *m/z* value. Almost all ionization sources can be interfaced to quadrupole mass analyzers, and their high scan rate allows coupling to chromatographic systems [60]. The FS mode is used for structure elucidation and the most sensitive SIM mode for quantitative measurements [63]. However, the SIM mode does not differentiate compounds with the same nominal mass and can lead to wrong results, especially if samples with complex matrices are analyzed.

- Triple quadrupole instruments ($Q_1q_2Q_3$) are tandem in space mass spectrometers whereby three quadrupole mass analyzers are linked together in series [64]. Precursor ions can be selected in Q_1, fragment ions formed in q_2 via collision-induced dissociation (CID), and separated in Q_3. Q_1 and Q_3 can work in both, FS or SIM mode. Filled with an inert gas (Ar or N_2) q_2 is used as collision cell. In combination with HPLC, $Q_1q_2Q_3$ have been described as workhorses of trace level quantitative analysis because of their reliability, high data acquisition rate, and short duty cycle (fraction of total operating time spent to measure target ions in the SIM mode) [43], allowing them to detect several fragmentation reactions in a single run, in the so-called multiple reaction-monitoring (MRM) mode.

ii) Ion trap

- There are two types of quadrupole ion trap (QIT) mass analyzers on the market, the cylindrical (3D) and the linear (2D). In both cases, the trap is filled with an inert gas, usually He, to cool the collected ions on one side – effecting an increase of the resolution – and to allow the execution of collision induced dissociation experiments after excitation of ion packets on the other side. QIT instruments work with as high scan rates as 52'000 *m/z*/s or 10 spectra/s [60], which makes them ideal detectors for chromatographic systems. Additionally, powerful structure elucidation can be performed by MS^n experiments. This technique consists of isolating precursor ions at a given *m/z* value, fragment them, isolate some of the formed fragment ions, and fragment them again. This can be done up to the 10^{th} generation of fragmentation.

For quantitative measurements, ion traps are usually operated in full scan MS/MS mode. In contrary to triple quadrupole analyzers, ion traps have high sensitivity in full scan mode due to variable accumulation times related to ion abundance. Low ion intensities lead to much longer scan times heading to a decrease of performances [43]. Another drawback of ion traps is the so-called "low-mass cut-off". This partial or complete suppression of ion detection in the low mass range is particularly problematic in MS/MS mode, when small fragment ions containing relevant structural information are not detected.

- Orbitrap and Fourier-transform ion cyclotron resonance (FT-ICR) mass spectrometers are ion traps allowing wide mass range detection with a high or extremely high resolving power and mass accuracy. Although these analyzers can be easily coupled with LC, their low scan rate of only around 1 scan per second do not allow

effective and precise quantitative determinations [65]. For this reason, Fourier-transform ion traps have only rarely been mentioned in scientific literature in combination with quantification [43].

iii) Time-of-flight (TOF)

- TOF analyzers identify ions according to the time they need to pass a given distance to a detector. This time is related to the acceleration voltage, the length of the field-free region, and the mass-to-charge ratio of the ions. The TOF analyzers provide high sensitivity at high scan rate of several hundred spectra per second in full scan mode and high mass range above 300'000 *m/z*. The newest TOF analyzers achieve good resolving power (resolution up to 60'000 full-width half-maximum) and good mass accuracy below 2 ppm with internal calibration [60]. The high scan rate in particularly make TOF analyzers perfect to be coupled with fast chromatographic methods, as fast-GC or UHPLC.

- Quadrupole TOF (QTOF) is a hybrid mass analyzer, combining the benefits of two analyzers: the possibility to perform CID with quadrupoles and the high performance with regards to speed, resolution, and sensitivity of TOF. The advantage of QTOF used for quantification, is the acquisition of full scan product ion spectra at high mass accuracy. The noise can be decreased and, at the same time, the amount of information collected increased [66].

An example of improved signal-to-noise ratio obtained by calculating accurate extracted ion chromatograms (HR-EIC) from data recorded at high-resolution is shown in Figure 28. In comparison to a mass window of ± 0.5 *m/z* (A), the sensitivity can be improved by a factor of 16 by using a mass window of ± 0.01 *m/z* (B).

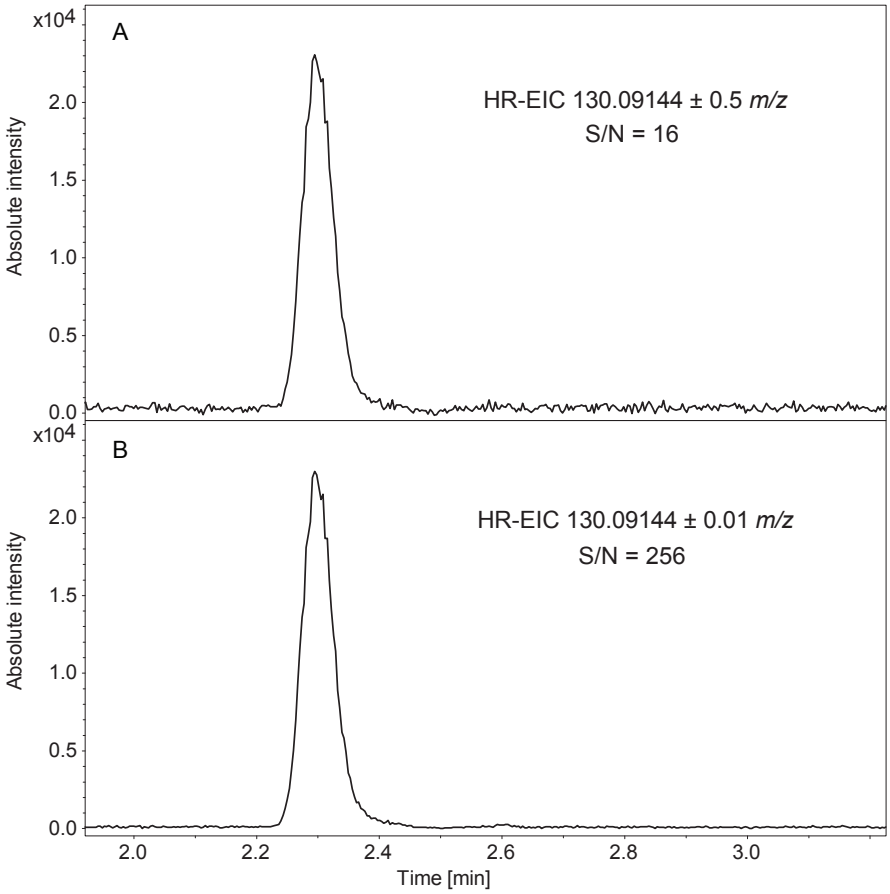

Figure 28: HR-EIC of *m/z* 130.09144 calculated with (A) 0.5 and (B) 0.01 mass width

iv) Tandem mass spectrometry

MS/MS is practicable with double focusing sector field, triple quadrupole, ion trap, and QTOF instruments. They can be categorized in tandem-in-time (ion traps) and tandem-in-space (double focusing sector field instruments, QqQ, QTOF) types. Both principles have their pro and contra. Ion traps permit multiple stage MS/MS experiments (MS^n) and have higher sensitivity in FS mode. However, quantification of analytes present at very different concentrations is difficult due to the limited dynamic range (two to three orders of magnitude). The low-mass cut-off is also a severe drawback because ions with low *m/z* ratios are discriminated or even not detected below $1/3^{rd}$ of the mass of the precursor ions without special parametrization [22, 67]

Triple quadrupoles are the most widely used tandem in space instruments. They allow operation in four different MS/MS acquisition modes, product ion, precursor ion, constant neutral loss, and selected or multiple reaction monitoring (SRM/MRM) scans (see figure 29).

- *Product ion scan* is certainly the most common MS/MS mode. Precursor ions at a specific *m/z* value are selected in the first quadrupole (Q_1). They are then transferred to the collision cell (q_2) where they collide with inert gas (N_2 or Ar) and where fragmentation occurs to form product ions and neutral species. The ions are transferred into the third quadrupole (Q_3), which scans over the mass range and delivers the product ion mass spectra.

- In the *precursor ion scan* mode, Q_3 is set to a specific *m/z* value (fragment ions of interest). Q_1 is scanning over the mass range transferring the ions of different *m/z* ratios separately into the collision cell (q_2) and finally to Q_3. This allows the detection of all precursor ions sharing the same fragment. In peptide chemistry for example, compounds containing glycine or tryptophan can be recognized if Q_3 is set to *m/z* 30 or 159 corresponding to the respective immonium ions [68].

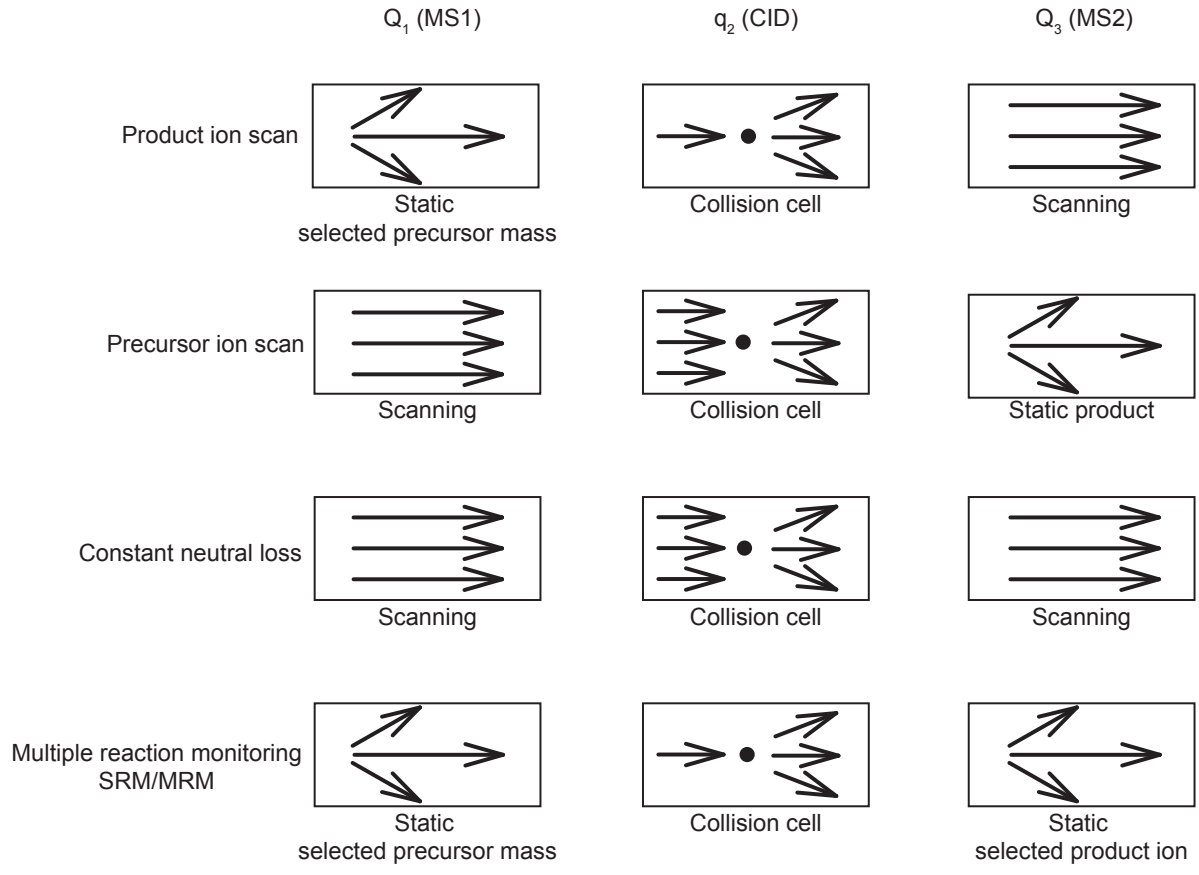

Figure 29: MS/MS scanning modes

- During *constant neutral loss* experiments, Q_1 and Q_3 are both scanning with a constant mass difference corresponding to a specific neutral loss that can usually be observed in a compound class. Typically neutral losses are water Δ=18 u, CO Δ=44u, NO_2 Δ=46 u [62].

- *Selected or multiple reaction monitoring* (SRM/MRM) is the method of choice for quantitative determinations using LC-MS/MS. Both mass analyzers Q_1 and Q_3 are set to fixed *m/z* values corresponding to a fragmentation reaction that is specific for a compound. Then, Q_1 and Q_3 switch simultaneously to a different value corresponding to another fragmentation reaction. Modern mass analyzers can switch very quickly, allowing the detection of more than 100 components within one second. MRM is the most selective and sensitive method, because only one mass is fixed in MS1 and MS2 at the same time removing all chemical noise [62].

Figure 30 illustrates the LC-MS/MS chromatogram recorded under MRM conditions. In this example the sample was a TpT solution that was irradiated with UV light. The instrument was set to two MS transitions (*m/z* 545 → 447 and *m/z* 545 → 432), which allowed the detection of four photoproducts. Both parameters, mass of fragment ions and RT, are essential for the description of each photoproduct.

To conclude, MS/MS is the method of choice for quantitative determinations, in particular when components of complex matrices are analyzed. The sensitivity of GC and HPLC-MS experiments is improved because MS/MS increases selectivity of detection and reduces chemical noise. SRM and MRM experiments can be performed with $Q_1q_2Q_3$, QTOF and ion trap instruments whereby triple quadrupole mass analyzers provide the highest duty cycles and are therefore more sensitive if several compounds have to be quantified.

Compared to MS, MS/MS provides a higher degree of confidence in the target structure detected and can also be extremely useful for structure elucidations, in particular when mild ionization sources are used [69].

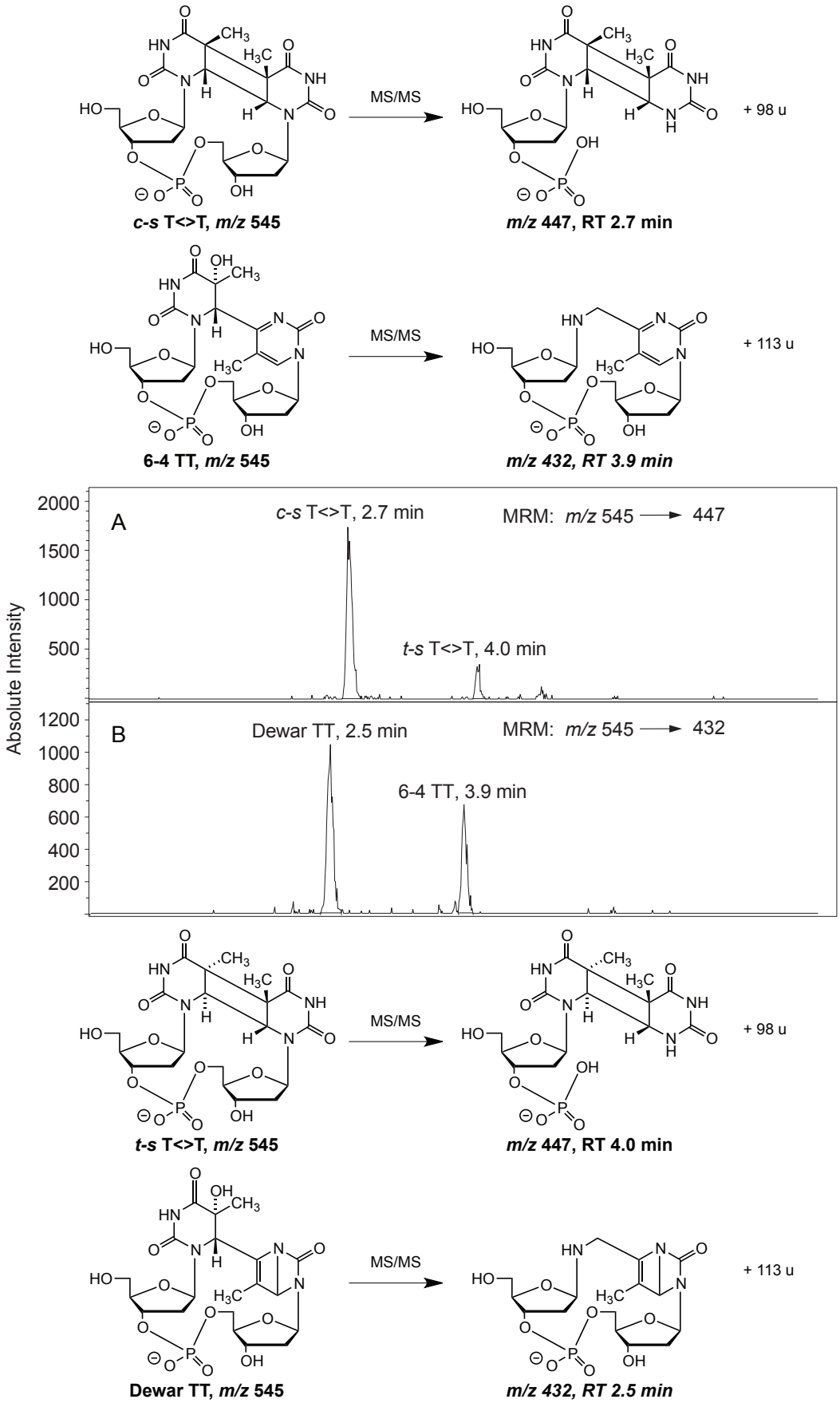

Figure 30: Photoproducts of TpT determined in MRM mode with Q_1 set at *m/z* 545 and Q_3 at (A) *m/z* 447 and (B) *m/z* 432, respectively

Criteria for method selection

For choosing the most appropriate quantitative analytical method, it is essential to consider the properties of analyte, matrix, and available instrumentation in relation to sample complexity and limit of detection. Sample preparation and chemical derivatization procedure, chromatographic method, ionization mode and mass analyzer will be chosen depending on these properties. Most of the modern quantification procedures are based on GC and HPLC and only such methods will be discussed below.

i) Analyte properties

Molecular weight, polarity, stability, and concentration are properties of an analyte that have to be considered for sample preparation procedure, need of chemical derivatization, chromatographic method, and especially choice of the ionization mode. Volatile compounds with low molecular weight below around 600 g/mol are ionized under EI/CI conditions. Polar molecules are well ionized with ESI, less polar with EI, CI, or APCI. Further, stability of the analyte is often related to the polarity and a chemical derivatization maybe requested when a GC-EI/CI procedure has to be used. The analyte concentration is also a concern as it influences (a) the choice of the domain of the calibration curve, and (b) the presents of the analyte in the linearity of detector response. This is particularly important for the concentration-dependent ESI method. When analyte concentration is high, the limit of quantification is also strongly depending on the mass analyzer (e.g. $Q_1q_2Q_3$, QIT, or QTOF) and acquisition mode (e.g. SIM or MRM) that have been chosen.

ii) Sample complexity

Number and concentration range of the target analytes also influence selection of the analytical method. For example, if several volatile compounds with similar physical properties have to be quantified, GC-MS will be often the method of choice because of the high chromatographic separation efficiency. Complex mixtures can be separated and, if some of the components are still co-eluting, on-line coupling to a MS often still allows the quantification thanks to detection of some specific fragment ions of these co-eluting compounds [70].

A high variety of analytes, mid-polar to polar and small to large, can be analyzed with HPLC-MS. Samples can be straightforwardly measured after extraction in contrary to GC where labile and/or polar molecules have to be derivatized prior to injection. The

recent development of ultra-high performance liquid chromatography (UHPLC) with stationary phases below 2 µm particle size dramatically increased separation efficiency, sample throughput (less than 5 min per run are possible), and sensitivity.

iii) Matrix complexity

Quantification of analytes from complex matrices like e.g. urine, plasma, and environmental or plant extracts requires reproducible sample preparation procedures to obtain best accuracies. These procedures usually involve solid-phase (SPE) or liquid-liquid (LLE) extraction. Extraction conditions (solvent, buffer, stationary phase) have to be chosen according to the complexity of the matrix and to the chromatographic method that will be used. Biological matrices contain hundreds of potential interfering components with the analyte that should be removed prior analysis. Otherwise, matrix effects could lead to poor reproducibility of chromatographic separations and ion suppression effects.

Choosing an MS/MS mass analyzer can partially solve the problems of analyzing complex matrices. The detection is selective, filtering the interfering signals improving signal-to-noise ratio.

In any case, addition of internal standards (IS) is essential for quantitative determinations. Matrix effects can be compensated and accuracy increased. The choice of the IS is very important and its structure should be closely related to the structure of the target analyte. Otherwise, ion-suppression effects occur and the ratio of the detector response between both compounds will vary and lead to poor quantitative results [71].

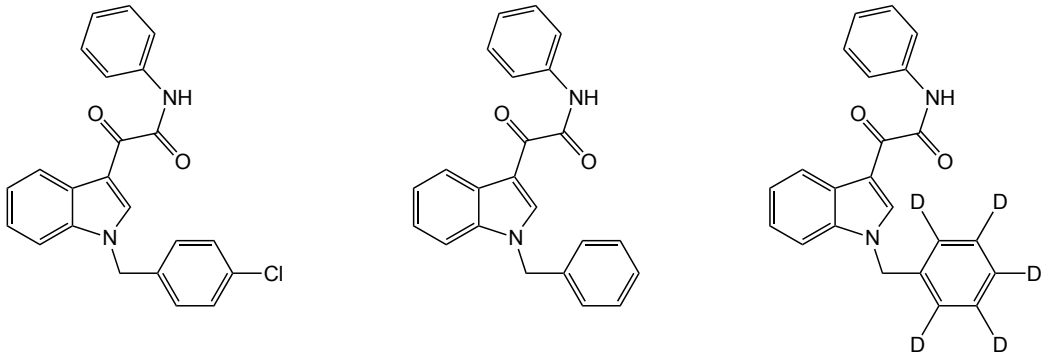

D-24851 Analogous internal standard SIL internal standard

Figure 31. Analog and SIL structure of D-24851 that have been used for quantitative determinations [71]

Stable isotopically labeled (SIL) compounds are the most appropriate internal standards used for quantitative measurements with MS detection since they show the same chromatographic and mass spectrometric (ionization efficiency and fragmentation) properties (example shown in Figure 31). SIL standards are usually labeled with ^{13}C, ^{15}N, ^{17}O or D (deuterium) atoms [72].

It is noteworthy that deuterium-labeled compounds have to be stable. Exchange between deuterium and hydrogen would result in a lower recovery of the SIL [73, 74]. SIL internal standards have to be as pure as possible to avoid interferences with the analyte response that could lead to inaccurate results. These requirements make standards either very expensive or not available. Internal standards with analog structure can thus be preferred [73-75].

1.3 Bibliography

[1] Stryer, L., *Biochemistry*, Third ed., W. H. Freeman and Company, **1988**.
[2] Kypr, J., Kejnovska, I., Renciuk, D., Vorlickova, M., *Nucleic Acids Res.* **2009**, *37*, 1713.
[3] Carr, S. M., **2010**, http://www.mun.ca/biology/scarr/A_B_Z_DNA.html, 2010
[4] Watson, J. D., Gann, A., Levine, M. K., Bell, S. P., Baker, T. A., *Molecular Biology of the Gene*, Sixth ed., Benjamin-Cummings Publishing Company, **2007**.
[5] Yakovchuk, P., Protozanova, E., Frank-Kamenetskii, M. D., *Nucleic Acids Res.* **2006**, *34*, 564.
[6] Pray, L., **2008**, http://www.nature.com/scitable/topicpage/discovery-of-dna-structure-and-function-watson-397
[7] Cooper, G. M., *The Cell: A Molecular Approch*, Second ed., Sunderland (MA): Sinauer Associates, **2000**.
[8] Caterino, T. L., Hayes, J., *Nat. Struct. Mol. Biol.* **2007**, *14*, 1056.
[9] Goldberg, A. D., Allis, C. D., Bernstein, E., *Cell* **2007**, *128*, 635.
[10] Feil, R., Fraga, M. F., *Nat. Rev. Genet.* **2012**.
[11] Jaenisch, R., Bird, A., *Nat. Genet.* **2003**, *33 Suppl*, 245.
[12] Portela, A., Esteller, M., *Nat. Biotechnol.* **2010**, *28*, 1057.
[13] Eyre-Walker, A., Keightley, P. D., *Nat. Rev. Genet.* **2007**, *8*, 610.
[14] Bertram, J. S., *Mol. Aspects Med.* **2000**, *21*, 167.
[15] Robertson, K. D., *Nat. Rev. Genet.* **2005**, *6*, 597.
[16] Semmler, A., Smulders, Y., Struys, E., Smith, D., Moskau, S., Blom, H., Linnebank, M., *Clin. Chem. Lab. Med.* **2008**, *46*, 1398.
[17] Maxwell, A., McCudden, C. R., Wians, F., Willis, M. S., *LabMedicine* **2009**, *40*, 171.
[18] Ravanat, J.-L., Martinez, G. R., Medeiros, M. H. G., Di Mascio, P., Cadet, J., *Tetrahedron* **2006**, *62*, 10709.
[19] Su, D. G., Fang, H., Gross, M. L., Taylor, J. S., *Proc. Natl. Acad. Sci. USA* **2009**, *106*, 12861.
[20] Sanglier, S., Leize, E., Dorsselaer, A., Zal, F., *J. Am. Soc. Mass Spectrom.* **2003**, *14*, 419.
[21] Cadet, J., Sage, E., Douki, T., *Mutat. Res.* **2005**, *571*, 3.
[22] Garrido Frenich, A., Plaza-Bolanos, P., Martinez Vidal, J. L., *J. Chromatogr. A* **2008**, *1203*, 229.
[23] Triolo, A., Arcamone, F. M., Raffaelli, A., Salvadeori, P., *J. Mass Spectrom.* **1997**, *32*, 1186.
[24] Hannon, M. J., *Chem. Soc. Rev.* **2007**, *36*, 280.
[25] Wan, K. X., Shibue, T., Gross, M. L., *J. Am. Chem. Soc.* **2000**, *122*, 300.
[26] Hemminki, K., Koskinen, M., Rajaniemi, H., Zhao, C., *Regul. Toxicol. Pharmacol.* **2000**, *32*, 264.
[27] Ghosh, D., Kosenkov, D., Vanovschi, V., Williams, C. F., Herbert, J. M., Gordon, M. S., Schmidt, M. W., Slipchenko, L. V., Krylov, A. I., *J. Phys. Chem. A* **2010**, *114*, 12739.
[28] Strekowski, L., Wilson, B., *Mutat. Res.* **2007**, *623*, 3.
[29] Tse, W. C., Boger, D. L., *Chem. Biol.* **2004**, *11*, 1607.
[30] Fenn, J., Mann, M., Meng, C., Wong, S., Whitehouse, C., *Science* **1989**, *246*, 64.

[31] McLafferty, F. W., *Science* **1981**, *214*, 280.
[32] Heck, A. J., Van Den Heuvel, R. H., *Mass Spectrom. Rev.* **2004**, *23*, 368.
[33] Beck, J. L., Colgrave, M. L., Ralph, S. F., Shell, M. M., *Mass Spectrom. Rev.* **2001**, *20*, 61.
[34] Hofstadler, S. A., Griffey, R. H., *Chem. Rev.* **2001**, *101*, 377.
[35] Loo, J. A., *Int. J. Mass Spectrom.* **2000**, *200*, 175.
[36] Rosu, F., Gabelica, V., Houssier, C., De Pauw, E., *Nucleic Acids Res.* **2002**, *30*, e82.
[37] Mouret, S., Baudouin, C., Charveron, M., Favier, A., Cadet, J., Douki, T., *Proc. Natl. Acad. Sci. USA* **2006**, *103*, 13765.
[38] Wang, Z., Cui, M., Song, F., Lu, L., Liu, Z., Liu, S., *J. Am. Soc. Mass Spectrom.* **2008**, *19*, 914.
[39] Wang, Z., Cui, M., Song, F., Lu, L., Liu, Z., Liu, S., *J. Am. Chem. Soc.* **2008**, *19*, 914.
[40] Miller, J. C., Miller, J. N., *Analyst* **1988**, *113*, 1351.
[41] Snyder, L. R., Kirkland, J. J., Dolan, W., *Introduction to modern liquid chromatography*, 3 ed., John Wiley & Son, Ltd, **2010**.
[42] Basilicata, P., Miraglia, N., Pieri, M., Acampora, A., Soleo, L., Sannolo, N., *J. Chromatogr. B* **2005**, *818*, 293.
[43] Boyd, R. K., Basic, C., Bethem, R. A., *Trace Quantitative Analysis by Mass Spectrometry*, John Wiley & Son, Ltd, **2008**.
[44] Huber, L., *Validation and Qualification in Analytical Laboratories*, Second ed., CRC Press, **2007**.
[45] Sparkman, O. D., Penton, Z. E., Kitson, F. G., *Gas Chromatography and Mass Spectrometry: A Practical Guide*, Second ed., Elsevier, **2011**.
[46] Guillarme, D., Nguyen, D. T., Rudaz, S., Veuthey, J. L., *Eur. J. Pharm. Biopharm.* **2008**, *68*, 430.
[47] Lacorte, S., Fernandez-Alba, A. R., *Mass Spectrom. Rev.* **2006**, *25*, 866.
[48] Núñez, O., Moyano, E., Galceran, M. T., *Trends Analyt. Chem.* **2005**, *24*, 683.
[49] Picó, Y., Blasco, C., Font, G., *Mass Spectrom. Rev.* **2004**, *23*, 45.
[50] Picó, Y., Font, G., Ruiz, M. J., Fernandez, M., *Mass Spectrom. Rev.* **2006**, *25*, 917.
[51] Chebbah, C., Pozo, O. J., Deventer, K., Van Eenoo, P., Delbeke, F. T., *Rapid Commun. Mass Spectrom.* **2010**, *24*, 1133.
[52] Guddat, S., Thevis, M., Schanzer, W., *Biomed. Chromatogr.* **2005**, *19*, 743.
[53] Lee, K. M., Kim, H. J., Jeong, E. S., Yoo, H. H., Kwon, O. S., Jin, C., Kim, D. H., Lee, J., *Rapid Commun. Mass Spectrom.* **2011**, *25*, 2261.
[54] Korfmacher, W. A., Cox, K. A., Ng, K. J., Veals, J., Hsieh, Y., Wainhaus, S., Broske, L., Prelusky, D., Nomeir, A., White, R. E., *Rapid Commun. Mass Spectrom.* **2001**, *15*, 335.
[55] Park, J. H., Park, Y. S., Rhim, S. Y., Kim, H. J., Jhee, O. H., Lee, Y. S., Lee, M. H., Shaw, L. M., Kang, J. S., *Biomed. Chromatogr.* **2009**, *23*, 1350.
[56] Stendel, R., Scheurer, L., Schlatter, K., Stalder, U., Pfirrmann, R. W., Fiss, I., Möhler, H., Bigler, L., *Clin. Pharmacokinet.* **2007**, *46*, 513.
[57] Casado-Vela, J., Cebrián, A., Gómez del Pulgar, M. T., Lacal, J. C., *Clin. Transl. Oncol.* **2011**, *13*, 617.
[58] Keshishian, H., Addona, T., Bugess, M., Mani, D. R., Shi, X., Kuhn, E., Sabatine, M. S., Gerszten, R. E., Carr, S. A., *Mol. Cell Proteomics* **2009**, *8*, 2339.
[59] Zhang, X., Wei, D., Yap, Y., Li, L., Guo, S., Chen, F., *Mass Spectrom. Rev.* **2007**, *26*, 403.

[60] Hesse, M., Meier, H., Zeeh, B., Bienz, S., Bigler, L., Fox, T., *Spektroskopische Methoden in der Organische Chemie*, 8 ed., Georg Thieme Verlag, **2012**.
[61] Kebarle, P., Verkerk, U. H., *Mass Spectrom. Rev.* **2009**, *28*, 898.
[62] Lemière, F., *LCGC Europe* **2001**, *Dec 2*, 2.
[63] Kärrman, A., van Bavel, B., Järnberg, U., Hardell, L., Lindström, G., *Anal. Chem.* **2005**, *77*, 864.
[64] Johnson, J., Yost, R. A., Kelley, P. E., Bradford, D. C., *Anal. Chem.* **1990**, *62*, 2162.
[65] Makarov, A., Denisov, E., Kholomeev, A., Balschun, W., Lange, O., Strupat, K., Horning, S., *Anal. Chem.* **2006**, *78*, 2113.
[66] Grimalt, S., Pozo, O. J., Sancho, J. V., Hernández, F., *Anal. Chem.* **2007**, *79*, 2833.
[67] Soler, C., Mañes, J., Picó, Y., *J. Chromatogr. A* **2005**, *1067*, 115.
[68] Colzani, M., Bienvenut, W. V., Faes, E., Quadroni, M., *Rapid Commun. Mass Spectrom.* **2009**, *23*, 3570.
[69] Sinha, R. P., Häder, D.-P., *Photochem. Photobiol. Sci.* **2002**, *1*, 225.
[70] Alder, L., Greulich, K., Kempe, G., Vieth, B., *Mass Spectrom. Rev.* **2006**, *25*, 838.
[71] Stokvis, E., Rosing, H., Beijnen, J. H., *Rapid Commun. Mass Spectrom.* **2005**, *19*, 401.
[72] Bergeron, A., Furtado, M., Garofolo, F., *Rapid Commun. Mass Spectrom.* **2009**, *23*, 1287.
[73] Chavez-Eng, C. M., Constanzer, M. L., Matuszewski, B. K., *J. Chromatogr. B* **2002**, *767*, 117.
[74] Wieling, J., *Chromatographia* **2002**, *55*, 107.
[75] Kato, K., Jingu, S., Ogawa, N., Higuchi, S., *J. Pharm. Biomed. Anal.* **2000**, *24*, 237.

CHAPTER 2

METHOD DEVELOPMENT TO STUDY NON-COVALENT DNA COMPLEXES

2.1 Introduction

Non-covalent interactions with DNA or RNA are essential in a variety of biological processes [1-3]. These interactions with specific regions of DNA are described by different binding modes such as intercalations, minor and major groove binding [4] based on *Van der Waals* forces, hydrogen bonds and electrostatic interactions. The presence of either adjacent AT- or GC-rich regions in the oligomer sequence can lead to selective binding between ligands and DNA [5, 6]. Non-covalent interactions have been investigated in more detail because they are of pharmacological interest. Some compounds such as polyamide drugs bind to the minor groove (AT-rich regions) of B-DNA. Other molecules, such as flavonoids, were suggested to bind DNA by intercalation with a minimal sequence selectivity (slight preference to GC-rich regions) [7].

At physiological pH, non-covalent complexes are formed between protonated polyamine derivatives and charged phosphate groups of oligonucleotides through electrostatic interactions. These complexes are known to stabilize the tertiary structure of DNA [8-10] and RNA [11, 12], to protect them from thermal and alkaline denaturation, enzymatic degradation, shear breakage, or radiation damage [8]. Members of this class of compounds have already been used to inhibit prostate cancer [13] and HIV-1 protease [14].

Biological activity related to non-covalent interactions of DNA/RNA duplexes with small organic molecules have been investigated using many analytical techniques, e.g. NMR [10, 12, 15], X-ray crystallography [5, 16], footprinting [6], and differential scanning calorimetry [8]. These methods are often laborious and/or require large quantities of material.

Mass spectrometry (MS) is known as one of the most sensitive analytical tools that requires very small amounts of substance (pmol or less). Thermo-labile molecules are usually measured with atmospheric pressure ionization (API) techniques by which they are charged and transferred from solution into the gas phase. In particular, electrospray ionization (ESI) is a soft and sensitive ionization technique and usually yields quasi-molecular ions with low fragmentation. This technique is particularly suitable for the investigation of polar molecules such as polyamines, flavonoids or larger biomolecules such as oligonucleotides, proteins, or DNA. Due to the mildness of this ionization method, non-covalent complexes built on very weak interactions are preserved during the transfer from the liquid to the gas phase. Thus, ESI-MS has proven to be a powerful tool for analyzing organic molecules/DNA complexes [17] and was successfully employed to determine the binding affinity of drugs with DNA [4, 18-20].

One example illustrated in Figure 1 shows the investigation of the binding affinity of the ligand *trans*-**D1** in presence of three different ds DNA sequences, which vary in their AT- and GC-content [20]. GC-content decreases from DNA1 to DNA3. In this study, three signals corresponding to free DNA, 1:1 complexes (DNA/ligand) and 1:2 complexes (DNA/ligand) are compared (highlighted with the red frame). A significant trend is observed. With the decrease of GC-content in the DNA sequences signal of 1:1 and 1:2 complexes drop compared to the increase of the signal of free DNA. This shows that the *trans*-**D1** bis-intercalator favored GC-rich sequences selectivity [20]. This indicates that selective binding interactions between ligands and DNA can be investigated using ESI-MS.

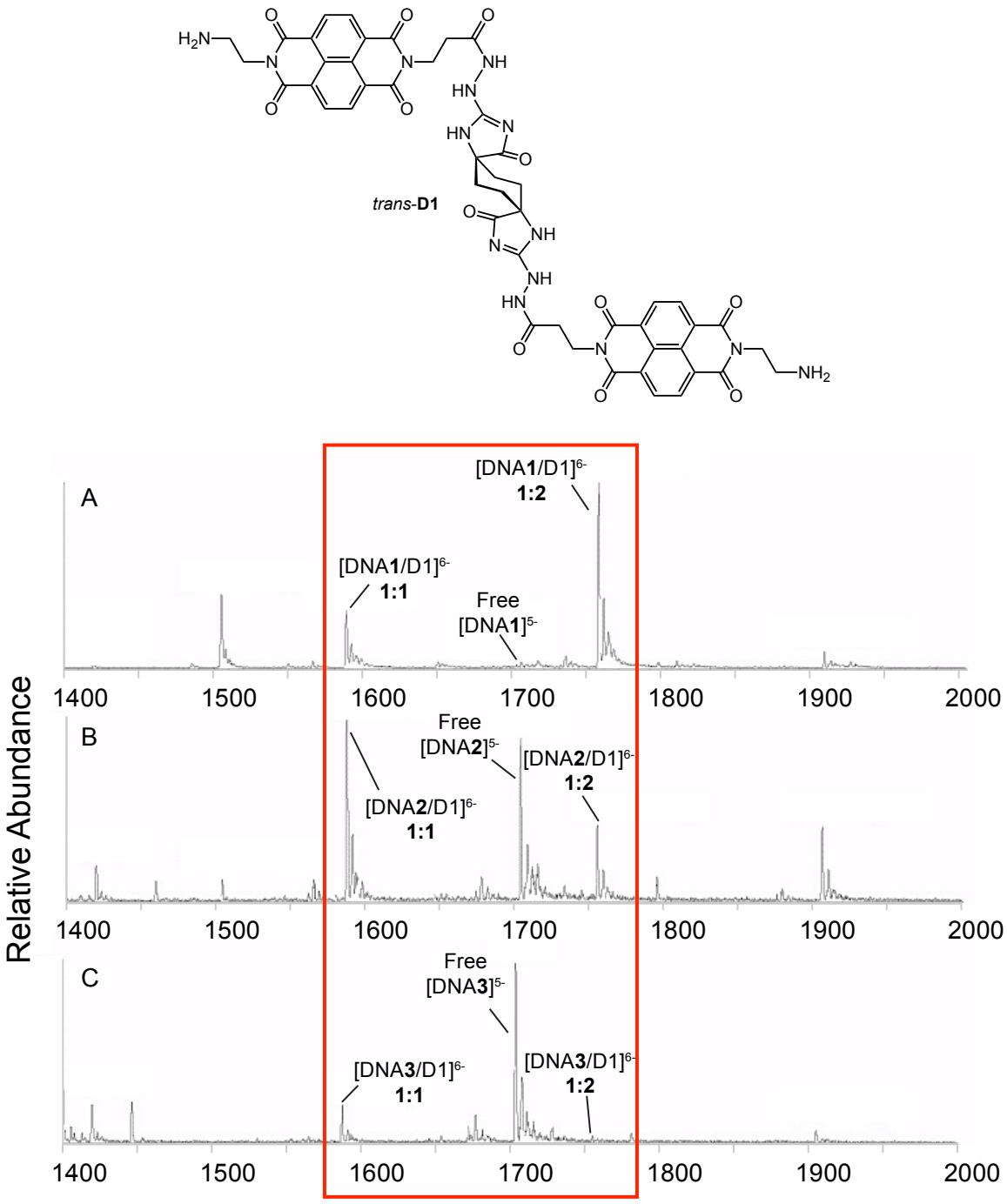

Figure 1: ESI-MS investigation of the binding affinity of the drug *trans*-**D1** with three different double stranded DNA sequences (reproduced after [20]).
A) DNA1, d(GCGGGGATGGGGCG/CGCCCCATCCCCGC)
B) DNA2, d(GCGGGAATTGGGCG/CGCCCAATTCCCGC, and
C) DNA3, d(GCGGAAATTTGGCG/CGCCAAATTTCCGC).

As discussed previously in chapter 1.1.4, the proportionality between analyte concentrations in solution and their response obtained with ESI-MS is generally accepted. However, the correlation is restricted to molecules with similar ionization efficiencies under given conditions. When this criterion is fulfilled, structure-activity relationship (SAR) studies between small organic molecules and DNA oligomers can

be performed with ESI-MS. All the non-covalent studies between DNA and ligands cited above were performed with short DNA sequences (< 20 bases). There are two main advantages of using short oligomers over genomic DNA: First, short DNA sequences have much lower molecular masses (M_R), which simplify the resulting spectra; second, only specific regions and selective complexations with drugs can be investigated (Chapt. 1.1.4). As discussed above, the selectivity can be tested using various AT- or GC-rich sequences. The strength of the binding mode between ligands and double stranded (ds) DNA has been estimated by *Wang et al.* performing collision induced dissociation (CID) experiments [7] or by *Wan et al.* with competitive experiments between two different ligands and one ds DNA sequence [3].

Within this project, an analytical method based on ESI-MS with a high-resolution Bruker maXis QTOF mass spectrometer (ESI-HR-QTOF-MS) was developed for investigating non-covalent complexes between short ds DNA sequences and small organic molecules such as flavonoids, polyamines or polyamine derivatives. The objectives were the following: (1) to implement an ESI-HR-QTOF-MS method using continuous flow electrospray ionization, to characterize and to estimate the binding affinities of these interactions. The choice of the instrument was set because it was the most sensitive MS available in our laboratory, and non-covalent studies have not been performed on this specific instrument so far. If reliable results regarding sensitivity and reproducibility, were obtained for non-covalent interactions with this setup, additional studies could be performed in this field; (2) to compare our own data obtained for the non-covalent complexes between various flavonoids and three ds DNA sequences with the results reported by Wang and coworkers using a less sensitive LCQ ion trap mass spectrometer [7]; (3) to examine if the chosen ds DNA shows any selectivity towards ethidium bromide (EthBr, described as intercalator ligand [18]), and 4',6-diamidino-2-phenylindole (DAPI, described as a minor groove binder [21]); and (4) to apply the method and verify if interactions between polyamine and their derivatives with ds DNA can be investigated.

2.2 Formation of double stranded DNA

For our investigations, the three different synthetic DNA oligomer sequences where chosen with similar molecular mass (M_R) but with different AT and GC contents (ds1, ds2, and ds3, see Table 1). They were selected according to the previous study done

by *Wang et al.* in order to have comparative data [7] and allowing to validate our newly developed ESI-HR-QTOF-MS method. One of the sequences, ds1, contains two adjacent TT bases located at the beginning of the sequence ss1b. For ds3, four adjacent TTAA bases are present in the middle of both single strands. The ds2 sequence contains six adjacent T and A bases in the center of the sequence. All three sequences show various positions and numbers of AT bases in order to compare them according to their selectivity with different ligands.

Name	Sequence	T_m (°C)	M_R (Da)
ds1	d(**AA**CTCCCGGCACAC/GTGTGCCGGGAG**TT**) (ss1a/ss1b)	46/46	8524.5
ds2	d(GGCG**AAATTT**GCGG/CCGC**TTTAAA**CGCC) (ss2a/ss2b)	44/44	8523.5
ds3	d(GGCGG**AATT**CGCGG/CCGCC**TTAA**GCGCC) (ss3a/ss3b)	48/48	8525.5

Table 1: Complementary oligonucleotide sequences used for non-covalent interaction studies

In order to form the expected ds DNA, it is essential to know the melting temperature (T_m) of the ds DNA. T_m corresponds to the temperature at which half of DNA strands are in a double helical and half in a single strand state [22]. This temperature strongly depends on the length of the oligonucleotides. The 14-mer DNA strands used in this study have a calculated T_m of ca. 46°C (according to the manufacturer).

The ss DNA oligomers employed in this study were obtained as 100 µM aqueous solutions and used as they were. To form the ds DNA helices, equal amounts of two complementary ss DNA solutions were mixed in NH_4OAc buffer (500 mM), and heated at 95°C for 15 min, which is clearly above the ds DNA T_m (ca. 46°C). At such temperatures, only free ss and no ds DNA were expected in solution. Finally, the solutions were slowly cooled to room temperature to form the thermodynamically more stable ds DNA. With this procedure ds DNA stock solutions of 10 µM concentration were prepared and further used for complexation experiments and ESI-MS analyses.

2.3 Optimization of the ESI-MS method

DNA complexes investigations by ESI-MS require maximal sensitivity to be successful. To obtain optimal conditions, solvent additives and instrument parameters had to be optimized. The synthetic ds DNA shown in Table 1 were evaluated first using the most appropriate solvent for direct infusion ESI-MS analyses. In a second step, the most important MS parameters were tuned to minimize adduct formation and fragmentation while keeping S/N maximum.

2.3.1 Solvent and buffer optimization

Direct infusion ESI-MS of ds DNA using H_2O/MeOH/$NH_4CH_3CO_2$ as a solvent mixture in the negative ionization mode is known to yield the best response fords DNA [3, 7]. Samples were thus prepared by mixing 10 µL of ds DNA stock solution (containing 500 mM $NH_4CH_3CO_2$) with 90 µL of a 3:1 (v/v) MeOH/50 mM $NH_4CH_3CO_2$ solution. The parameters used to acquire the preliminary data were defined by tuning the instrument with a commercial tune mix, composed of phosphazen derivatives (Bruker).

Typical data obtained for ESI-MS of ds DNA sequences with a M_R of ca. 8'500 Da is illustrated using ds1 (Figure 2). Under such conditions, the spectrum shows an intensive signal of five times negatively charged ds DNA (ds1 $^{5-}$). A signal (with less than 10 % relative intensity) is observed for ds1 $^{4-}$ ions. Single stranded molecules were also detected as ss1a $^{3-}$ and ss1b $^{3-}$ ions, originating from material that did not anneal properly or from decomposition occurring during the ionization process.

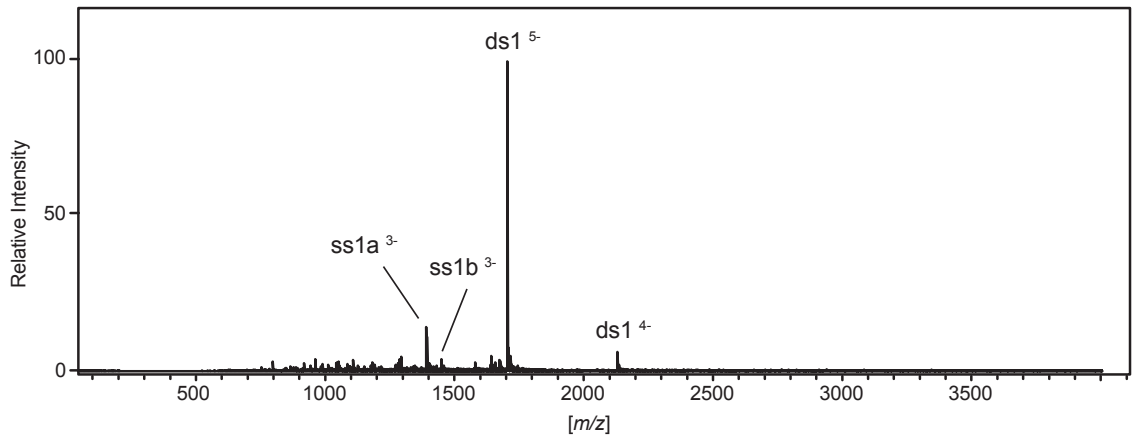

Figure 2: ESI-MS of ds1 measured at 1 µM concentration in MeOH/aqueous $NH_4CH_3CO_2$ 60 mM 3:1

The MS analysis of oligonucleotides is difficult because the polyanionic backbone has a high affinity to ubiquitous cationic contaminants e.g. potassium and sodium ions, resulting from HPLC purification procedures or DNA synthesis (sample handling in glassware). These adducts, lead to signal multiplication at one charge state reducing the sensitivity of ESI-MS analyses and complicating data interpretation (Figure 3 A).

In order to reduce the formation of adducts of alkali metal ions, a solution consisting of a propan-2-ol/(aqueous 2.5 mM piperidine + 2.5 mM imidazole v/v) 1:1 (called spray solution) was added to the sample solution in a 9:1 ratio. The combination of a strong base such as piperidine with a weaker base such as imidazole has been described to reduce cation adduction and therefore improve the signal intensity [23, 24]. *Muddiman et al.* have proposed two different mechanisms for the reduction of Na adducts to the ds DNA backbone. Suppression of alkali adducts possibly results [23]:

(1) both bases form hydrogen bonds with the DNA backbone, thereby displacing Na cations. Upon transfer of ds DNA from solution to the gas phase, neutral loss of piperidine and imidazole occurs leading to protonated DNA molecule.

(2) both bases interact with the Na cations, which leads to have ds DNA free of Na adducts in solution, and can be detected without Na adducts.

The comparative ESI-MS data of ds1 measured without and with addition of spray solution are illustrated in Figure 3. A decrease of adducts formation and an increase of sensitivity can be observed.

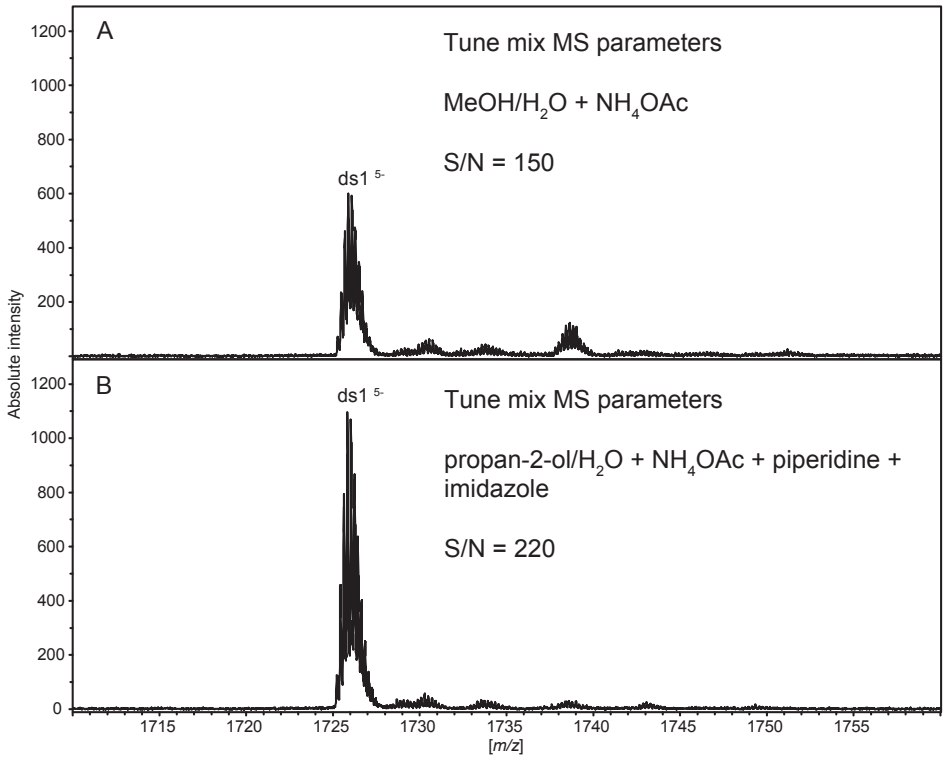

Figure 3: ESI-MS of ds1 prior and after optimization of the sample solvent. The region of the 5– ions is zoomed. 10 µL DNA stock solution + 90 µL spray solution consisting of (A) MeOH/aqueous NH_4OAc 50 mM 3:1 and (B) propan-2-ol/(aqueous 2.5 mM piperidine + 2.5 mM imidazole v/v) 1:1

2.3.2 MS parameters optimization

Optimal MS instrument parameters often depend on the analyte investigated. This is particularly the case when labile molecules or non-covalent interactions have to be measured. Several variables of the maXis QTOF mass spectrometer were therefore optimized such as source conditions (temperature and N_2 flow), transfer time from the ion source to the TOF, collision energy, and ion cooler in front of the TOF. Regarding the collision cell, a minimum energy is already necessary to cool the ions and have optimal ion transmission. In contrast, high collision energies can lead to dissociation of the double strands and even fragmentation of single strands. In our case, ions have passed through the cell with an optimal collision energy of 8-10 eV giving us the best ion transmission with maximal sensitivity and with minimal fragmentation reactions. The task of this device is to focuse the internal energy of ions and to define the size of the ion packets before they enter the TOF, in order to increase the sensititviy. However, if too many ions are collected, they start to collide, resulting in fragmentation and loss of resolution.

Figure 4 illustrates the increase of sensitivity of ds1 DNA by a factor of 1.7 obtained after instrument parameter optimization compared to the method based on the Bruker calibration tune mix.

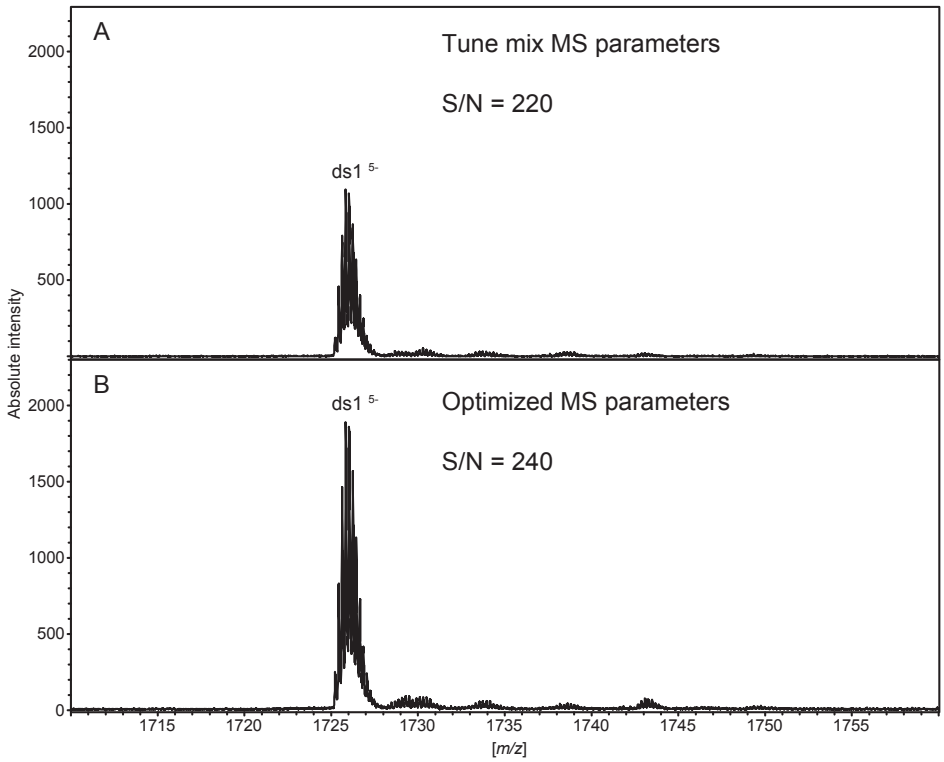

Figure 4: ESI-MS of ds1 (10 µL stock solution + 90 µL of a propan-2-ol/(aqueous 2.5 mM piperidine + 2.5 mM imidazole v/v) 1:1 acquired before (A) and after (B) tuning of the mass analyzer. The region of the 5– ions is zoomed.

2.3.3 Summary

The sample solutions and the instrument parameter methods were optimized in order to obtain the highest sensititvity for the signal of ds DNA five times negatively charged (ds DNA^{5-}), with a minimum fragmentation and adduct formation. With this set of optimized parameters, the efforts will now be put on the investigation of the non-covalent interactions between ds1-3 and our ligand library.

2.4 Investigation of non-covalent interactions

The primary goal was to check the suitability of maXis QTOF mass spectrometer to investigate non-covalent interactions between ds DNA and various classes of ligands. Two classes of natural compounds, polyamines [8-12] and glycosylated flavonoids and their aglycone derivatives [7], were investigated because they are known to bind

DNA and RNA. Hydroxycinnamic acid derivatives of polyamines, which should behave like polyamines were also studied.

Finally, two DNA stains, ethidium bromide (EthBr) and 4',6-diamidino-2-phenylindole (DAPI), widely used for fluorescence detection, were tested. They should give us an indication of the selectivity of the sequences, since EthBr principally interacts with DNA by intercalation [18] and DAPI by minor groove binding [21].

The study of the aforementioned non-covalent interactions was performed with the same ESI-MS conditions as the ones optimized for free ds DNA (see Chap. 2.2.2). Solutions of ds1-3 DNA (10 µL, 10 µM) and ligand (10 µL, 40 µM) were mixed and diluted in a 1 to 4 ligand excess with 80 µL of optimized solution containing 2.5 mM of piperidine and imidazole additives in order to improve the S/N and suppress the formation of adducts. All samples were prepared and measured consecutively with continuous flow ESI-MS in the negative, full scan mode.

The relative DNA binding affinities were estimated by means of MS signal intensities reflecting the relative concentrations of the several complexes present in solution. Ion species in solution were determined relative to the most abundant 5– ions and the fraction of bound DNA (fb_{DNA}) was calculated in mol %[1] using the following equation:

$$(1) \quad \textit{Fraction of bound DNA}\,(\textit{mol}\%) = \frac{I_{(1:1)} + I_{(1:2)} + I_{(1:3)} \cdots}{I_{(DNA)} + I_{(1:1)} + I_{(1:2)} + I_{(1:3)} \cdots} X 100$$

I represents the relative intensity of free DNA or DNA-ligand complexes at a specific charge state.

[1] MS is a concentration sensitive detector and the ratio of signal intensities can therefore be correlated to the mol ratio

2.4.1 Interactions of DNA with flavonoids

Non-covalent interactions between flavonoids and duplex or triplex DNA have been investigated in detail using ESI-MS [3, 7, 25]. Flavonoids formed preferentially intercalation complexes due to their interactions with GC-rich regions of DNA and occurring via strong π-π stacking. Comparative complexation studies of different classes of flavonoids with ds DNA further revealed that the position of the OH-groups on their different ring systems are influencing the binding properties and that glycoside substitution enhanced complex formation [7].

The goal of this study was principally to confirm that complex formation between ds DNA and a broad range of flavonoid classes (flavone, isoflavone, flavanone, and flavanol) can be investigated with the maXis QTOF mass spectrometer. The resulting data should then be compared to reported ones obtained with a thermo LCQ ion trap [7]. Direct data comparison of the fraction of bound DNA obtained from different MS platforms is essential, as it can lead to different ESI spectra due to differences in ionization energy, pressure, temperature and acceleration voltage. Nevertheless, the relative complexation affinity of the flavonoid ligands with the three ds DNA should remain the same.

Six ligands were measured in presence of ds1, ds2 and ds3 in order to evaluate the ESI-MS method developed on the maXis QTOF instrument (see Chapt 2.3). The ds DNA sequences were chosen in analogy to those used by *Wang et al.* [7]. The ligands were selected to be able to compare mono-glycosilated flavone (vitexin) with the corresponding aglycone (apigenin) as well as with glucose, to obtain reference values for fb_{DNA} and to compare them with literature. In addition, flavonol, isoflavone, flavanone *C*- and *O*-glycosides, glycoside and rhamnosyl derivatives were also tested. The complete ESI-MS complexation data together with the one found in the literature is summarized in Table 2. Only ds1 from *Wang et al.* is mentioned in Table 2 because the values for ds 2 and ds 3 are reported to follow the same trend [7].

		Fraction of bound DNA (mol%)			
		ds1 $^{5-}$	**ds2 $^{5-}$**	**ds3 $^{5-}$**	**ds1 $^{5-}$ Literature [7]**
apigenin (flavone aglycone) (ap)	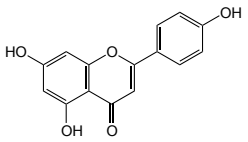	17	13	20	25
glucose (glu)	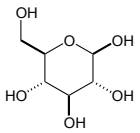	0	0	0	–
vitexin (flavone-8-*C*-glu) (vi)	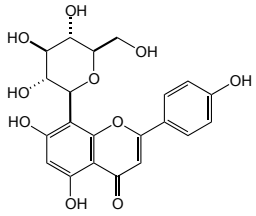	28	26	29	74
genistin (isoflavone-7-*O*-glu)	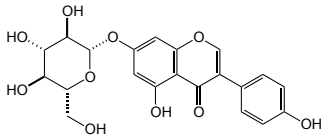	18	13	15	60
liquiritin (flavanone-4'-*O*-glu)	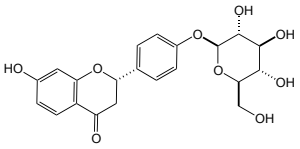	9	6	7	57
quercitrin (flavonol-3-*O*-rha)	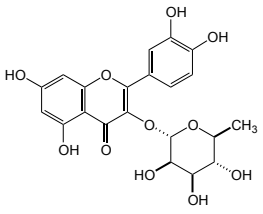	8	6	6	–

Table 2: Comparison between the fb_{DNA} (mol%) measured with maXis ESI-QTOF-MS and published data (LCQ ion trap) obtained for solutions of ds1, ds2, and ds3 in presence of a four-fold ligand excess

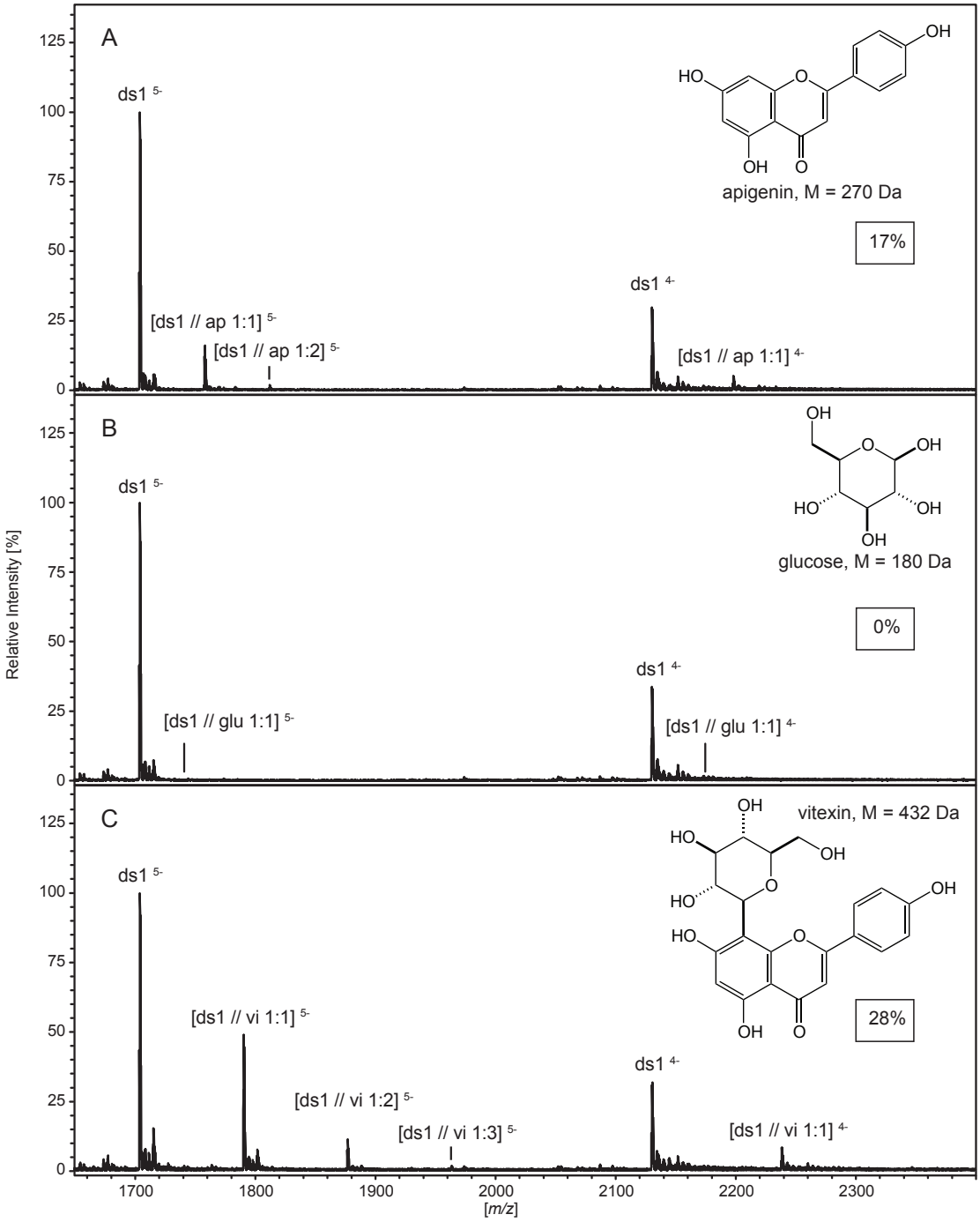

Figure 5: ESI-MS spectra of ds1 d(**AA**CTCCCGGCACAC/GTGTGCCGGGAG**TT**) mixed with (A) apigenin, (B) glucose and (C) vitexin in a 1:4 ratio. Calculated fb_{DNA} (in mol%) is framed.

At a first glance it appears that all values of fb_{DNA} obtained are significantly lower than those published [7]. Since the samples had an identical ligand to ds DNA ratio of 1 to 4, the lower signal intensities corresponding to the complexes might be due to the different instrumentation used or to the different concentrations of sample solutions (samples measured with the maXis QTOF were diluted 20x in order to avoid saturation of the detector).

Comparison of the values of fb_{DNA} calculated from the maXis QTOF data lead to a more differentiated interpretation. In line with published results, no differences of binding affinities were observed within the different DNA strands ds1, ds2 or ds3. The higher values observed for a glycosylated flavone (vitexin) compared to the corresponding aglycone (apigenin) has been reproduced and glucose was not interacting at all (see Figure 5). This supports the fact that flavonoids and not glucose moieties are essential for the interactions with ds DNA. However, a differentiation of flavonoids of various classes using the developed method seemed to be risky, although in both cases, maXis and published data, vitexin presented the highest binding affinity with ds DNAs. In particular the mono-glycosylated liquiritin and genistin lead to values of fb_{DNA} that were similar or much lower than the ones obtained for apigenin (9, 18 and 17 mol%, respectively). This is in disagreement with the results of *Wang et al.* where aglycone flavonoid showed a tendency to lower binding affinities than the glycosylated one.

In conclusion, the method developed in Chapter 2.2 allowed investigations of the binding affinities between ds DNA and flavonoid derivatives. The fact is that the absolute values of fb_{DNA} obtained were lower than in reference data. Although the glycosylated flavone vitexin displayed the highest affinities to ds1, no significant selectivities of ligands to any ds DNA sequences or of ds DNA to ligands were observed.

2.4.2 Interaction of ds DNA with fluorescent tags

According to the literature, EthBr is known to interact with ds DNA as an intercalating tag, whereby this type of molecules are non-specific binders, with a slight affinity for GC-rich regions [18]. On the other hand, DAPI is a very strong minor groove binder, with a preference for sequences containing three or more consecutive AT base pairs [21].

The synthetic ds DNA sequences chosen (see chapter 2.2.1, Table 1) contain various amounts of AT-rich domains found in the middle (ds2 four AT base pairs, ds3 six AT base pairs) or at the end of the oligonucleotide chain (ds1 two AT base pairs). With this choice of sequences, it should be possible to verify: (1) if signals corresponding to the complexes can be detected with ESI-MS; (2) if the number of AT base pairs has an influence on the constant of complex formation; and (3) if the

position of the AT base pairs has an influence on the ligand selectivity. The ESI mass spectra of the complexes were measured with the method optimized for free DNA.

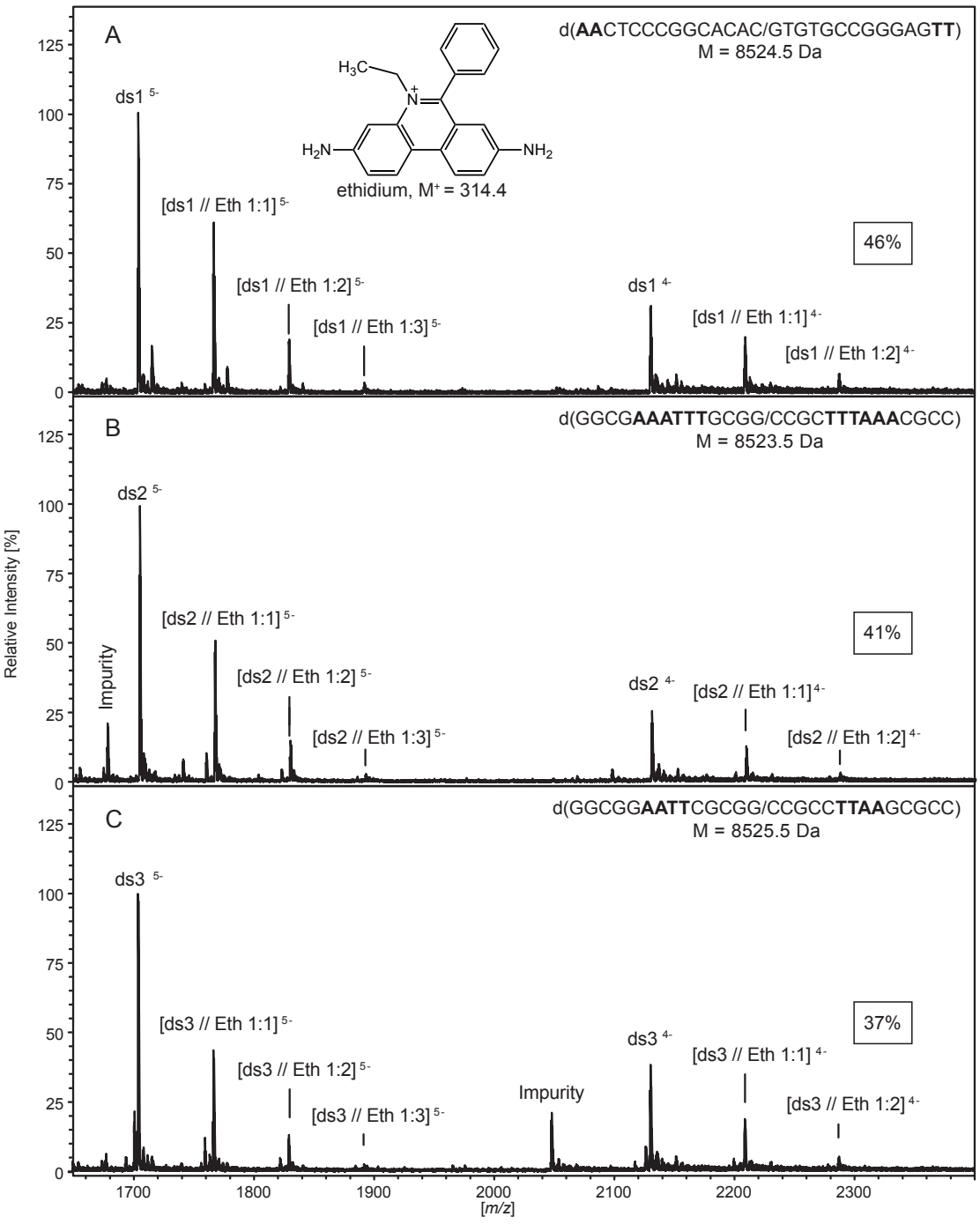

Figure 6. ESI-MS spectra of ethidium (Eth) complexation with ds1, ds2, and ds3 DNA in a 1 to 4 ratio. Calculated fb_{DNA} (in mol%) is framed

Analogous to free ds DNA, the ds DNA // Eth complexes formed preferably ions with a charge state of 5– under these ESI-MS conditions. The spectra show relatively high signal intensities corresponding to free ds DNA (see Figure 6). Furthermore, Eth seemed to interact a bit stronger with ds1 (46 %), the DNA with the highest number

of GC base pairs in a row (six compared to four and five for ds2 and ds3 respectively). These observations provide some evidence about the slight preference of intercalators for GC-rich sequences.

The ESI-MS analysis of the solution containing DAPI mixed with the ds DNA, compared to Eth, led to big differences of fraction of bound DNA (see Figure 7).

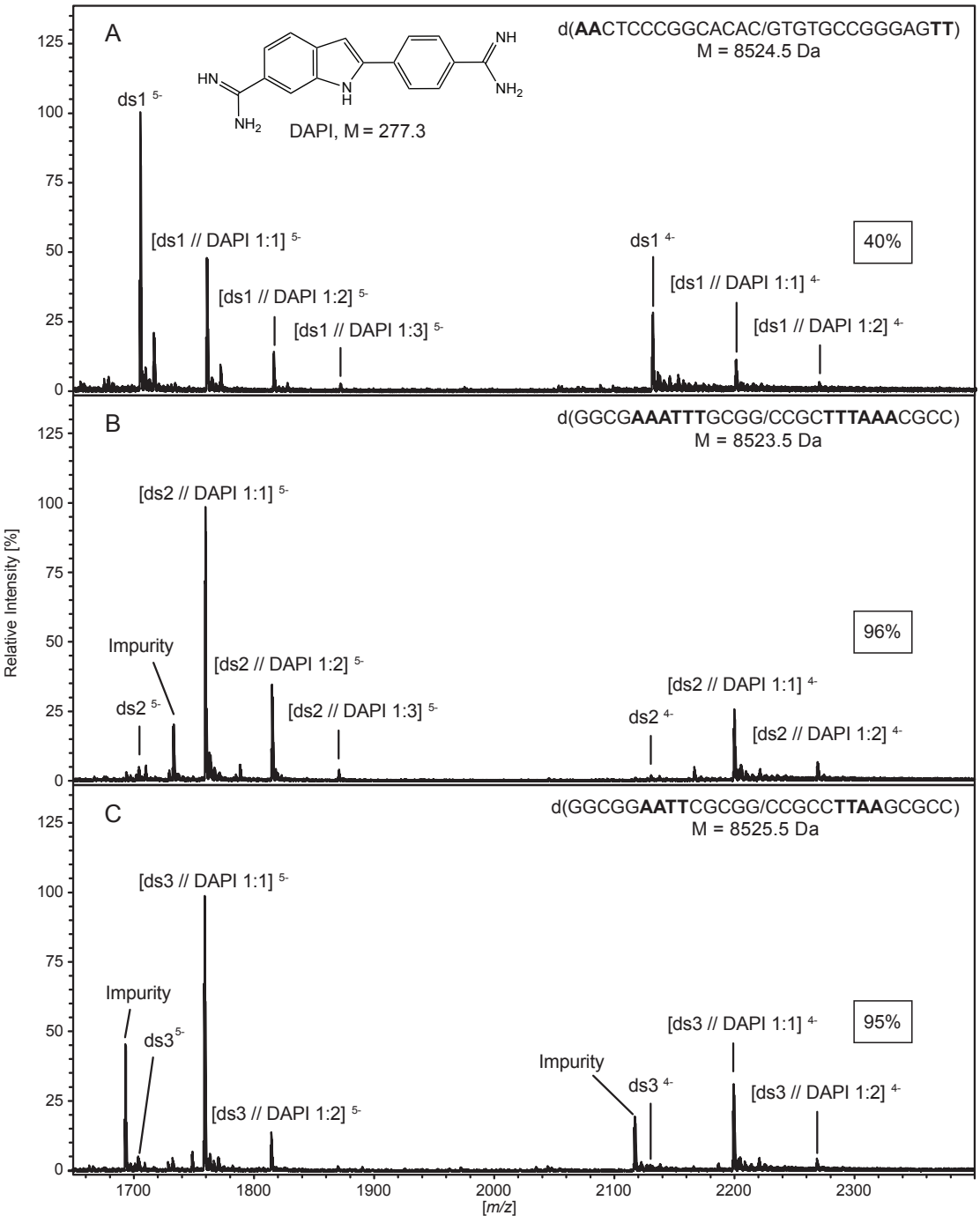

Figure 7. ESI-MS spectra of DAPI complexation with ds1, ds2, and ds3 DNA in a 1 to 4 ratio. Calculated fb_{DNA} (in mol%) is framed.

Again, the complexes with a 5– charged state are preferably formed and their response will be used for the determinations of the fraction of bound DNA.

The affinity of DAPI to ds1 DNA was obtained in the range already observed for Eth complexes (fb_{DNA} = 40%). However, this value rose up to 96 and 95 % for ds2 and ds3 sequences, respectively. Stronger interactions of the minor groove binder DAPI with the AATT-containing site are completely in agreement with the published DNA association binding constant (*K*) obtained by fluorescence spectroscopy [26]. In this work, the binding of DAPI with different $(A/T)_4$ sequences in a stable 28-mer hairpin was studied, showing much stronger affinities for the AATT site (association constant K_a = 5.5 x 10^8 M^{-1}) compared to e.g. TAAT or TTAA (ca. 2 x 10^7 M^{-1}). In our case, both ds2 and ds3 but not ds1 DNA contain AATT sequences.

In conclusion, the data obtained for Eth and DAPI confirm that ESI-MS with a maXis QTOF can be used as an investigation method for the analysis of non-covalent interactions between ds DNA and intercalators and minor groove binders.

In this case, ESI-MS signals of DAPI complexes with ds 2 and 3 were very abundant (> 95 mol % of fb_{DNA}), in contrast to residual signals observed in spectra of Eth complexes, corresponding to free oligonucleotides. This demonstrates that the developed method is able to detect the presence of a specific binding site as AATT in an oligomer sequence.

ESI-MS measurement of weaker intercalating interactions lead to a low part of bound DNA (< 50 mol %) and further experiments are required to validate the method regarding the recognition of GC-rich sequences and the mechanism of interaction.

2.4.3 Interactions of ds DNA with polyamines and derivatives

Polyamines have been described as major and minor groove binders with a preference for AT-rich regions of DNA [8, 21]. Furthermore, cinnamic acid derivatives of polyamines have been isolated in high amounts from plant material, e.g. pollen of *Aphelandra sp.* [27] or *Alnus glutinosa, Betula verruscosa* and *Pterocarya fraxinifolia* [28]. Non-covalent interactions of such derivatives have, to our knowledge, never been investigated previously. The objective was therefore to see if the ESI-MS method developed (see Chapt. 2.3) is appropriate to study interactions with other secondary metabolites, the polyamines, and to see if a substitution with cinnamic acid has an influence on their binding affinities towards ds DNA. In order to assess

the complexation properties, a library of available linear polyamines (spermine and spermidine), cinnamate derivatives ((*E*)-ferulic and *p*-coumaric acid), and cinnamate polyamine conjugates were selected and analyzed in presence of the synthetic ds1, ds2 and ds3 used previously.

		Fraction of bound DNA (mol%)		
		ds1 $^{5-}$	**ds2** $^{5-}$	**ds3** $^{5-}$
spermidine (spd)	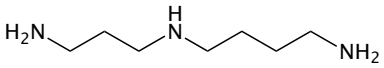	2.3	2.1	2.2
spermine (spm)	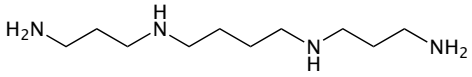	1.7	1.7	1.2
(*E*)-ferulic acid	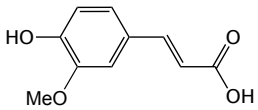	0	0	0
p-coumaric acid (cou)	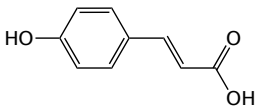	0	0	0
N-(*E*-coumaroyl) putrescine	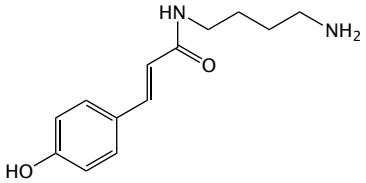	2.6	2.5	2.8
1,14-bis(*E*-cinnamoyl) spermine (1,14-cin spm)	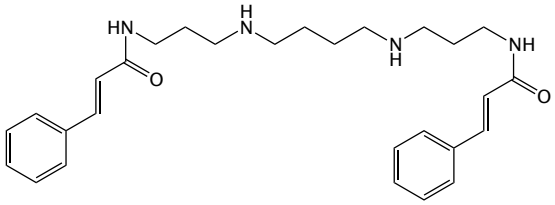	4.2	3.3	3.6
5,10-bis(*E*-cinnamoyl) spermine (5,10-cin spm)	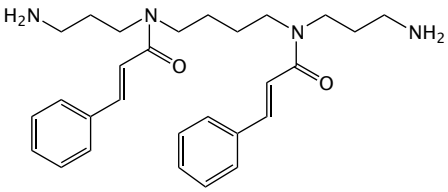	4.1	4.4	4.4

Table 3: fb_{DNA} (mol%) obtained from the ESI-MS analyses of ds1, ds2, and ds3 performed in presence of a four-fold excess of polyamines, cinnamic acids and polyamine derivatives

Compared to flavonoids, very low binding affinities were measured between spermine and spermidine with the ds DNA sequences (between 1.2 to 2.3 mol%) eventhough strong interactions were expected considering those observed by X-ray

diffraction across the binding groove of the B-DNA duplex $[d(CGCGAATTCGCG)]_2$ [26] (see Table 3 and Figure 8).

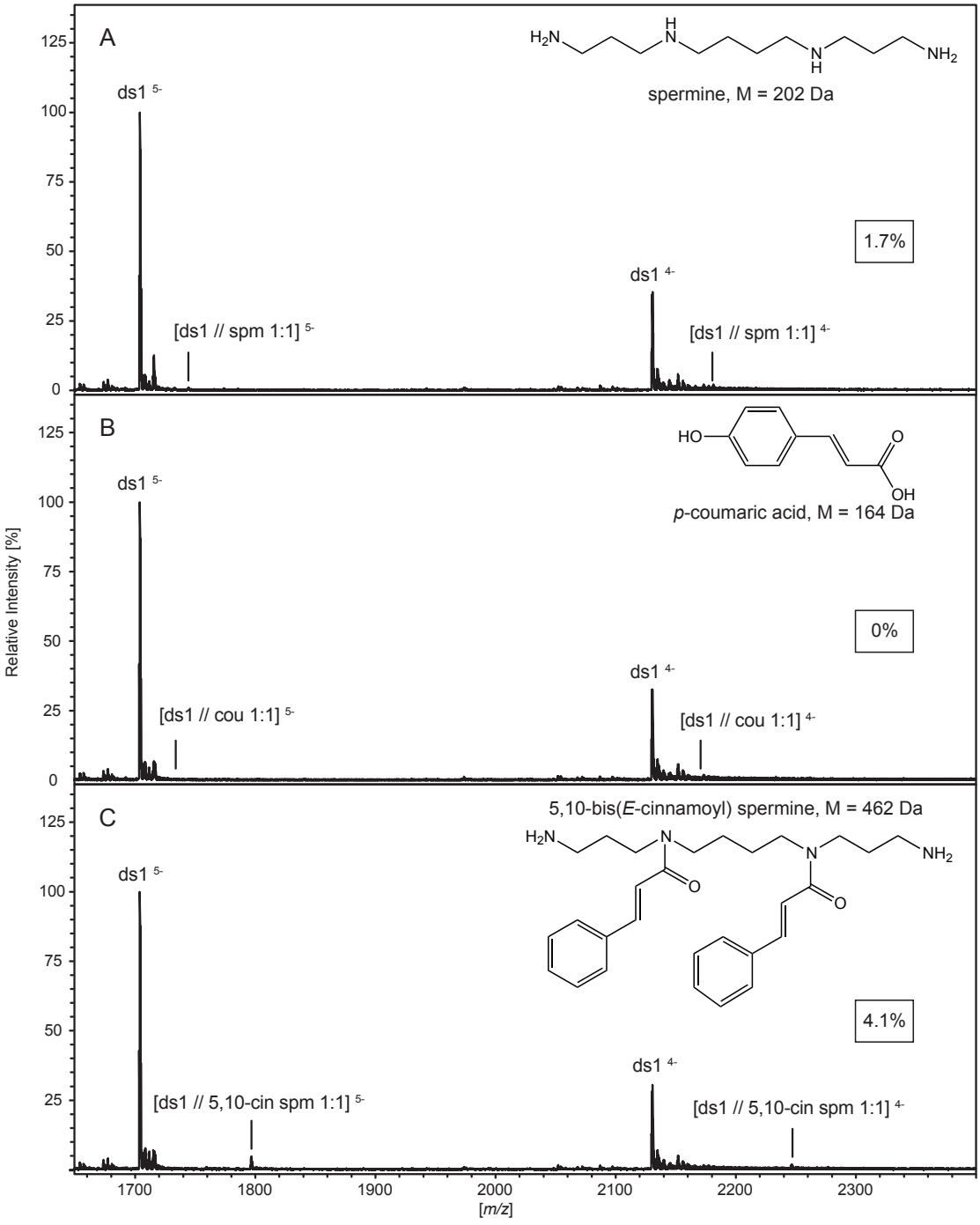

Figure 8: ESI-MS spectra of ds1 d(**AA**CTCCCGGCACAC/GTGTGCCGGGAG**TT**) mixed with (A) spermine, (B) *p*-coumaric acid and (C) 5,10-bis(*E*-cinnamoyl) spermine in a 1:4 ratio. Calculated fb_{DNA} (in mol%) is framed.

(*E*)-ferulic and *p*-coumaric acid did not show any affinity to DNA. The polyamine derivatives showed a two times higher fb_{DNA}, compared to the free polyamines. As introduced earlier in the chapter, it may be possible that the observed ESI-MS signals,

representing complexation of ds DNA with polyamine and polyamine derivatives, arise from electrostatic interactions between the polyamine backbone and the negatively charged phosphate groups of DNA. SAR studies showed that the most stable complexes did not only result in simple electrostatic spanning of the anionic DNA backbone by protonated spermine [21].

Poor information concerning the relative interactions of polyamines, hydroxycinnamic acid derivatives of polyamines and hydroxycinnamic acids with ds DNA were gained in this study due to low binding affinities observed with the ESI-MS method developed. Nevertheless, no interaction of hydroxycinnamic acids with ds DNA were observed, and higher affinities of acyl-polyamines compared to free polyamines spermidine and spermine were detected (1,2 - 2,3 compared to 2.4 - 4.4 mol %).

2.5 Conclusion and outlook

The aim of this project was to develop a sensitive method based on direct-infusion ESI high-resolution QTOF-MS in order to investigate non-covalent interactions between synthetic DNA sequences containing 14 base pairs and small organic molecules. The synthetic ds DNA ds1, ds2, and ds3 were used for optimizing sample solution and instrument parameters, and for the complexation studies.

The ESI-MS analyses were performed in the negative ionization mode to get a minimal formation of adducts. The sample solvent appeared to be an essential parameter and best results were obtained with addition of imidazole and piperidine to the DNA dissolved in a mixture of propan-2-ol/aqueous NH_4OAc. Some specific MS parameters were also critical to obtain optimal S/N, in particular collision energy and ion cooler.

Non-covalent interactions between ds1, ds2, and ds3 and a library of glycosylated and aglycone flavonoid derivatives (apigenin, genistin, liquiritin and vitexin) were investigated using the optimized ESI-MS conditions and the results were compared to published data. It appeared that the same compound, vitexin, showed the highest binding affinities to DNA (30 mol %). But compared to literature data, the values of fractions of bounded DNA obtained were all lower and their relative order was sometimes different. This could be due to harder electrospray ionization conditions (compared to literature, a different instrument and ion source have been used) or lower solution concentrations of ligand and ds DNA.

In a second part, DAPI and EthBr were chosen to assess the method with regard to the selectivity of the interactions between ligands and ds DNA containing different number of AT base pairs. These ligands are known as minor grove binders and intercalators, respectively. Eth exhibited almost equal affinities of ca. 50 mol% of fraction of bound DNA to all sequences. However, DAPI was much more selective and displayed high binding affinities of approximately 100 mol% to ds2 and ds3. The ds DNA ds2 and ds3 contain AAATTT and AATT sites, respectively. These sites are known to form preferentially minor grove bindings. It appears therefore that the method developed here could be used to study interaction mechanisms as long as the binding affinities are high enough. This was not the case with the interactions between flavonoids and ds DNA. In this case, the method was not sensitive enough to reproduce literature data.

Finally, the non-covalent interactions of polyamine and their derivatives with ds DNA were investigated with the same optimized ESI-MS method. Although successful NMR and XRay investigations have been published, it appeared that binding affinities of polyamine derivatives were clearly weaker (< 5 mol%) than those of flavonoid derivatives and the DNA fluorescent tags DAPI and Eth (data summarized on Figure 9). Nevertheless, it seemed that the substitution of polyamines with cinnamic acid derivatives increased the binding affinities toward ds DNA.

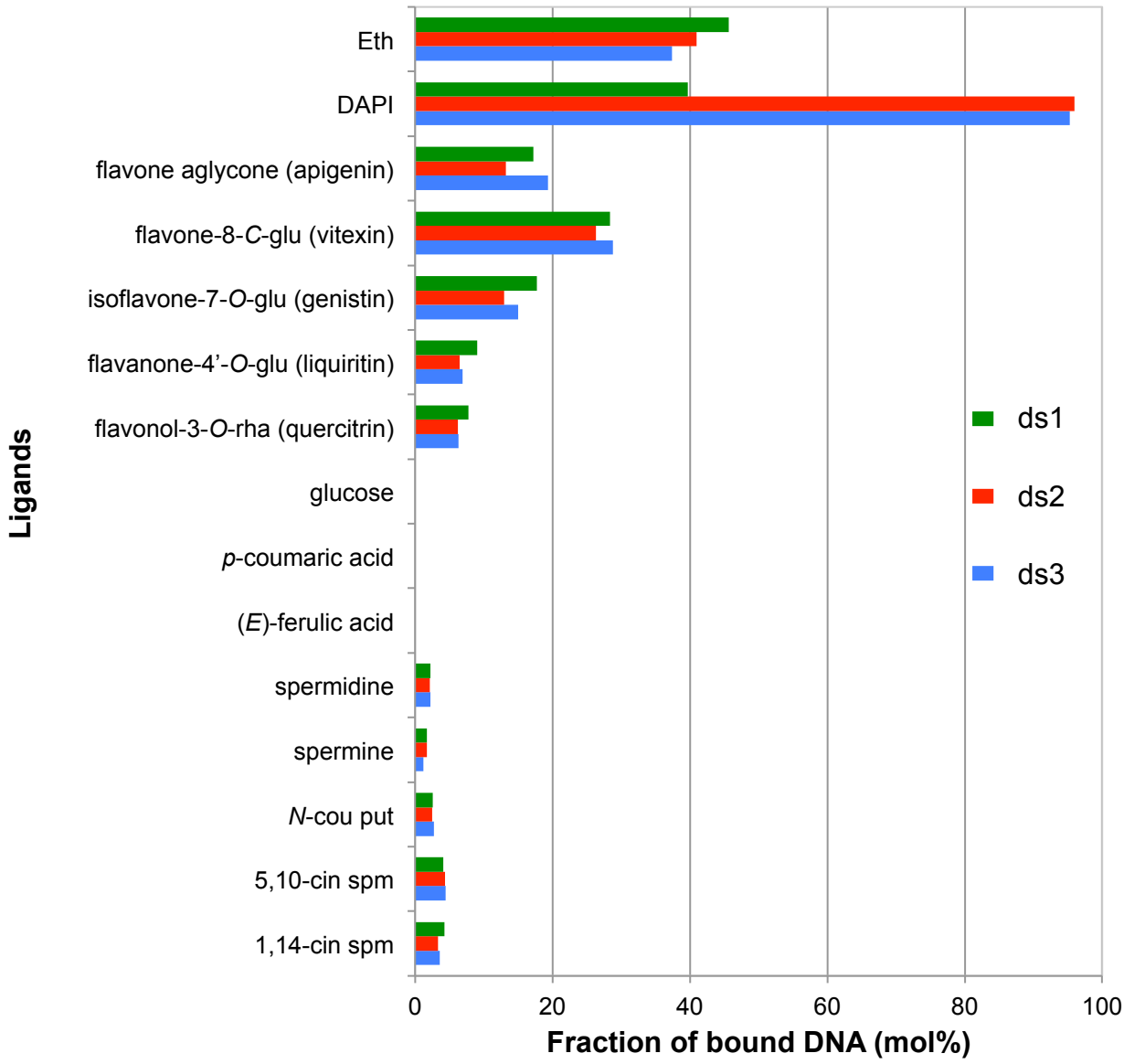

Figure 9: Overview of DNA-binding affinites of the investigated ligands with ds1, ds2 and ds3

In the future, some competitive experiments with two ligands and one ds DNA sequence should be performed in order to correlate the relative ion abundance with the binding affinities [3]. This would be also essential for correlating the relative values of fractions of bounded DNA by the different ligands under investigation. Furthermore, a larger variety of flavonoid and polyamine derivatives should be compared in order to confirm the first observations and to assess the method as a tool for investigating the binding modes of DNA with small organic molecules.

2.4. Experimental part

2.4.1 Chemicals and ligands

Propan-2-ol, ammonium acetate ($NH_4CH_3CO_2$), triethylamine (Et_3N) (all in LC-MS Ultra Chromasolv® quality), piperidine (puriss), imidazole (puriss), and glacial acetic acid (puriss) were obtained from Sigma-Aldrich (Buchs, Switzerland). The 14mer complementary single strand DNA sequences used to form ds1 (ss1a and ss1b), ds2 (ss2a and ss2b), and ds3 (ss3a and ss3b) were purchased from Microsynth (100 µM, HPLC purified, Balgach, Switzerland). LC-MS grade H_2O (< 2 ppb) was obtained by purification of deionized H_2O with a MilliQ gradient apparatus equipped with a BioPack® ultrafiltration module (Millipore, Milford, MA, USA).

Spermine tetrahydrochloride, spermidine trihydrochloride, (*E*)-ferulic acid, *p*-coumaric acid, glucose, 4',6-diamidino-2-phenylindole (DAPI), ethidium bromide (EthBr) and vitexin were purchased from Sigma-Aldrich, quercitrin and apigenin from Extrasynthese (Lyon Nord, France), and liquiritin and genistin from Chengdu Biopurify Phytochemicals Ltd. (Chengdu, China) in the best qualities available. *N*-(*E*-Coumaroyl) putrescine, 1,14- and 5,10-bis(*E*-cinnamoyl) spermine were synthesized in our laboratories [29].

2.4.2 Instrumentation

On-flow ESI-MS

ESI-MS data were obtained from a maXis UHR-QTOF mass spectrometer (Bruker Daltonik GmbH, Bremen, Germany) equipped with an ESI source. Acquisitions were performed under continuous-flow injection conditions at a flow rate of 6.7 µL/min. ESI parameters: end plate offset (–500 V), capillary (4500 V), nebulizer gas (N_2, 0.4 bar), dry gas (N_2, 4 L/min), dry temperature (160 °C). MS parameters: funnel RF (3200 Vpp), ISCID energy (0 eV), multipole RF (350 Vpp), ion energy (4 eV), low mass (350 *m/z*), collision energy (22 eV), collision RF (1000 Vpp), ion cooler RF (600 Vpp), transfer time (125 µs), and pre-puls storage (25 µs). Mass spectra were acquired as soon as the MS signal intensities were stable during 1 min in the negative mode at a resolution of 20'000 (FWHM), in the full scan mode, in the mass range *m/z* 50 – 3500 and with a scan rate of 2 Hz.

2.5.3 Experimental description

Formation of ds DNA and complex solutions

For the study of non-covalent interactions between ligands and ds DNA, three different solutions are necessary: the ds DNA, ligand and the spray.

The ds DNA stock solution: stock solutions of double strand oligonucleotides were purchased at a concentration of 100 µM in MilliQ water. Annealing solution was obtained by mixing 10 µL of each complementary single strand solution (ssa and ssb) with 80 µL of 500 mM ammonium acetate solution. The annealing solution was heated to 95°C for 15 minutes in a Techne® Dri-Block® heater (Model DB-3D, Staffordshire, UK). The block heater was then switched off and slowly cooled to room temperature overnight. The final concentration of the ds DNA stock solution was 10 µM. After one weak, the stock solutions were freshly prepared.

The ligand solution: All ligands were prepared at a concentration of 40 µM. Flavonoids and hydroxycinnamic acids were diluted in MeOH and the polyamines and their derivatives in H_2O.

The spray solution: One solution of 2.5 mM piperidine and one solution of 2.5 mM imidazole were prepared. They were mixed together in a 1:1 ratio with a final 1.25 mM concentration of piperidine and imidazole. This 1:1 solution is then mixed volume to volume *(v/v)* with propan-2-ol to have the final spray solution with a 0.625 mM concentration of piperidine and imidazole.

For ds DNA signal optimization 10 µL of the resulting double strand DNA stock solution (10 µM) was diluted to 100 µL with the spray solution prior mass spectrometric analyses.

For complexation studies, 10 µL of ds1, ds2 or ds3 (10 µM) with 10 µL ligand (40 µM) and diluted with 80 µL of spray solution were prepared prior to mass spectrometric analysis.

2.5 Bibliography

[1] Geall, A. J., Al-Hadithi, D., Blagbrough, I. S., *Bioconjugate Chem.* **2002**, *13*, 481.
[2] Hemminki, K., Koskinen, M., Rajaniemi, H., Zhao, C., *Regul. Toxicol. Pharmacol.* **2000**, *32*, 264.
[3] Wan, K. X., Shibue, T., Gross, M. L., *J. Am. Chem. Soc.* **2000**, *122*, 300.
[4] Tse, W. C., Boger, D. L., *Chem. Biol.* **2004**, *11*, 1607.
[5] Quintana, J. R., Lipanov, A. A., Dickerson, R. E., *Biochemistry* **1991**, *30*, 10294.
[6] Wade, W. S., Mrksich, M., Dervan, P. B., *J. Am. Chem. Soc.* **1992**, *114*, 8783.
[7] Wang, Z., Cui, M., Song, F., Lu, L., Liu, Z., Liu, S., *J. Am. Soc. Mass Spectrom.* **2008**, *19*, 914.
[8] Esposito, D., Del Vecchio, P., Barone, G., *J. Am. Chem. Soc.* **1997**, *119*, 2606.
[9] Kim, M. S., Diamond, S. L., *Bioorg. Med. Chem. Lett.* **2006**, *16*, 5572.
[10] van Dam, L., Nordenskiöld, L., *Biopolymers* **1999**, *49*, 41.
[11] Frydman, B., Westler, W. M., Samejima, K., *J. Org. Chem.* **1996**, *61*, 2588.
[12] Frydman, L., Rossomando, P. C., Frydman, V., Fernandez, C., Frydman, B., Samejima, K., *Proc. Natl. Acad. Sci. USA* **1992**, *89*, 9186.
[13] Frydman, B., Porter, C. W., Maxuitenko, Y., Sarkar, A., Bhattacharya, S., Valasinas, A., Reddy, V. K., Kisiel, N., Marton, L. J., Basu, H. S., *Cancer Chemother. Pharmacol.* **2003**, *51*, 488.
[14] Ma, C.-m., Nakamura, N., Hattori, M., *Chem. Pharm. Bull.* **2001**, *49*, 915.
[15] Pelton, J. G., Wemmer, D. E., *Biochemistry* **1988**, *27*, 8088.
[16] Liquori, A. M., Costantino, L., Crescenzi, V., Elia, V., Giglo, E., Puliti, R., De Santis Savino, M., Vitagliano, V., *J. Mol. Biol.* **1967**, *24*, 113.
[17] Gale, D. C., Smith, R. D., *J. Am. Soc. Mass Spectrom.* **1995**, *6*, 1154.
[18] Gabelica, V., De Pauw, E., Rosu, F., *J. Mass Spectrom.* **1999**, *34*, 1328.
[19] Griffey, R. H., Sannes-Lowery, K. A., Drader, J. J., Mohan, V., Swayze, E. E., Hofstalder, S. A., *J. Am. Chem. Soc.* **2000**, *122*, 9933.
[20] Mazzitelli, C. L., Chu, Y., Reczek, J. J., Iverson, B. L., Brodbelt, J. S., *J. Am. Soc. Mass Spectrom.* **2007**, *18*, 311.
[21] Strekowski, L., Wilson, B., *Mutat. Res.* **2007**, *623*, 3.
[22] SantaLucia, J. J., *Proc. Natl. Acad. Sci. USA* **1998**, *95*, 1460.
[23] Muddiman, D. C., Cheng, X., Udseth, H. R., *J. Am. Soc. Mass Spectrom.* **1996**, *7*, 697.
[24] Greig, M. J., Griffey, R. H., *Rapid Commun. Mass Spectrom.* **1995**, *9*, 97.
[25] Wan, C., Cui, M., Song, F., Liu, Z., Liu, S., *Int. J. Mass Spectrom.* **2009**, *283*, 48.
[26] Breusegem, S. Y., Clegg, R. M., Loontiens, F. G., *J. Mol. Biol.* **2002**, *312*, 1049.
[27] Werner, C., Hu, W., Lorenzi-Riatsch, A., Hesse, M., *Phytochemistry* **1995**, *40*, 461.
[28] Meurer, B., Wray, V., Wiermann, R., Strack, D., *Phytochemistry* **1988**, *27*, 839.
[29] Jengtens, C., Hofmann, R., Guggisberg, A., Bienz, S., Hesse, M., *Helv. Chim. Acta* **1997**, *80*, 966.

CHAPTER 3

THE QUANTIFICATION OF PHOTOPROTECTION

3.1 Introduction

The protection of DNA from damage induced by UV-radiation is of critical importance to all organisms that are exposed to sunlight. Evolution due to effects of UVB radiation on aquatic and terrestrial plant ecosystems concerns different aspects like comparison of growth and physiological responses to various levels of solar UVB or induction (initiation) of UV-absorbing compounds, their chemical characterization, and their localization. A comparative assessment of the physiological function of UV-absorbing compounds as protective UV-screens for plants has been described [1].

In DNA, UV-induced damage occurs mainly by photodimerization of two adjacent pyrimidines, mostly thymine bases, in the same polynucleotide chain. These lesions are named cyclobutane pyrimidines (*c-s* T<>T and *t-s* T<>T) and pyrimidine (6-4) pyrimidone (6-4 TT) dimers, whereby the *c-s* T<>T is the major photoproduct formed. The 6-4 TT photoproduct can further photoisomerize into Dewar TT valence isomer under UVB irradiation (Figure 1).

DNA mutations induced by UV-light have been associated with skin cancer [2, 3]. Different endogen or exogen protection mechanisms exist for human beings to protect from damage by UV-irradiation, such as gene *p53* with a function of repairing damaged DNA, or sunscreen application.

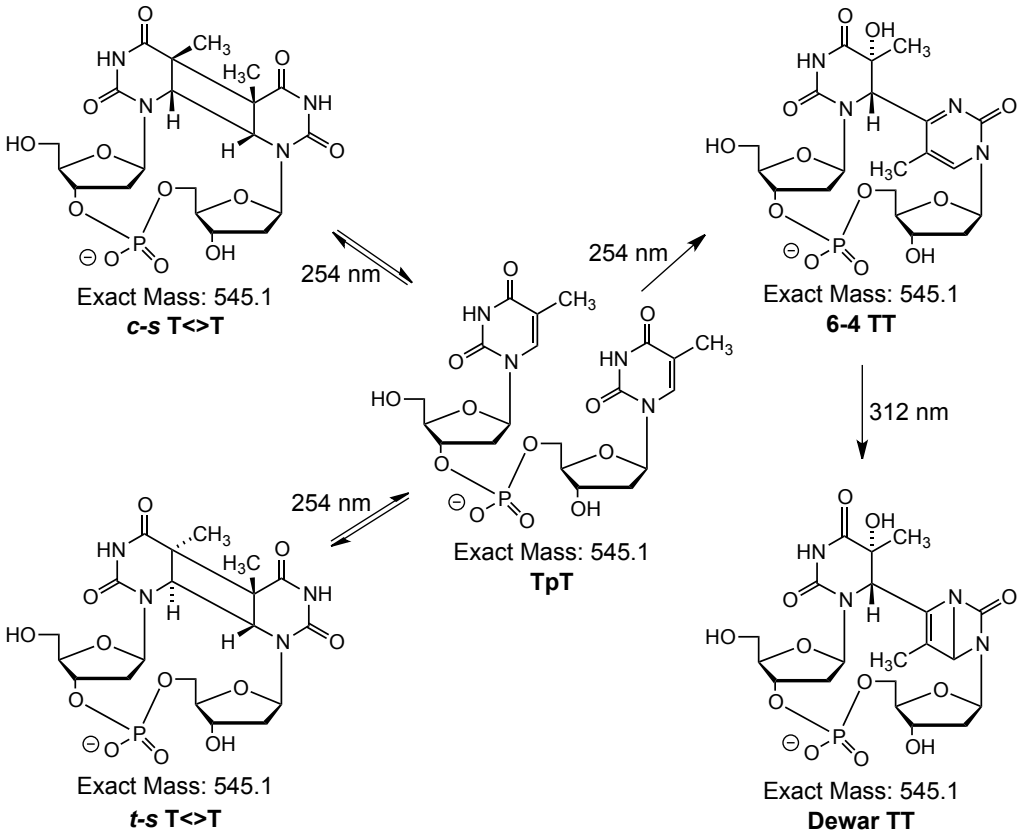

Figure 1: Structures of thymine dimeric photoproducts induced by UV-light

In plants, secondary metabolites, such as mycosporine-like amino acids (MAA) [4], cuticular waxes [5], flavonoids [1, 6] and substituted (mono, di and tri) cinnamic acid derivatives of spermidine [7] have been described to play important roles in the protection from damage caused by UV-radiation. The mechanism of protection probably stems from the property of the secondary metabolite to absorb UV-light in the same range (230-300 nm) as DNA (Figure 2). For example DNA damage caused by UV-irradiations was shown to be higher in mutants of *Zea mays* that are specifically defective in flavonoid accumulation [6], than in the wild type.

Some cinnamic acid derivatives of spermidine were found in high concentrations in the pollen of different plants of the family of Betulaceae, Fagaceae and Juglandaceae [7-9]. These secondary metabolites absorb light in a way that could be beneficial for protection of plant genetic material [10]. Furthermore, they undergo a reversible daylight-induced *E/Z* isomerization, which may be a way of dissipating the energy of UV-irradiation.

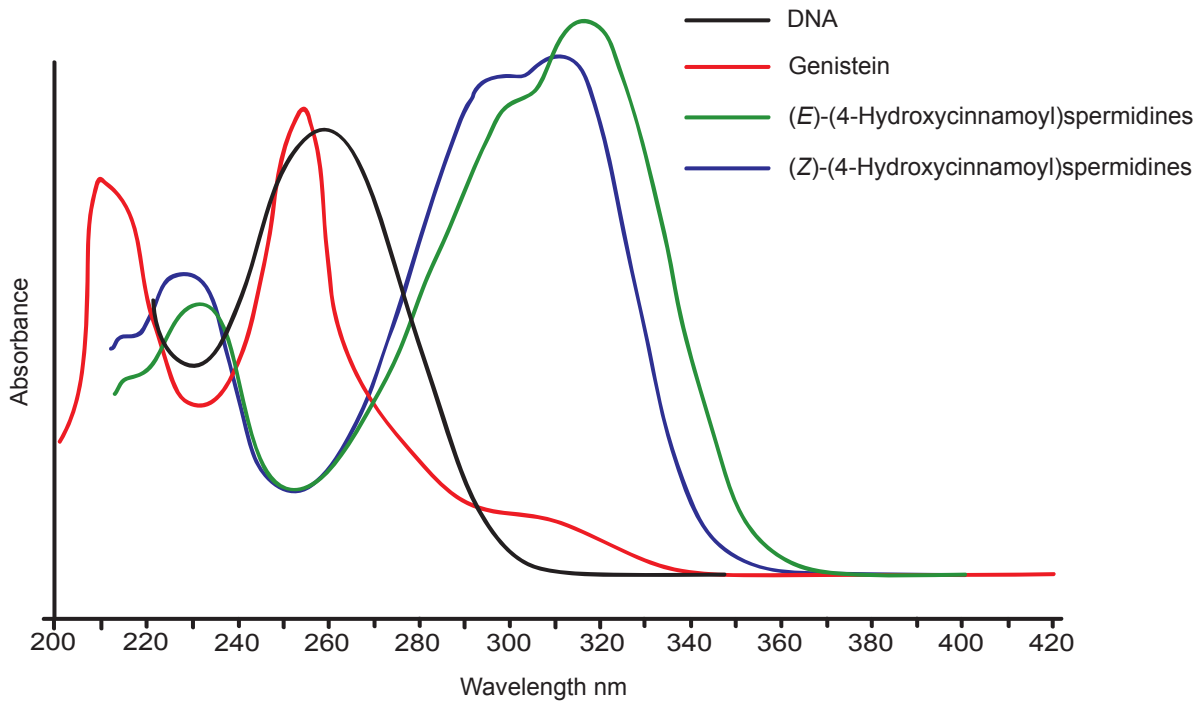

Figure 2: UV-absorbance of DNA, genistein, flavonoid, and (*E/Z*)-(4-hydroxycinnamoyl)-spermidine derivatives.

Several analytical methods have been developed to follow the mutagenicity of UV-irradiation on DNA, in particular IR- [11] and UV- [12] spectroscopy, chromatography [13, 14] and enzyme-linked immunosorbent assays (ELISA) [15]. Since the quantum yield of the photoproducts formation is very low (maximum of 2 % for *c-s* T<>T [2]), sensitive analytical methods are required for the investigation of these DNA mutations. The most specific and sensitive assay for the detection of DNA photoproducts is based on monoclonal antibodies [6].

Mass spectrometry (MS) is known to be one of the most sensitive analytical techniques, as it needs only very small amounts (pmol or less) of analyte. The extent of DNA mutation by formation of photoproducts has also been determined by methods based on MS. Quantitative liquid chromatography tandem mass spectrometry (HPLC-ESI-MS/MS in the MRM mode) approaches, compared to full scan MS (HPLC-ESI-MS), have the advantage of increased selectivity and sensitivity [2, 16]. Such instrumentation allows additionally qualitative investigations and the characterization of unknown DNA lesions.

In this project, analytical methods based on ultra high performance liquid chromatography (UHPLC) and mass spectrometry (MS) have been developed for investigating the effects of UV-light irradiation between thymidylyl(3'-5')thymidine

(TpT) and synthetic ds DNA, in presence of organic molecules. The selected molecules, mostly secondary metabolites, are potentially acting as UV-filters.

In the first part of the chapter, complete optimization of the experimental setup including irradiation box, chromatographic separation, and MS using a Waters UPLC coupled to a maXis QTOF mass spectrometer (HR-QTOF-MS), is presented in detail. The objectives were to form photoproducts with the highest yield, to separate them in a short time with the best sensitivity and determine their relative quantities.

Various classes of UV-filter compounds have been described [6, 8]. The goal of this project is to evaluate UV-filter properties of our target molecules either at 254 or 312 nm. TpT or synthetic ds DNA solutions were therefore irradiated in presence of UV-absorbing metabolites and the formation of photoproducts monitored using the previous optimized analytical method.

3.2 Development of the quantification and irradiation methods

Optimization of the experimental setup was performed with a 10 µM solution of TpT dissolved in H_2O/MeCN, which was irradiated in a quartz micro-cuvette according to the procedure described by *Douki et al.* [2] to obtain the photoproducts. This solution was then used to optimize the chromatographic and mass spectrometric conditions.

3.2.1 Optimization of fast chromatography

Photoproduct dimers are highly polar compounds with similar structures. They are poorly retained and therefore difficult to separate on reversed-phase (RP) material (C18 columns). However, a good separation is necessary to avoid ion suppression in the MS and in order to obtain reproducible quantitative data.

Various RP columns with particle sizes between 1.7 and 3 µm were tested (see Table 1). The conditions were optimized to have an optimal retention and separation of the photoproducts *c-s* T<>T and Dewar TT ($1.4 < R_s < 2.0$), and the latter in the shortest analysis time [17].

Additive	Mobile phase (minimal portion of organic solvent)	Column	R_s [1]	Flow [mL/min]	Analysis time [min]
0.1% HCOOH	H_2O/MeCN (> 3 %)	Waters Acquity BEH, 50 x 1 mm, 1.7 µm	0.0	0.25	5
10 mM NH_4HCO_2	H_2O/MeOH (> 3 %)	Waters Acquity BEH, 100 x 2.1 mm, 1.7 µm	0.0	0.35	6.3
5 mM NH_4HCO_2	H_2O/MeOH (> 3 %)	Waters Acquity BEH, 50 x 2.1 mm, 1.7 µm	0.0	0.20	8
5 mM NH_4HCO_2	H_2O/MeOH (> 10 %)	Interchim Uptisphere UP3NEC#20QS, 200 x 2.1 mm, 3 µm	0.5	0.2	11
5 mM NH_4HCO_2	H_2O/MeOH	Interchim Uptisphere UP3HDO#20QS, 200 x 2.1 mm, 3 µm	1.2	0.2	11
5 mM NH_4HCO_2	H_2O/MeOH	Interchim Uptisphere PLP, 100 x 2.1 mm, 2.2 µm	1.5	0.25	7
5 mM NH_4HCO_2	H_2O/MeOH	YMC-PACK ODS-AR, 150 x 4.6 mm, 3µm	1.7	0.80	9
5 mM NH_4HCO_2	H_2O/MeOH	YMC-Hydrosphere C18, 150 x 4.6 mm, 3µm	1.7	0.90	8
5 mM NH_4HCO_2	H_2O/MeOH	Waters Acquity HSS T3 C18, 100 x 2.1 mm, 1.8 µm	2.0	0.30	7.5
5 mM NH_4HCO_2	H_2O/MeOH	Waters Acquity HSS C18, 100 x 2.1 mm, 1.8 µm	1.7	0.32	7.8

Table 1: Overview of the chromatographic conditions tested (gradient elution). HPLC columns highlighted in blue do, and green do not tolerate the use of 100 % aqueous mobile phase, respectively. R_s was calculated using the peaks corresponding to *c-s* T<>T and Dewar TT.

First, an Acquity® BEH (Bridged Ethylene Hybrid) column with 1.7 µm particle size was tested using different additives (HCOOH and NH_4HCO_2) and organic solvents (MeCN and MeOH). The next column tested was an Uptisphere® NEC (non-end-capped[2]) column. Although both columns were operated at their tolerance aqueous phase content limit of 97 and 90 %, respectively, the results were insufficient with a maximal R_s of 0.5 (green part in Table 1).

The following columns were chosen with respect to their tolerance for 100 % aqueous mobile phase (blue part in Table 1). They were obtained from different manufacturers and have various carbon content, silanol activity, pore sizes and C18 functionalization.

[1] The resolution factor defining the chromatographic separation between compounds A and B is defined as $R_S = \frac{(t_R)_B - (t_R)_A}{(W_{1/2})_A + (W_{1/2})_B}$ ($W_{1/2}$ = peak width at 50 % relative intensity).

[2] Non-encapped columns have silica based reversed phase sorbents with extra silanol residues for strong retentions of polar compounds

The best results were obtained with the Waters Acquity HSS C18 column. This trifunctional C18 stationary phase, with 1.8 µm particle size is endcapped, and shows low silanol activity. The mobile phase consisting of H_2O and MeOH was buffered with 5 mM NH_4HCO_2. Using this combination, the photoproducts were separated in a 4 minutes gradient and a total run time of 7.8 minutes (Figure 3), which is almost 40 % faster than published data (total time 20 minutes) [2].

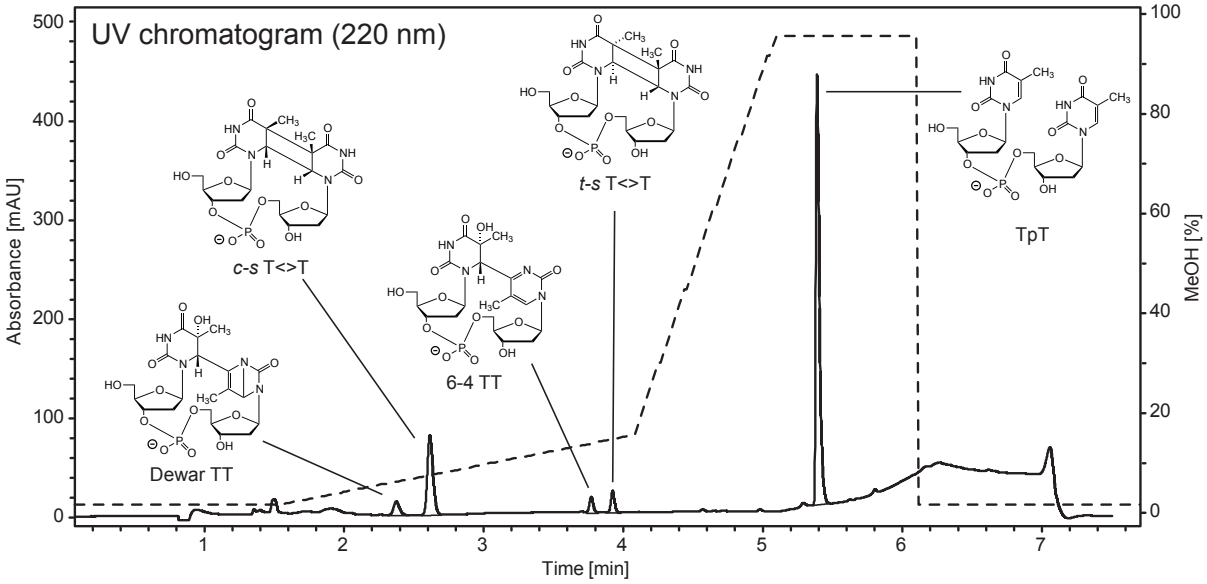

Figure 3: UV-chromatogram (left scale) showing the optimized separation of the photoproducts with an HSS C18 column. A gradient of H_2O/MeOH + 5 mM NH_4HCO_2 buffer was used (dotted line, right scale).

3.2.2 MS method optimization

After chromatographic separation, the photoproducts were detected by ESI-MS with a high-resolution maXis QTOF mass spectrometer in the full scan (FS-MS) or in the multiple-reaction monitoring (MRM) mode. To date, published data were obtained using triple quadrupole mass analyzers acquired in the MRM mode [2, 18].

Optimization of the MS/MS fragmentation parameters (precursor ions *m/z* 545) with direct injection of the irradiated TpT solution (3 µL/min flow rate) appeared to be challenging. Yields of fragment-ion formation varied a lot and were strongly depended on the structure of the different photoproducts. Baseline chromatographic separation was required with FS-MS mode since high-resolution extracted ion chromatograms (HR-EIC) for each photoproduct have identical monoisotopic masses (*m/z* 545.128). Finally, the data was processed with HR-EIC (± 0.01 *m/z*) in order to improve signal-to-noise ratio (S/N) and sensitivity at the same time. The developed

LC method (see Chapt. 3.2.1) did fulfill the peak resolution criteria, and could thus be used in combination with FS-MS. A direct comparison of both acquisitions, full scan MS and MRM modes, is shown in Figure 4.

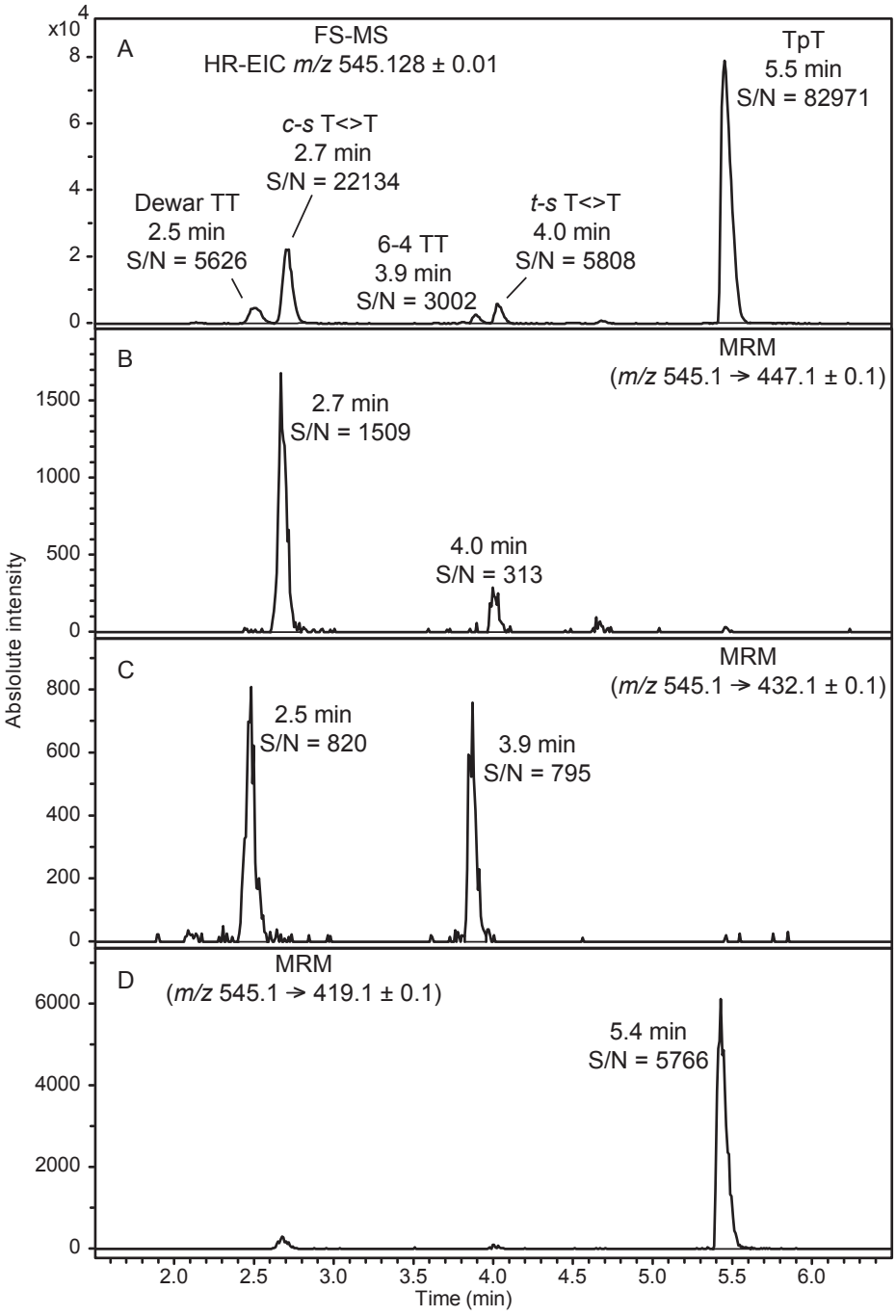

Figure 4: UHPLC-ESI-QTOF-MS analyses of a 10 µM TpT solution after irradiations at 254 (formation of *c-s* and *t-s* T<>T and 6-4 TT) and 312 nm (photoisomerization of 6-4 TT in Dewar TT). Acquisitions were performed in (A) FS-MS and (B-D) in MRM mode (precursor ions *m/z* 545.1). The S/N is given for each peak.

According to S/N, the use of FS-MS (Figure 4A) led to a much higher sensitivity (factor of ten) compared to MRM detection (Figure 4B-D). This is an important criterion in quantitative determinations. The higher S/N in the FS-MS method, and

therefore better sensitivity, was crucial because of the low quantum yield of mutations observed during irradiation of TpT and synthetic ds DNA.

Additional aspects relevant for quantification in general are, the correlation between relative amounts and ion responses, as well as the precision of the method. The relative areas of the five main photoproducts were therefore compared using both MS acquisition modes (Figure 5).

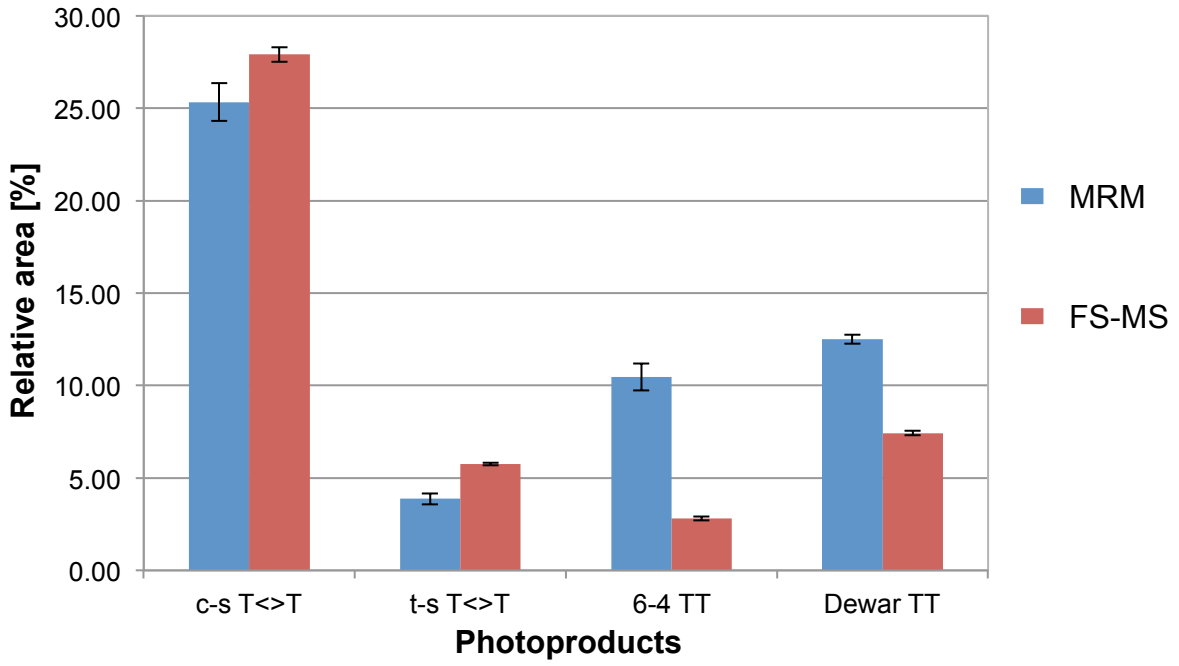

Figure 5: Relative response of all four photoproducts acquired in the FS-MS and in the MRM mode (n=5)

The two acquisition methods used, led to different relative signal responses. First, MS/MS fragmentations were strongly related to the structure of the precursor ions and each reaction generated different fragmentation yields and thus signal responses. Second, similar ionization efficiencies were prerequisited to obtain comparable FS-MS responses. As all photoproducts belong to the same class of compounds, the relative areas obtained from FS-MS data should probably better reflect the relative amounts in the samples.

A further advantage of the FS-MS over the MRM method is the lower systematic error due to its higher sensitivity. This is illustrated with the smaller error bars obtained after 5 injections of the same irradiated TpT solution (see Figure 5).

In conclusion, FS-MS was shown to be the method of choice. The higher selectivity of MRM methods would only be beneficial in the presence of more complex matrices.

In our case, this was not the problem because of good chromatographic separation (see Chapt. 3.2.1).

3.2.3 Optimization of the irradiation setup

The quantum yield of the photoreaction is very low (Φ = 0.02)[3] and only traces of the major product *c-s* T<>T can be isolated from e.g. irradiated calf thymus DNA [2]. It was therefore essential to find an efficient and reproducible irradiation method in order to form photoproducts with the highest yield. Three main points were thereby crucial: the UV-lamp, the sample container and the irradiation setup.

The lamp was chosen according to the system used by *Douki et al.* [2]. Two wavelengths can be selected, one at 254 nm to form *c-s* T<>T, *t-s* T<>T and 6-4 TT, and the other at 312 nm to transform 6-4 TT into Dewar TT.

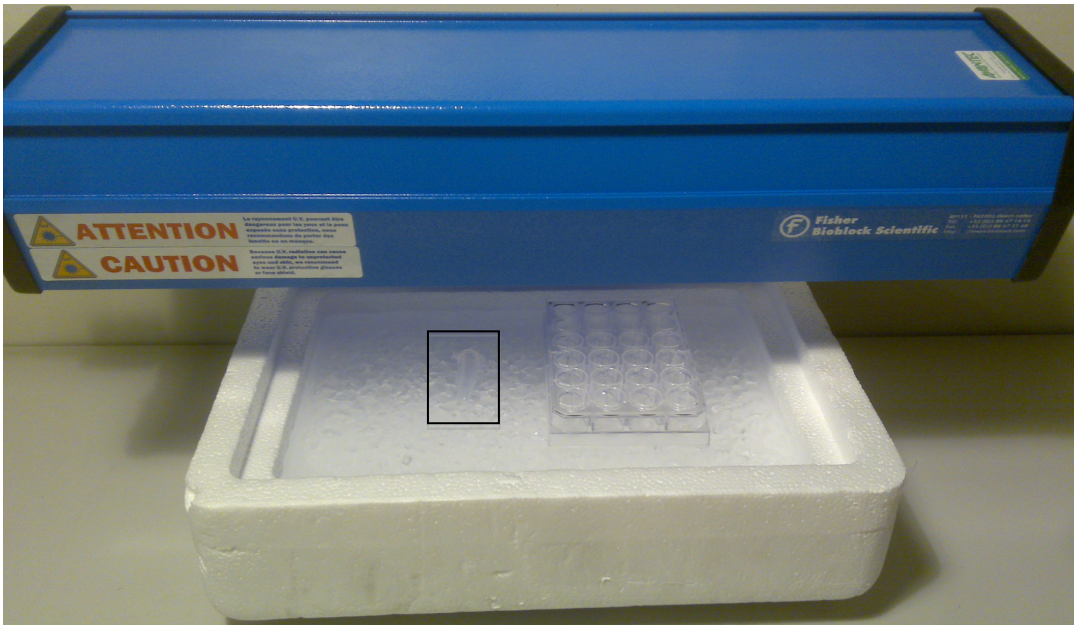

Figure 6: Irradiation setup with Eppendorf® tube (in the black frame) and microplate

Containers used for irradiation with different shape and materials have been tested. First irradiation experiments were performed using Eppendorf® tubes and micro-plates. These inexpensive consumables, allow irradiation of many samples at the same time and the analyte can be refrigerated in an ice bath (see Figure 6). They are

[3] The quantum yield is defined as: $\Phi = \frac{N_{prod}}{N_{ph,abs}} = N_A hc \frac{c_{prod} V}{P_{abs} \Delta t \lambda_{Lamp}}$ [15]

made of polypropylene, a material that absorbs UV-light at wavelengths below 300 nm (Figure 7, curve D). For this reason, irradiations had to be performed from the top with open containers. However, the surfaces of irradiation were small compared to the sample volumes and sample solvent was evaporating. This led to low yield of photoproducts and poor reproducibility.

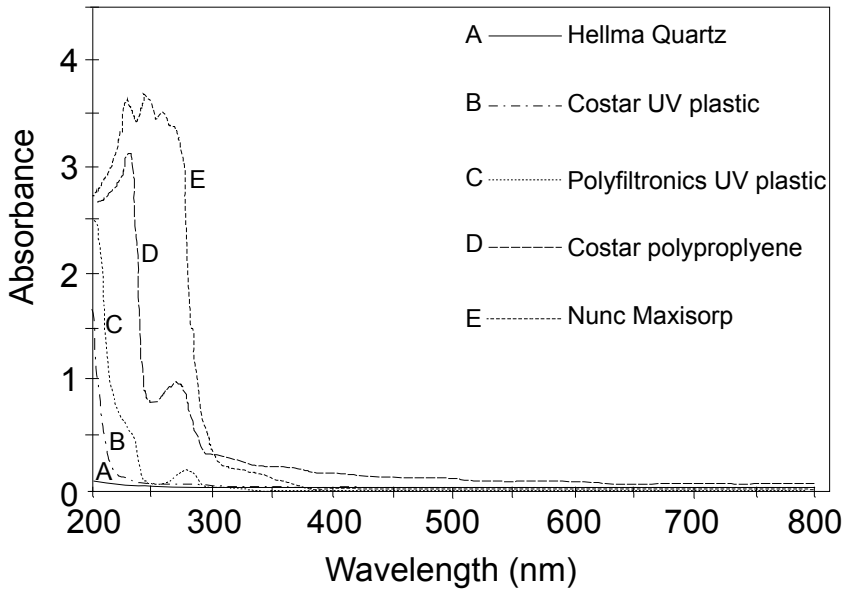

Figure 7: Background absorbance of (A) quartz and (B-E) various microplates[4]

The UV-light transparent quartz micro-cuvettes were finally chosen (see Figure 7, curve A). These cuvettes offer the largest surface of irradiation (5 cm^2) for a volume of only 500 µL. They can also be sealed with caps, avoiding evaporation during the long irradiation periods.

[4] P. Held, *The Importance of Using the Appropriate Microplate for Absorbance Measurments in the Ultraviolet Region of the Spectrum*, Technical Note, BioTeck Instruments, Inc, **2001**. Link: http://www.biotek.com/resources/articles/absorbance-measurement-ultraviolet-spectrum.html.

An irradiation box was finally constructed in order to achieve best reproducibility. This setup allowed uniform irradiations as the samples are shielded from daylight and defined irradiation distances of 20 to 95 cm between the lamp and the micro-cuvettes can be chosen. With this system it was also easy to place a second row of micro-cuvettes in front of the one containing TpT or DNA solutions.

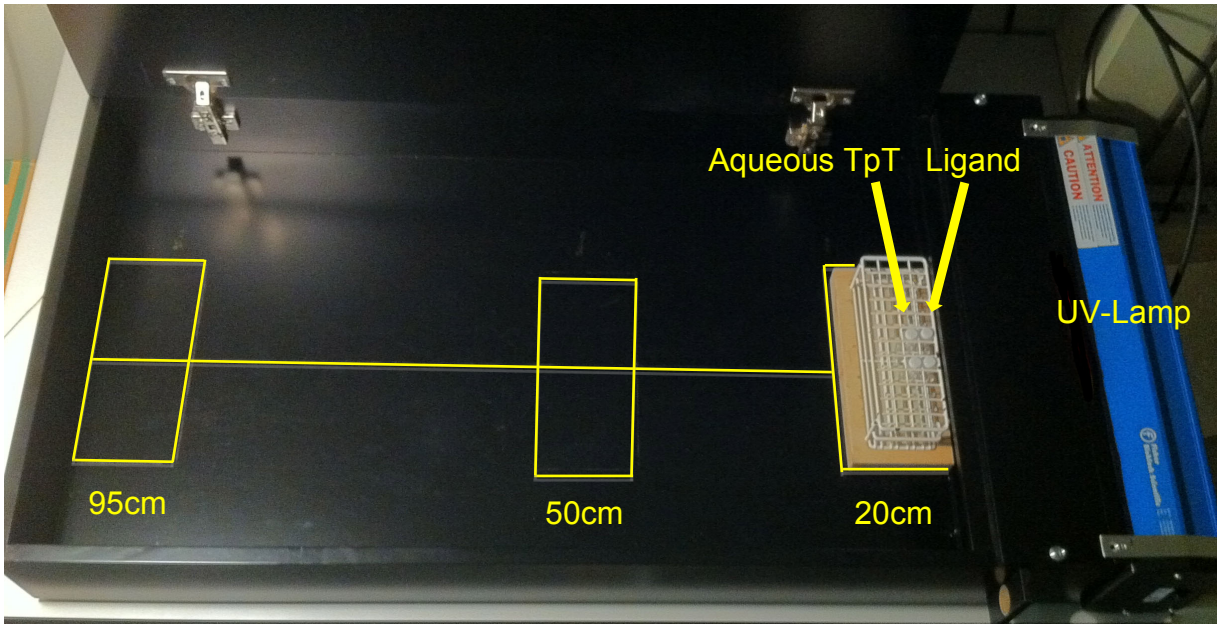

Figure 20: Irradiation setup consisting of a black box, quartz micro-cuvettes with caps, and three marked positions for experiments at e.g. 20, 50, or 95 cm distance from the UV-lamp

3.3 Estimation of the UV-protection factor

The primary objective of the project was the verification of the reliability regarding reproducibility, sensitivity and accuracy of the UV-irradiation instrumental set up developed in Chapter 3.2. Additionally, insight in the effectiveness of some plant secondary metabolites to act as UV-filters should be gained on the basis of some preliminary tests. These secondary metabolites were chosen with regard to their classification: flavones (apigenin and its *C*-glycoside derivative vitexin), anthocyanin (kuromanine), cinnamic acid (*p*-coumaric acid), polyamines (spermine and its 5,10-bis(*E*-cinnamoyl) derivative).

UV-filter		$Log_{10}\ \varepsilon_{254}$	$Log_{10}\ \varepsilon_{312}$
Apigenin (ap)	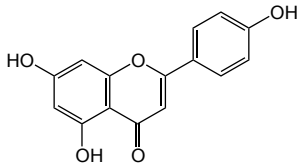	4.11	4.22
Vitexin (vi)	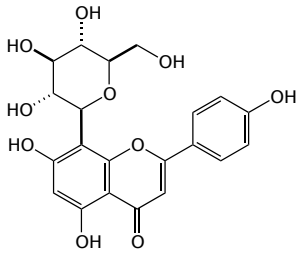	4.09	4.20
Kuromanin (ku)	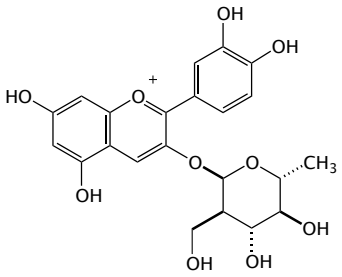	3.94	3.53
p-coumaric acid (cou)	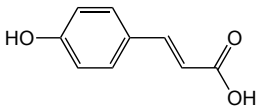	3.57	4.21
Spermine (spm)	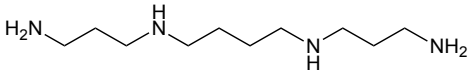	0	0
5,10-bis(*E*-cinnamoyl) spermine (5,10-cin spm)	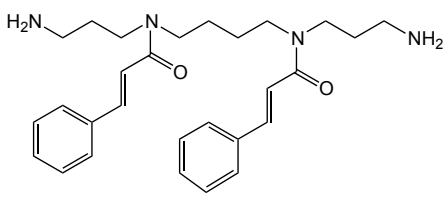	4.02	3.56

Table 2: UV-filters and their extinction coefficients ε at 254 and 312 nm, respectively

With this experimental setup, we tried to correlate absorption properties of the selected UV-absorbing molecules with their capacity to protect TpT or ds DNA against photoproduct formation. For this reason, the extinction coefficients[5] ($\log_{10}$ ε) of compounds shown in Table 2 were measured at 254 and 312 nm, which correspond to our irradiation wavelengths. It appeared that these molecules present similar $\log_{10}$ ε values except for spermine and *p*-coumaric acid at 254 nm, and kuromanin and 5,10-bis(*E*-cinnamoyl) spermine at 312 nm.

Three irradiation setups were therefore developed for the screening of the UV-filters. The first consisting of two cuvettes (one containing the TpT and the other the UV-filter solution), the second with a unique cuvette (containing both, the TpT and the UV-filter), and a third including a synthetic ds DNA instead of the TpT dimer.

3.3.1 Irradiation of TpT and UV-filter solutions in separated cuvettes

First experiments were performed in separate cuvettes and at the shortest distance from the UV-light source (20 cm). This arrangement should avoid problems of solubility and lead to maximal yields of photoproducts. Their formation was followed by UHPLC-ESI-HR-QTOF in the FS-MS mode by collecting aliquots of 40 µL of the TpT solutions and by integrating all photoproduct signals.

In a control assay accomplished with a pure TpT solution, steady state of *c-s* T<>T formation was already reached after ca. one hour irradiation at 254 nm (see Figure 9, TpT without UV-filter). These results are in agreement with the data published by *Douki et al.* [2].

The rate of photoproducts formed after irradiation of TpT, was used as reference data. The UV-filter solutions (50 µM) were then positioned in front of the dimer solutions
(10 µM). The kinetic of the photoproduct formation (*c-s* T<>T) was then followed in absence and in presence of three UV-filters (apigenin, vitexin and kuromanin) as presented in Figure 9.

[5] Molar extinction coefficient $\varepsilon = \frac{A}{C \cdot l}$, *A* corresponding to the absorbance measured at a defined wavelength divided by *C* the mole concentration of the absorbing material and *l* the path-length. SI unit: m^2/mol [19]

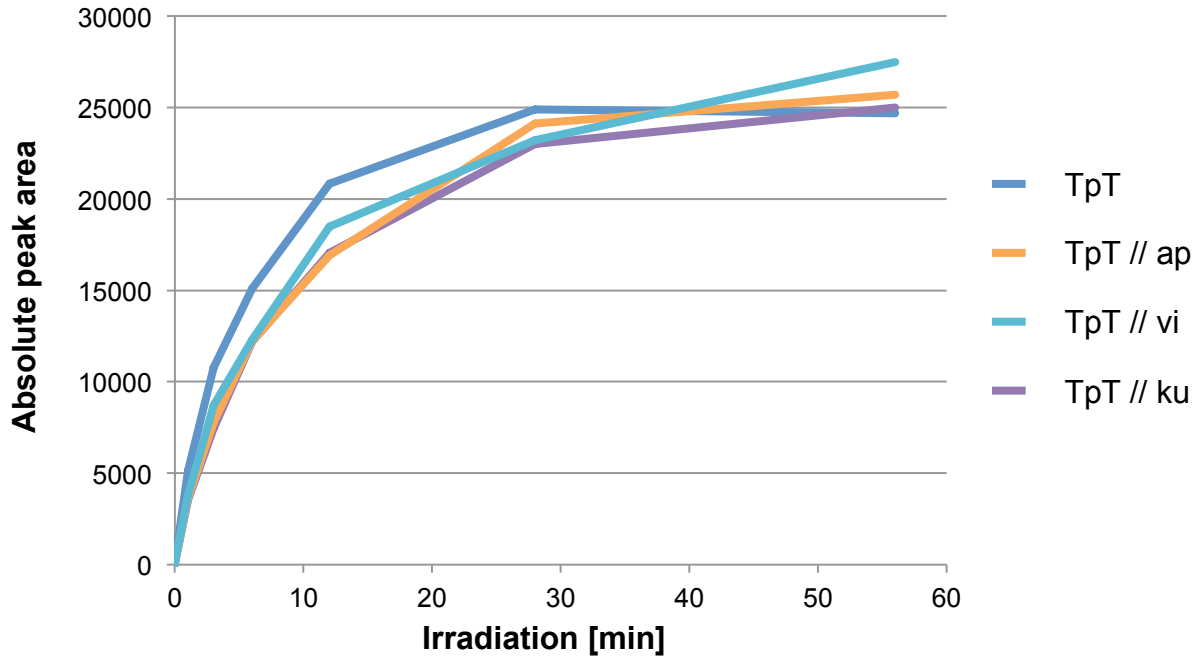

Figure 9: Formation of *c*-s T<>T as a function of irradiation duration λ = 254 nm, (solution of 10 µM TpT without and with a 1:5 molar ratio of apigenin, vitexin, and kuromanin, respectively) in a separate cuvette. Data were obtained from the HR-EIC of UHPLC-ESI-HR-QTOF-MS analyses.

The data were then processed allowing a more precise comparison of the formation of each photoproduct separately in presence of the various UV-filters (see Figure 10). It appears that the formation of photoproducts was mainly due to increased concentration of 6-4 TT and the major reaction product *c-s* T<>T dimer. Further, summation of the absolute peak areas of all photoproducts led to a better visibility of protection effects and to an improved reproducibility of the quantification. Although only two series of experiments were performed, it seems that good coefficients of variation (around 3 %) can be obtained for the quantification of the sum of all TpT photoproducts (see error bars in Fig 10).

Surprisingly, from all plant metabolites tested, only *p*-coumaric acid did not show any UV-protection effects at 254 nm. This can be explained with the relatively low extinction coefficient of 3.57 at this wavelength (Table 2). However, the results observed with spermine, a molecule lacking any UV-absorbing group, seem to contradict this assumption. In this case an overall protection effect of 2 % was observed. This is close to those observed with the other UV-filters (between 6 and 0.5 %). The most significant effects of UV protection (10 %) were observed with apigenin. Although this value is obtained for the molecule with the highest $\log_{10}$ ε

value at 254 nm, it is too risky at this stage of the research, to correlate the extinction coefficient values with the formation of TpT photoproducts.

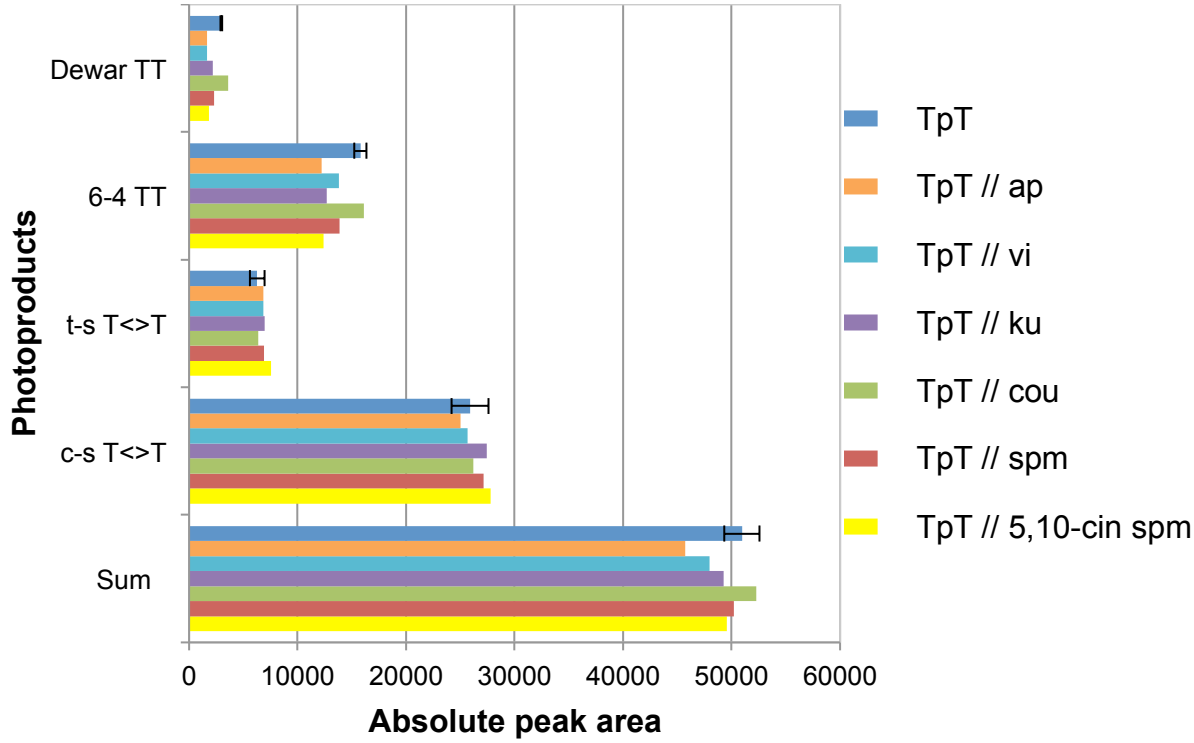

Figure 10: Formation of photoproducts after 56 min irradiation at 254 nm of an aqueous solutions of 10 µM TpT without and with a 50 µM UV-filter solution of apigenin, vitexin, kuromanin, *p*-coumaric acid, spermine or 5,10-bis(*E*-cinnamoyl) spermine prepared in a separate cuvette. Data were obtained from the HR-EIC of UHPLC-ESI-HR-QTOF-MS analyses.

With the hope of observing more significant effects, a second irradiation series was performed under the same conditions (concentration, distance and duration) at 312 nm. This wavelength is closer to the one of the UV-light reaching earth and probably closer to reality. The sum of the absolute peak areas were lower by a factor of 1/3 if TpT was irradiated at 312 nm (Figure 11) compared to the experiments achieved at 254 nm (Figure 10). The major compound formed is still *c-s* T<>T (see Figure 11)

Considering the UV-protection effects, spermine was, as expected from the $\log_{10}$ ε values, the only compound that did not show any photoprotection effects (Figure 11). The other plant metabolites exhibited similar mutation inhibitions of ca. 20 ± 3 %, although kuromanin and 5,10-bis(*E*-cinnamoyl) spermine have at 312 nm clearly a low $\log_{10}$ ε of only 3.53 and 3.56 compared to e.g. apigenin with a $\log_{10}$ ε = 4.22. It seems therefore possible, this time, to correlate the quantified UV-protection effect of the tested UV-filters tested with their extinction coefficients.

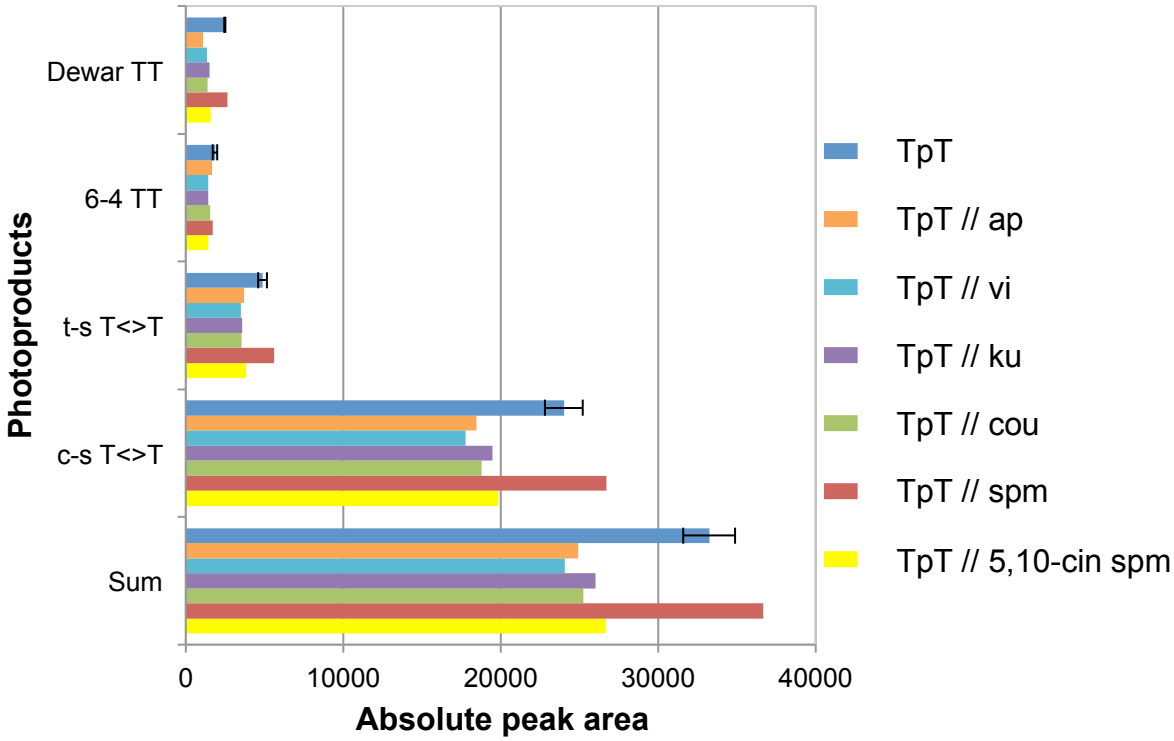

Figure 11: Formation of photoproducts after irradiating at 312 nm an aqueous solutions of 10 µM TpT during 56 min without and with 50 µM UV-filter solution of apigenin, vitexin, kuromanin, *p*-coumaric acid, spermine or 5,10-bis(*E*-cinnamoyl) spermine prepared in a separate cuvette. Data were obtained from the HR-EIC of UHPLC-ESI-HR-QTOF-MS analyses.

In conclusion, UV-protection effects can be monitored using our developed UHPLC-ESI-HR-QTOF method in the FS-MS mode, irradiating two micro-cuvettes in series, containing in one the TpT and in the other the UV-filter solution. The sensitivity and the accuracy (± 3 % at 312 nm) of the instrumental setup developed is satisfactory. The robustness of the assay needs to be probed by performing additional experiments. Irradiations at 254 nm lead to higher concentrations of mutation products than at 312 nm. However, the inhibition of the formation of photoproducts with our target filters is more evident if irradiations are performed at 312 nm with a maximum of 23 % for vitexin compared to only 10 % for apigenin at 254 nm.

At this stage of the project, it is may be too early to correlate the $\log_{10}$ ε values of the UV-filters with the quantification of the photoproducts formed in their presence. Nevertheless, the previous tests done at 312 nm appear to be more appropriate to perform further experiments with supplementary UV-filters with a broader range of extinction coefficients.

3.3.2 TpT irradiation in presence of a UV-filter using one cuvette

Preliminary irradiation tests of TpT (5 µM) and UV-filters mixed together were done using a 4-fold excess of one spermine derivative (1,14-bis(*E*-cinnamoyl) spermine, 20 µM) and one flavone glycoside (vitexin, 20 µM) in an aqueous solution. The cuvettes were irradiated at 254 nm for ca. one hour and photoproduct concentrations determined with the UHPLC-ESI-QTOF method in the MRM mode (see Chapter 3.2.2).

Figure 12 shows the extracted ion chromatogram of the major photoproducts at *m/z* 447 after 64 min irradiation of TpT at 254 nm in presence of 1,14-bis(*E*-cinnamoyl) spermine.

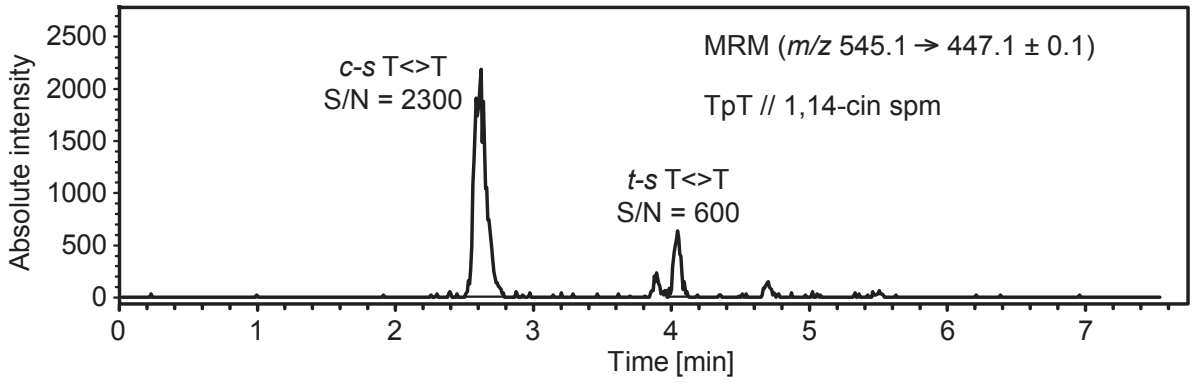

Figure 12: UHPLC-ESI-QTOF-MS/MS (*m/z* 545.1 → 447.1) of an aqueous solution of TpT and 4-fold excess of 1,14-bis(*E*-cinnamoyl) spermine after 64 min of irradiation at 254 nm

Similar to the two cuvettes experiment, sensitivity, chromatographic separation and peak width were reasonable and would allow quantification of the TpT photoproducts, but the S/N are about a factor of 3 lower (S/N = 2300 and 6200 for *c-s* T<>T and S/N = 2200 and 600 for *t-s* T<>T with one and two cuvettes, respectively). This can be attributed to the MRM method (as discussed in Chapter 3.2.2), which is less sensitive than the full scan one.

The quantification of the photoproducts with vitexin present in solution appeared to be more complicated as this flavonoid is not soluble in H_2O. The vitexin stock solution was therefore prepared in MeOH and then added to the aqueous TpT solution to obtain a final solvent mixture of H_2O/MeOH 3:2. The rest of the handling was exactly the same as in the experiment with 1,14-bis(*E*-cinnamoyl) spermine. Unfortunately, the chromatographic separation caused major problems

(see Figure 13) due to the injection of 5 µL sample solution containing a relatively high fraction of organic solvent in an almost exclusively aqueous mobile phase (only 1 % of MeOH)[6]

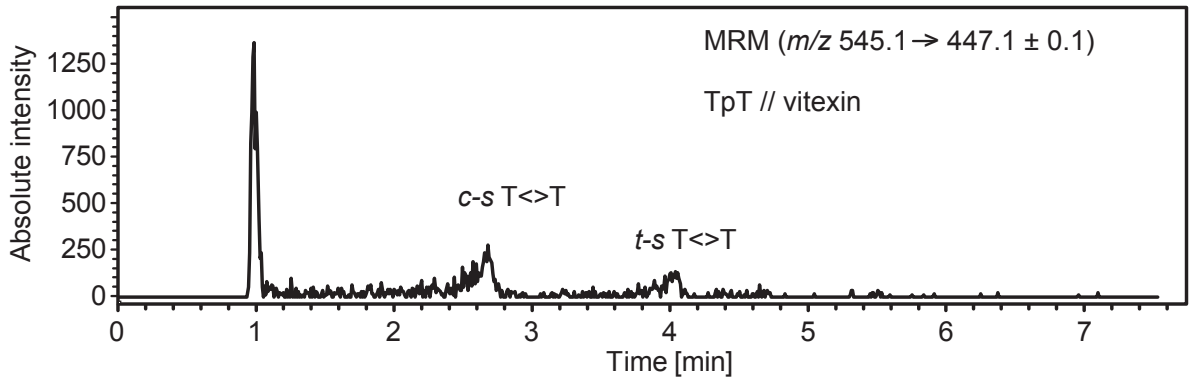

Figure 13: UHPLC-ESI-QTOF-MS/MS (*m/z* 545.1 → 447.1) of a solution of TpT and 4-fold excess of vitexin in H_2O/MeOH 3:2 after 64 min of irradiation at 254 nm

3.3.3 Irradiation of ds DNA in presence of a plant metabolite absorbing UV-light

This experiment was designed to test the influence of binding affinities between UV-filters and ds DNA strands, and derive their UV-protection capacity. Due to the problems encountered with the solubility of vitexin in pure H_2O (see Chapter 3.3.2), only a single experiment has been performed with an aqueous solution containing ds2 DNA (0.3 µM) and 1,14-bis(*E*-cinnamoyl) spermine (1.2 µM) in a 4-fold excess. This assay should prove the ability of the method to quantify the UV-protection using longer oligonucleotide chains (in this case, ds2 with 14 base pairs). After 2.5 hours irradiation at 254 nm (this wavelength has been chosen in order to get higher amounts of photoproducts than at 312 nm) ds DNA was enzymatically digested and photoproducts quantified with the UHPLC-ESI-QTOF method in the MRM mode (Figure 14). However, the overall yields (photoproduct formation, digestion and extraction) were very low and the signals just above the limit of detection (see Chapt. 1.2.2).

The very low photolysis yields are probably due to the presence of only 6 AT base pairs in ds2 DNA and the very small quantum yield of the reaction. The signals

[6] This known phenomenon has already been described [20]

obtained are at the moment too low to make any quantitative determination, but the sensitivity may be improved by e.g. applying the full scan ESI-MS conditions developed in Chapter 3.2.2, or irradiating for a longer time.

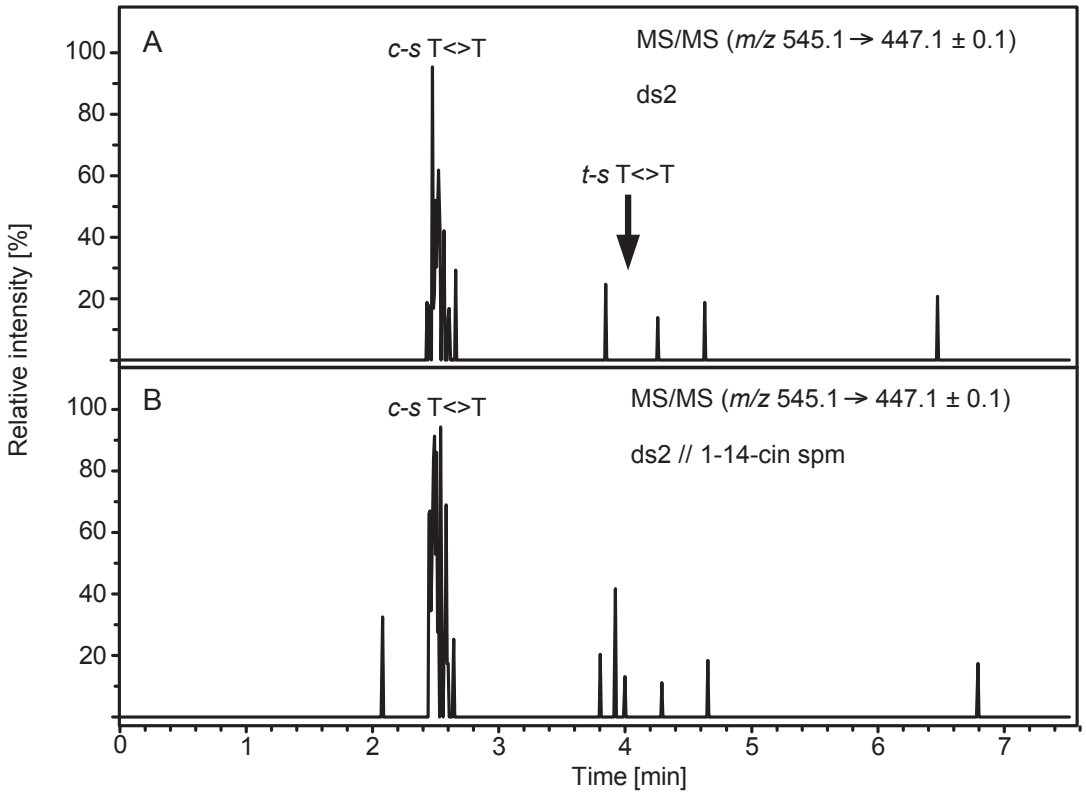

Figure 14: UHPLC-ESI-QTOF-MS/MS (*m/z* 545.1→ 447.1) of an aqueous solution of ds2 DNA (A) without and (B) with addition of a 4-fold excess of 1,14-bis(*E*-cinnamoyl) spermine after 2.5 h of irradiation at 254 nm and followed by enzymatic digestion

3.4 Conclusion and outlook

The aim of this part of the project was to develop a method allowing the quantification of the reactivity of DNA with regard to the formation of photoproducts after UV-light irradiations. It should also allow to verify that the presence in the solution of small organic molecules absorbing UV-light leads to a decrease of the amount of formed photoproducts.

In a first part, an irradiation device including black box, UV-lamp, and quartz micro-cuvettes was designed and tested in combination with a newly implemented analytical method based on fast UHPLC chromatography and high-resolution ESI-QTOF mass spectrometry (UHPLC-ESI-HR-QTOF-MS). This arrangement allowed the relative quantification of TpT photoproducts with good reproducibility, the full-scan MS detection showing better sensitivity and accuracy than the MRM mode.

An absolute quantitative procedure including external calibration curve using pure photoproducts was not developed as the preliminary experiments were only designed to prove that photoprotection effects could be monitored.

In a second part, the instrumental setup was assessed with regard to the reactivity of TpT and a synthetic double strand DNA (14 base pairs) to UV light in presence of plant secondary metabolites that were proposed as natural UV-filters [6, 8]. Three approaches were considered: (1) irradiation in separated cuvettes, one containing the TpT and the other the UV-filter solution, (2) irradiation of a unique cuvette containing solution of UV-filter mixed with TpT, and (3) irradiation a unique cuvette containing small organic molecules and synthetic ds DNA. Systems utilizing one cuvette were developed in order to tentatively correlate non-covalent interactions between DNA/small molecules with the efficiency of the UV-protection, an approach that failed at this stage of the project.

It appears that the quantitative determinations of photoprotection effects are possible with the system based on two cuvettes. Differentiations were clearer after irradiations at 312 (maximum of 23 % UV-protection effect) than at 254 nm (10 %). However, it seems risky at this stage of the project to attempt to correlate the results of the quantification of the photoproducts with the extinction coefficients $\log_{10} \varepsilon$ of the small organic molecules and to reach a conclusion on relative protection effects of different UV filters.

Preliminary experiments performed with the irradiation of a unique cuvette containing oligonucleotides and UV-filters led to problems of chromatography (a 5 µL injection of the solution containing irradiated TpT and vitexin disrupted chromatographic behavior) and of sensitivity (signal of photoproducts arising from the irradiation of synthetic ds DNA were close to or below the limit of detection).

If the approach of irradiating unique solutions has to be followed up, further optimizations of e.g. solvent mixtures containing some DMSO or UHPLC-MS quantification method have to be performed. A larger variety of UV-filters with a broad range of extinction coefficients have also to be tested in order to try to correlate extinction coefficients with UV-protection effects.

3.5 Experimental part

3.5.1 Chemicals, solvents and enzymes

Methanol (MeOH), acetonitrile (MeCN), ammonium formate, triethylamine (all in LC-MS Ultra Chromasolv® quality) and glacial acetic acid (puriss) were obtained from Sigma-Aldrich (Buchs, Switzerland).

Thymidylyl(3'-5')thymidine (TpT) was purchased from Microsynth (Balgach, Switzerland). TpT (dissolved in 600 µL of solvent A) was purified by HPLC (Prominence HPLC system from Shimadzu Scientific Instruments, Columbia, MD, USA) using a YMC-pack Basic 10Pµm column (10 µm, 150 x 10 mm, YMC Co.,Ltd., Kyoto, Japan). The chromatography was performed with a mobile phase consisting of 0.01 M triethylammonium acetate (eluent A, preparation of 2 L by addition of 5.6 mL of glacial acetic acid to MilliQ water followed by addition of ca. 27.8 mL of triethylamine to an adjusted pH of 7.0 ± 0.1) and MeCN (eluent B, Chromasolv). 100 µL solution of TpT was purified with a linear gradient elution from 5% to 25% of B within 7 min at a flow rate of 3 mL/min. The final solution of TpT used for the irradiation tests, is a 10 µM (NanoDrop control) solution in H_2O/MeCN 96:4 + 0.012 M $HNEt_3OAc$.

Protocol for ds DNA formation see Chapter 2.5.3. LC-MS grade H_2O (< 2 ppb) was obtained by purification of deionized H_2O with a MilliQ gradient apparatus equipped with a BioPack® ultrafiltration module (Millipore, Milford, MA, USA). Spermine tetrahydrochloride, *p*-coumaric acid, kuromanin chloride and vitexin were purchased from Sigma-Aldrich, apigenin from Extrasynthese (Lyon Nord, France) in the best qualities available. 5,10- and 1,14-bis(*E*-cinnamoyl) spermine derivatives were synthesized in our laboratories [21].

Nuclease P_1 from Penicillium citrinum was obtained from Sigma-Aldrich (Buchs, Switzerland). Shrimp Alkaline Phosphatase (SAP) was obtained from Promega (Madison, WI, USA). Calf Spleen phosphodiesterase, Type II, was obtained from Calbiochem, Merck (Darmstadt, Germany) and Snake venom phosphodiesterase, Type I, from MP Biomedicals (Santa Aba, CA, USA).

3.5.2 Instrumentation

UHPLC-ESI-MS

The photoproducts were quantified under following optimized conditions:

UHPLC-MS analyses were performed on an Acquity system (Waters, Milford, MA, USA) using an Acquity HSS C18 column (2.1 x 100 mm, 1.7 μm, Waters), Acquity BEH (50 x 1 mm, 1.7 µm, Waters), Acquity BEH (100 x 2.1 mm, 1.7 µm, Waters), Acquity BEH (50 x 2.1 mm, 1.7 µm, Waters), Acquity HSS T3 C18 (100 x 2.1 mm, 1.8 µm, Waters), Acquity HSS C18 (100 x 2.1 mm, 1.8 µm Waters), Uptisphere UP3NEC#20QS (200 x 2.1 mm, 3 µm, Interchim), Uptisphere PLP (100 x 2.1 mm, 2.2 µm, Interchim), YMC-PACK ODS-AR (150 x 4.6 mm, 3 µm, YMC), YMC-Hydrosphere C18 (150 x 4.6 mm, 3 µm, YMC)

Mobile phase of the optimized method consisted of H_2O (eluent A) and MeOH (B) both buffered with 5 mM of NH_4HCO_2. Elution at a flow rate of 0.32 mL/min started with 1 % of B during 1.5 min, followed by a linear increase to 15 % of B within 2.5 min, and finally to 95 % of B within 1 min. The wash step consisted in a plateau of 0.9 min at 95 % of B, and finally the column was re-equilibrated during 1.6 min until next injection. Sample solutions (5 µL) were injected using the “partial loop with needle overfill” technique. MeOH/H_2O 2:1 and H_2O were used as strong and weak needle wash solutions, respectively.

The UHPLC was connected to a high resolution maXis QTOF mass spectrometer (Bruker Daltonik GmbH, Bremen, Germany) equipped with the ESI source (ESI parameters: end plate offset (–500 V), capillary (4000 V), nebulizer gas (N_2, 1.8 bar), dry gas (N_2, 9 L/min), dry temperature (200 °C). MS parameters: funnel RF (200 Vpp), ISCID energy (10 eV), multipole RF (200 Vpp), ion energy (4 eV), low mass (100 *m/z*), collision energy (10 eV, He gas), collision RF (350 Vpp), ion cooler RF (200 Vpp), transfer time (100 μs), and pre-puls storage (10 μs). Full scan mass spectra were acquired in the negative full scan mode, at 20’000 resolution (FWHM), scan rate of 2 Hz, and between *m/z* 50 and 600. An external mass calibration below 2 ppm accuracy was performed between *m/z* 112 and 1064 just before starting a series of measurements with a 2 mM solution of sodium formate in H_2O/propan-2-ol 1:1. MS/MS spectra were acquired with almost the same parameters as in the full scan, only the collision energy was changed (25 eV).

3.5.3 Experimental description

a) Measurements of $Log_{10}\,\varepsilon$ values

Stock solution of apigenin (dissolved in MeOH), Vitexin (DMSO), Kuromanin (H_2O), *p*-coumaric acid (EtOH) and 5,10-bis(*E*-cinnamoyl) spermine (H_2O) were prepared at a concentration of 5 mM. The stock solutions were then diluted to concentrations of 0.05, 0.025 and 0.0125 mM with MeOH (apigenin, vitexin and *p*-coumaric acid) and with H_2O (kuromanin and 5,10-bis(*E*-cinnamoyl) spermine). Absorbance of 400 μL of each solution was measured between 200 and 450 nm in quartz micro-cuvettes with a UV spectrophotometer SpectraMax M5 (Molecular Device, Sunnyvale, CA, USA). The extinction coefficients were calculated from the linear slope obtained after plotting the absorbances at 254 and 312 nm over the concentrations.

b) UV irradiations

The solutions were irradiated with a UV-lamp (VL-215.MC, Vilber Lourmat, Marne-la-Vallée, France) that was switched on at least one hour in advance. Two rows (in the experiment with two cuvettes) of quartz micro-cuvettes with caps (400 µL, 115F-QS, Hellma GmbH & Co. KG, Müllheim, Germany) were positioned in a 100 x 12 mm tube rack, the oligonucleotide at a distance of 20 cm from the lamp and the UV filter solution in front of them. In the experiment with one row, the micro-cuvettes were positioned in a 100 x 12 mm tube rack at a distance of 20 cm from the lamp.

c) Determination of photoprotection factors

The determination of the phototprotection factor was measured using always the 10 μM TpT solution in H_2O/MeCN 96:4 + 0.012 M $HNEt_3OAc$, 50 μM UV-filters diluted either in MeOH (apigenin, vitexin) or in H_2O (*p*-coumaric acid, spermine, 5,10-bis(*E*-cinnamoyl) spermine, kuromanin) and 20 μM ds2 (see Chapter 3.5.1).

2 micro-cuvettes (first containing TpT, the second UV-filter): 200 μL TpT is added in a first one and 200 μL of UV-filter is added in a second micro-cuvette. Irradiation of three different series consisting of three UV-filters and a control experiment with pure H_2O were performed at 254 or 312 nm. Aliquots (40 μL) of TpT were collected after 0, 1, 3, 6, 12, 28 and 56 minutes irradiation time and 5 μL were injected in the UHPLC-ESI-HR-QTOF-MS system.

1 micro-cuvette (TpT + UV-filter): 200 μL of TpT were mixed with 160 μL UV-filter and diluted with 40 μL of H_2O. The irradiation of the single micro-cuvette was performed at 254 nm. Aliquots (40 μL) of the solutions were collected after 0, 1, 2, 4, 8, 16, 32 and 64 minutes irradiation time and 5 μL were injected in the UHPLC-ESI-QTOF-MS/MS system.

1 micro-cuvette (ds2 + UV-filter): 10 μL of ds2 were mixed with 16 μL of UV-filter and diluted with 74 μL H_2O. The irradiation of the single micro-cuvette was performed at 254 nm. One aliquot (20 μL) was collected after 150 minutes irradiation time. Procedure of enzymatic digestion: the aliquots were diluted with 80 μL H_2O and 10 μL of buffer (ammonium acetate 200 mM, $CaCl_2$ 100 mM, pH 6. Then 1 μL (1 U) of Nuclease P1 and 1 μL (0.008 U) of calf spleen phosphodiesterase are added. The resulting solution was incubated in a dry-block (Techne Dri-block DB-3D) for 2 h at 37°C. Then, 10 μL of a second buffer (500 mM Tris, 1 mM EDTA, pH 8), 2 μL (0.004 U) of snake venom phosphodiesterase and 5 μL (5 U) of shrimp alkaline phosphatase were added. The samples were incubated in the dry-block at 37°C for two additional hours, and 5 μL were then directly injected in the UHPLC-ESI-QTOF-MS/MS sytem.

3.6 Bibliography

[1] Rozema, J., Björn, L. O., Bornman, J. F., Gaberscik, A., Häder, D. P., Trost, T., Germ, M., Klisch, M., Gröniger, A., Sinha, R. P., Lebert, M., He, Y.-Y., Buffoni-Hall, R., de Bakker, N. V., van de Staaij, J., Meijkamp, B. B., *J. Photochem. Photobiol. B* **2002**, *66*, 2.

[2] Douki, T., Court, M., Sauvaigo, S., Odin, F., Cadet, J., *J. Biol. Chem.* **2000**, *275*, 11678.

[3] Hemminki, K., Koskinen, M., Rajaniemi, H., Zhao, C., *Regul. Toxicol. Pharmacol.* **2000**, *32*, 264.

[4] Sinha, R. P., Sinha, J. P., Gröniger, A., Häder, D.-P., *J. Photochem. Photobiol. B* **2002**, *66*, 47.

[5] Robberecht, R., Caldwell, M. M., *Oecologica* **1978**, *32*, 277.

[6] Stapleton, A. E., Walbot, V., *Plant Physiol.* **1994**, *105*, 881.

[7] Meurer, B., Wray, V., Wiermann, R., Strack, D., *Phytochemistry* **1988**, *27*, 839.

[8] Meurer, B., Wiermann, R., Strack, D., *Phytochemistry* **1988**, *27*, 823.

[9] Meurer, B., Wray, V., Grotjahn, L., Wiermann, R., Strack, D., *Phytochemistry* **1986**, *1986*, 433.

[10] Youhnovsky, N., Bigler, L., Werner, C., Hesse, M., *Helv. Chim. Acta* **1998**, *81*, 1654.

[11] Germ, M., Mazej, Z., Gaberscik, A., Häder, D. P., *J. Photochem. Photobiol. B* **2002**, *66*, 37.

[12] Klisch, M., Häder, D. P., *J. Photochem. Photobiol. B* **2002**, *66*, 60.

[13] Gröniger, A., Häder, D. P., *J. Photochem. Photobiol. B* **2002**, *2002*, 54.

[14] van de Staaij, J., de Bakker, N. V., Oosthoek, A., Broekman, R., van Beem, A., Stroetenga, M., Aerts, R., Rozema, J., *J. Photochem. Photobiol. B* **2002**, *66*, 21.

[15] Megerle, U., Lechner, R., Konig, B., Riedle, E., *Photochem. Photobiol. Sci.* **2010**, *9*, 1400.

[16] Churchwell, M. I., Beland, F. A., Doerge, D. R., *Chem. Res. Toxicol.* **2002**, *15*, 1295.

[17] Snyder, L. R., Kirkland, J. J., Dolan, W., *Introduction to modern liquid chromatography*, 3 ed., John Wiley & Son, Ltd, **2010**.

[18] Zhang, F., Bartels, M. J., Pottenger, L. H., Gollapudi, B. B., Schisler, M. R., *Rapid Commun. Mass Spectrom.* **2005**, *19*, 2767.

[19] Chalmers, J. M., Griffiths, P. R., *Handbook of Vibrational Spectroscopy, Vol. 5*, Wiley: New-York ed., **2002**.

[20] Dolan, J. W., Alsehli, B., *LCGC Europe* **2012**, *25*, 564.

[21] Jengtens, C., Hofmann, R., Guggisberg, A., Bienz, S., Hesse, M., *Helv. Chim. Acta* **1997**, *80*, 966.

CHAPTER 4

DETERMINATION OF THE METHYLATION GRADE OF DNA

4.1 Introduction

Epigenetics are related to many biological phenomena as e.g. biological development/differentiation, cellular differentiation, aging, environmental influences, or diseases (Figure 1). Epigenetic factors consist in stable chemical modifications in a way to affect gene transcription, silencing or activation. They influence the phenotype without any changes in the genotype. Two major epigenetic mechanisms, histone modification and DNA methylation have been described [1-3].

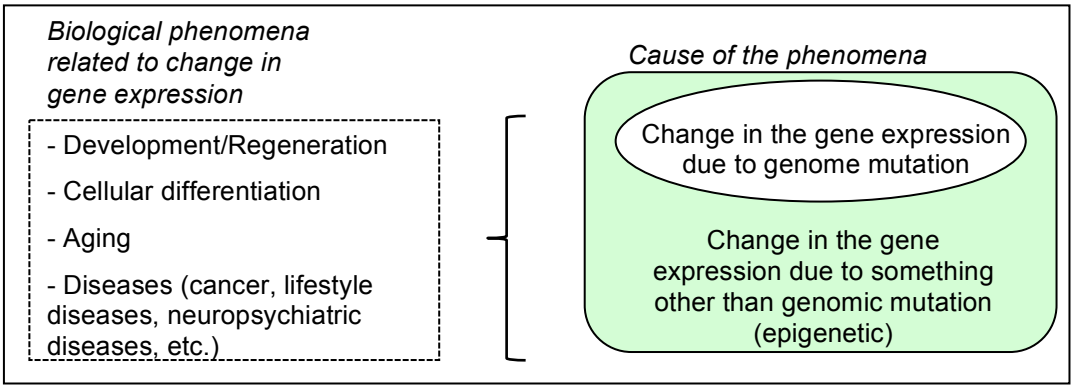

Figure 1: Epigenetics in various biological phenomena (reproduced after [2])

The growing interest in epigenetics is mainly due to a high activity in genome sequencing and in the mechanisms of genome regulation, and is illustrated by an increasing number of publications by a factor of about five the last ten years on that topic [2] (see Chapt. 1.1.2 for more details).

DNA methylation is a fundamental epigenetic modification of gene expression and plays an important role in the regulation of many cellular processes as embryonic development, transcription, chromatin structure, inactivation of X chromosomes, chromosome stability and genomic imprinting [4]. Aberrant DNA methylation has also been associated with human ailments [4]. Cancer is certainly one of the most cited diseases related to DNA methylation in literature [4-7].

As an application example, the increase of the S-adenosyl methionine/S-adenosyl homocysteine (SAM/SAH) ratio (see Chapt. 1.1.3) has been associated with sepsis in rodents [8]. This change implies a deregulation in the methylation process during sepsis. Although the rodent model does not exactly compare with the human one, the data obtained encourage further studies in order to find a correlation between sepsis and SAM/SAH ratio in human patients (See Chapter 5 for application).

A further connection has been noticed between the smoking behavior and its influence on the global DNA methylation [9]. The findings of this study lead to the conclusions that possibly oncological, neuropsychiatric, or addictive diseases could be affiliated to DNA methylation.

Various analytical methods have been developed to quantify the methylation grade in human and in calf thymus (CT) DNA. They are mainly based on GC-MS, HPLC-UV, and HPLC-MS (Table 1). A relatively broad range of methylation grade could be determined for human leukocytes (4.0 – 5.4 mol%) and CT DNA (4.75 – 8.1 mol%). Only a few of these methods show low standard deviations (std dev) or coefficients of variation (CV's) synonymous of high precision. Low accuracy in DNA methylation grade suggests low precision measurement because these analytical methods are not necessary appropriate to determine it.

From all the procedures based on GC, accurate determination of the methylation grade have been obtained for CT DNA with flame ionization detector (FID) [10] and for human DNA with electron capture detector (ECD) [11]. These methods are sensitive and low amounts of DNA, below 1 µg, are required. However, the major drawback of both methods is the time-consuming sample preparation, in particular derivatization and solid phase extraction steps [11]. Further, a long time analysis of around 25 min, is inappropriate for handling numerous samples.

HPLC-UV methods lead also to good and excellent accuracy for CT and human leukocyte DNA, respectively [12]. However these methods have also their drawbacks

in long analysis times (23 to 70 min), required several µg of DNA, and a dangerous procedure of DNA hydrolysis with hydrofluoric acid. A higher sensitivity and best time analysis of 12 min are achieved with MS detection, in particular in the MS/MS mode (Table 1).

Analytical method	Methylation grade found in human leukocyte DNA [mol% ± std dev]	Methylation grade found in CT DNA [mol% (CV %)]	Analysis time [min]	Amount of DNA requested [µg]	Lit.
GC-FID	–	6.75 (3.0)	Not indicated	< 1	[10]
GC-ECD	4.04 ± 0.26	5.7 (8.2)	25	0.35	[11]
HPLC-UV	–	6.5 (3.8)	> 23	Not indicated	[13]
HPLC-UV	–	8.1	> 17	1	[14]
HPLC-UV	–	8.1	-	-	[15]
HPLC-UV	–	6.65 (15)	70	< 10	[16]
HPLC-UV	4.56 ± 0.05	–	70	1 - 5	[12]
^{32}P-base analysis	–	4.76 (5.7)	1080	1	[17]
Fluoroimmuno-assay	–	4.75	-	-	-
EI-MS	–	6.43	-	1 - 20	[18]
GC-EI-MS	–	5.7 (7)	> 10	0.2	[19]
GC-EI-MS	–	6.6 (6.5)	> 5	1	[20]
GC-EI-MS	5.0 - 6.0	–	> 6	5	[21]
LC-ESI-MS	5.4 ± 0.1	–	13	1	[22]
LC-ESI-MS/MS	**4.0 ± 0.44**	**6.5 (3.5)**	12	1	[23]
LC-ESI-MS/MS	4.7 ± 0.8	–	14	1	[24]

Table 1: Analytical methods used for the quantification of DNA methylation. Performances are presented as mean ± standard deviation or mean (inter-assay CV) in mol% (Reproduced after [23]).

Superior sensitivity and high throughput were the reasons to combine an high performance liquid chromatography (HPLC) and ESI-MS/MS has been chosen for the development of a method to determine the methylation grade in human leukocyte DNA and CT DNA. The best values obtained were 4.0 ± 0.44 mol% methylation grade for healthy humans and of 6.5 % (CV 3.5%) for calf thymus DNA [23].

In biological variability studies, a large number of patient and control samples have to be measured in order to have enough data for statistical relevance.

The main goal of this project was to develop a robust analytical method to quantify the absolute amount of 5-methylcytosine in DNA samples based on UPLC-ESI-HR-QTOF-MS using a maXis UHR-QTOF coupled to an UPLC system. This method would be then used to find a relationship between the methylation grade of DNA and various diseases as e.g. sepsis, alcoholics, and cancer. *Kok et al.*

developed a method for the determination of the methylation grade of CT and human DNA [23]. Our developed method has to be as good as the published data, and, if possible, in a shorter time analysis for an increased sample throughput.

4.2 Development of the quantification method

4.2.1 Transfer to UHPLC and high-resolution QTOF MS

In the most accurate method developed by Kok and coworkers, approximately 1 µg of DNA was hydrolyzed under acidic conditions with formic acid resulting in the free bases. Because the 5-position of cytosine is the only reactive site that has been observed in DNA methylation, the global DNA methylation was only determined by quantifying cytosine and 5-methylcytosine. They found a methylation grade of 4.0 ± 0.44 mol% for healthy humans and 6.5 % (CV 3.5 %) for calf thymus DNA [23]. Detection and quantification of the hydrolysis products were performed by LC-ESI-MS/MS, allowing fast and sensitive analyses without derivatization.

The first step was to transfer the method to an UHPLC system in order to increase the sample throughput while maintaining a good chromatographic separation, using same solvents (H_2O and MeCN) and buffer (nonafluoro-1-pentanoic acid, NFPA). The major modifications were the selection of an Acquity BEH C18 stationary phase with smaller particle size (1.7 compared to 3.5 µm), smaller column dimensions (inner diameter of 2.1 instead of 4.6 mm), and an adapted flow rate (0.5 instead of 1.0 mL/min).

The UHPLC system was connected to Bruker maXis high-resolution mass spectrometer (QTOF) equipped with an electrospray ionization source. The instrument parameters were optimized with a solution of commercially available cytosine. Due to the insufficient MS/MS sensitivity of the QTOF mass analyzer for fragment ions below *m/z* 100, data were collected in the full scan mass range instead of the published multiple reaction-monitoring mode (MRM). Quantification was finally achieved with an improved selectivity using integration of high-resolution extracted ion chromatograms (HR-EIC) with ± 0.05 *m/z* width.

Unfortunately, the NFPA buffer used in this method had to be replaced in spite of excellent performances in terms of peak shape, width, sensitivity, and speed. This ion-pairing agent used for separating the highly hydrophilic cytosine and 5-

methylcytosine on a C18 reversed phase column lead to major contamination of the UHPLC-MS instrumentation in the negative ionization mode. A huge effort in flushing the solvent pumping system was afterward necessary to reduce the intensity of the long-lasting ESI-MS signals of deprotonated NFPA and restore acceptable analytical performances.

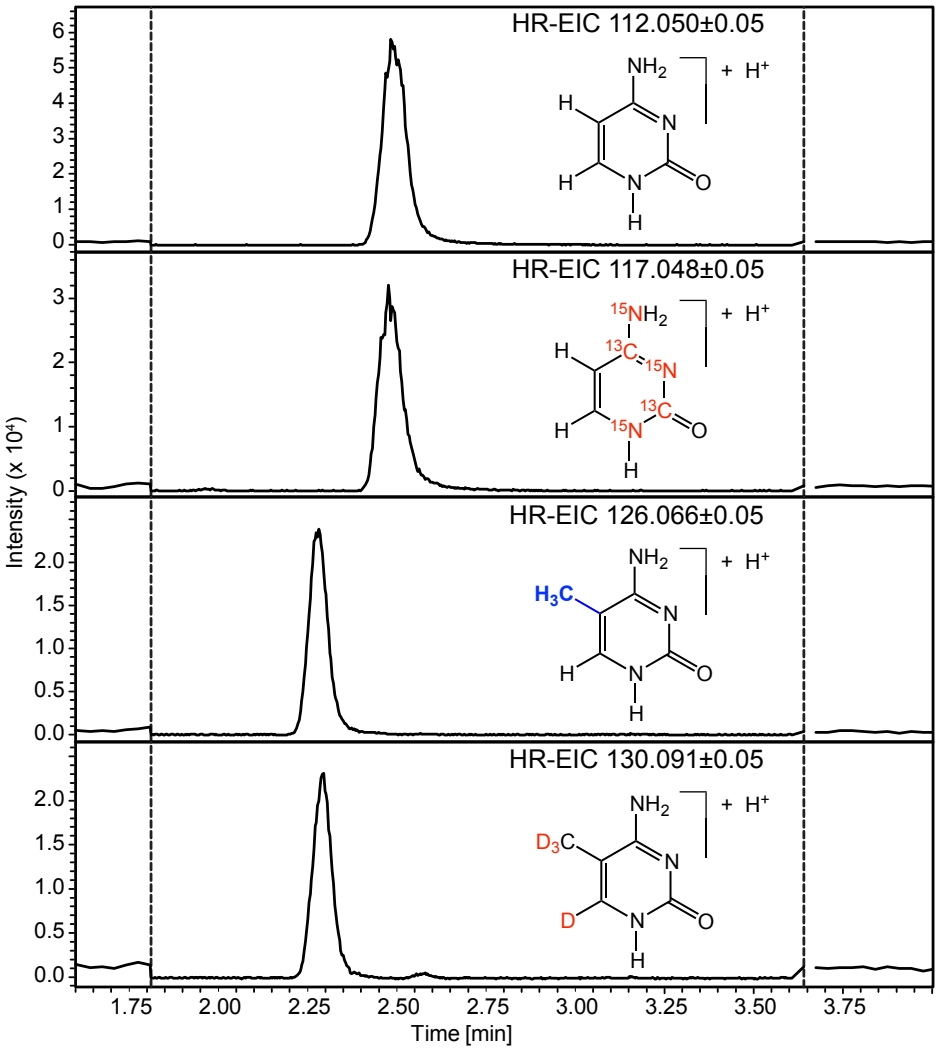

Figure 2: HR-EIC of cytosine and 5-methylcytosine and their respective labeled internal standards 2,4-[$^{13}C_2$,$^{15}N_3$]-cytosine and 5',5',5',6-[$^{2}H_4$]-5-methylcytosine

Several C18 endcapped or non-endcapped reversed phase columns have consequently been tested with various solvents and buffers, in vain. Finally, normal phase chromatographic conditions including an Acquity BEH Amide column, H_2O and MeCN as solvent, and 10 mM NH_4HCO_2 + 0.125 % HCOOH as additives were

fulfilling the requirements for the separation of cytosine and 5-methylcytosine within less than 5 minutes (Figure 2)[2].

The robustness and sensitivity of the optimized UHPLC and ESI-HR-QTOF-MS method was then tested by measuring the methylation grade of 10 CT DNA samples prepared from the same stock solution. To obtain maximal accuracy, internal standards (ISTD), consisting of 2,4-[$^{13}C_2$,$^{15}N_3$]-cytosine and 5',5',5',6-[$^{2}H_4$]-5-methyl-cytosine, were added to the DNA samples prior hydrolysis with concentrated formic acid, according Kok's procedure [23]. Cytosine and 5-methylcytosine were quantified by means of the Bruker QuantAnalysis® software using calibration curves with 6 points. The analysis of the 10 samples of 1 µg CT DNA was then repeated a second time and the amounts recalculated with the previously used calibration curve in order to test the stability of the analytical system. The mol% ratios of cytosine and 5-methylcytosine shown in Figure 3 were finally calculated from these absolute amounts (see Chapt. 4.4.4)

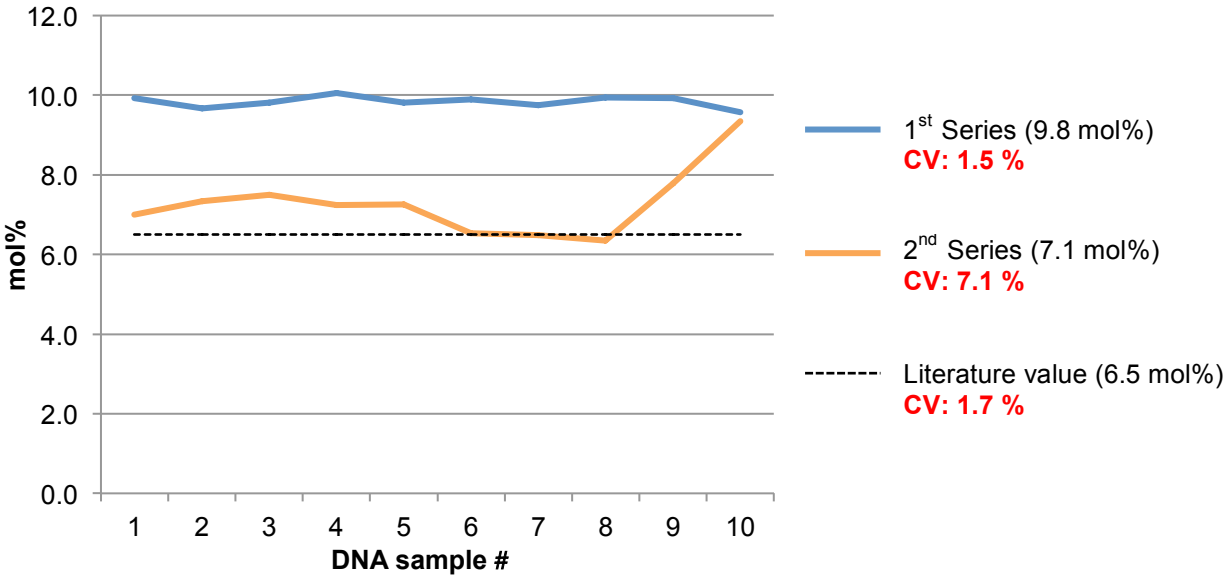

Figure 3: Double determination of methylation grade (mol%) of 10 CT DNA samples with the newly developed UHPLC-ESI-HR-QTOF-MS method by applying the same calibration curve. 1st injection series in blue, 2nd in orange; mean value in brackets, CV in red, and literature value as black dashed line.

Obviously, the accuracy and the coefficient of variation varied a lot. The dual determinations were therefore repeated five times including new calibration curves and using the same commercially available CT DNA. Again, the results were not

[2] Method developed according to Waters® Application Note WA64081, Acquity UPLC BEH Amide Column, Application notebook, 2009, p. 31

reproducible with degrees of methylation varying between 6.5 and 12.7 %, and CVs between 1.4 and 14.8 %.

Comparing the data sets obtained, it seemed that the uncertainties could arise from the instrumental setup. The first handling of the troubleshooting was to exclude improper sample preparations, unreliable calibration curves, and lacking hydrolysis. A series of 10 hydrolyzed CT DNA samples was therefore sent to Kok's laboratory in Holland in order to determine their degree of methylation and CVs. The 10 samples were double-checked using a unique calibration curve, leading to an average degree of methylation of respectively 7.12 % (CV of 1.45 %) in the first and of 7.09 % (1.58 %) in the second series. Therefore, there is no reason to distrust the preparation of the samples and the solutions used for calibration.

The next step was to localize the origin of the discrepancies observed in the UHPLC-ESI-HR-QTOF-MS method. Astonishingly, the poor accuracy could not be correlated with the variable CV's. Looking at the analytical procedure, the DNA concentrations were checked prior hydrolysis with a NanoDrop instrument (± 2 % accuracy), peaks corresponding to cytosine and 5-methylcytosine are base-line separated (see Figure 2), standard ESI conditions including widely used solvents (H_2O, MeCN, and NH_4HCO_2 buffer) were chosen in combination with most appropriately labeled internal standards and a 6 point calibration curve used.

The accuracy and stability of the UHPLC-ESI-HR-QTOF-MS method, including phenomena of adsorption, carry over, and decomposition, were then checked with the determination of the absolute amount of cytosine and 5-methylcytosine of the hydrolysis of a unique CT DNA sample (1 µg).

After complete hydrolysis of the DNA sample, the measured amounts of cytosine and 5-methylcytosine can be compared to the theoretical value. CT DNA purchased from Sigma-Aldrich was certified to contain 42 % of GC base pairs [25]. A complete hydrolysis of 1 µg DNA would theoretically gives 72 ng of cytosine[3]. This cytosine is partially methylated (6.5 mol% according to published data [23]) leading to calculated absolute amounts of cytosine and 5-methylcytosine of 66.7 and 5.3 ng, respectively.

[3] $\frac{1\,\mu g\ DNA \times 42\,\% \times 111.04\ g/mol\ M_R^{cytosine}}{650.09\ g/mol\ M_R^{GC}}$

Average masses of 67.3 ± 4.4 and 7.1 ± 0.3 ng were obtained for the determination of cytosine and 5-methylcytosine in this unique sample. The intra-assay stability with CV values of around 5 % can be considered as acceptable, although better precision was expected for the analysis of a unique sample. As comparison, Kok's laboratory reached precisions below 2 % for the determination of the methylation grade in 10 CT DNA samples.

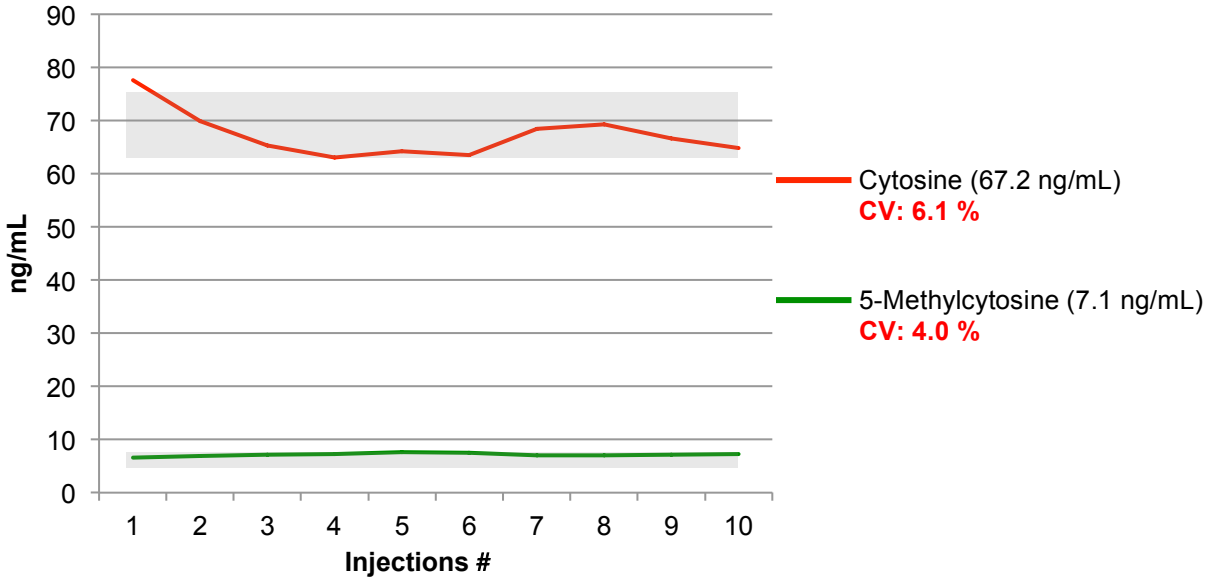

Figure 4: Absolute amounts of cytosine and 5-methylcytosine determined 10 times from the hydrolysis of one CT DNA sample (1 µg). The mean values are shown in brackets, the intra-assay coefficient of variation in red, and the std dev in grey

The average amount of 67.2 ng cytosine obtained from the UHPLC-ESI-HR-QTOF-MS is extremely close to the theoretical value. However, the measured quantity of 5-methylcytosine is clearly above the theoretical one (7.1 ± 0.3 compared to 5.3 ng; + 33 %). This amount lead to a degree of methylation of 8.5 mol% that is definitively higher than the expected value of around 6.5 to 7 mol%.

As for the determination of the methylation grade in 10 CT DNA samples performed previously, the CV values do not explain the mismatch. A inappropriate preparation of the 5-methylcytosine standard solutions used for the calibration curve was further considered and rejected for two main reasons: (1) The calibration curve with 6 points between 1 and 16 ng showed an excellent correlation coefficient (R = 0.999871, see Figure 5) and (2) exactly the same standard solutions were used in Kok's laboratory and the values of methylation grade obtained there were within the expectations (7.1 mol%, CV of 1.45 %).

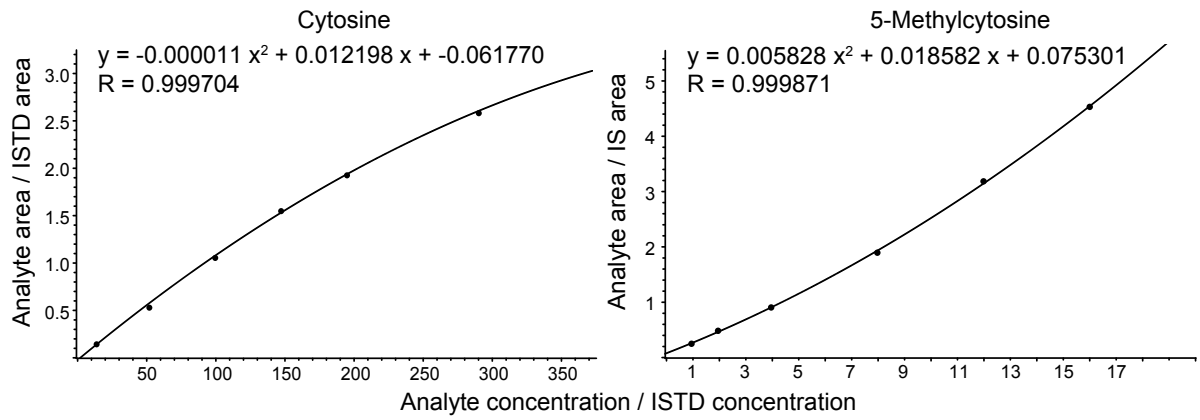

Figure 5: Calibration curves obtained for cytosine and 5-methylcytosine with the maXis QTOF expressed in relative ng amounts related to corresponding relative signal areas

To conclude, the method transfer failed because of a lack of reproducibility in terms of accuracy and precision (CVs). Obviously, the DNA methylation grades obtained from the QTOF are random in spite of the use of the most appropriate labeled ISTDs and of good calibration curves. As miscarried sample preparations or calibration solutions can be excluded, a fundamental problem of mass analyzer and ion response has to be considered. The use of a QTOF mass analyzer in full scan mode is the major difference in comparison to the published method based on multiple reaction monitoring (MRM) data acquisition with triple quadrupole mass spectrometer, nowadays the gold standard in quantitative determinations. Therefore, further MS detection techniques will be considered.

4.2.2 Evaluation of mass analyzers

The Bruker maXis QTOF ™ mass analyzer presented above was principally developed for measuring 'large' charged molecules. In the case of cytosine and 5-methylcytosine, quantification of ions below *m/z* 130 is asked for. Special dedicated instrument tuning was required for measuring in such a low mass range and these extreme adjustments may have caused unexpected problems including e.g. non-reproducible ion transmission and response.

Further mass analyzers were then evaluated in order to define which one is the most appropriate to quantify DNA methylation in terms of precision and accuracy. At the same time, it should also be possible to find out whether the poor data quality is related to ion suppression, detector saturation, or data processing issues.

Next to the Bruker maXis™ QTOF, a Bruker HCT™ ion trap and an AB Sciex API 3200 Qtrap™ linear ion trap running in the triple quadrupole acquisition mode were chosen in order to have different kinds of mass analyzers, acquisition modes (full scan or MS/MS, Chapt. 1.2.3) and processing software. Electrospray ionization and standardized chromatographic conditions including the previously optimized UHPLC method (see Chapt. 4.2.1) were chosen each time in order to simplify data assessment. The selected MS-acquisition conditions can be summarized as follows:

- *QTOF* acquisitions performed in the full-scan mode (*m/z* 0-200) and chromatograms extracted at high resolution (HR-EIC ± 0.05 *m/z*) to increase method selectivity and sensitivity (enhanced signal-to-noise ratio).
- The *ion trap* used in the full-scan mode (*m/z* 0-200, ± 0.1 *m/z*). The scan rate was too low to acquire all four MS/MS transitions in MRM mode. In this case, only one data point per chromatographic peak and MRM transition was obtained, which is definitively not sufficient for quantitative determination.
- Quantitative analyses on the *Qtrap* performed in the most selective and sensitive MRM mode. The published MS/MS transitions from *m/z* 112.10 to 95.10, 117.10 to 99.09, 126.10 to 109.108, and 130.10 to 113.10 were chosen for the detection of cytosine, 2,4-[$^{13}C_2$,$^{15}N_3$]-cytosine, 5-methylcytosine, and 5',5',5',6-[$^{2}H_4$]-5-methylcytosine, respectively.

a) Reproducibility of the ratio of peak areas

In order to have a reliable appraisal of the mass analyzer ion responses, a single standard solution containing a defined ratio of cytosine and 5-methylcytosine was prepared. Concentrations of 1000 and 40 ng/mL, respectively, corresponding to a ratio of 3.6 mol% were chosen to be comparable to the values obtained after hydrolysis of 1 µg human DNA. Reproducibility of ten measurements was then evaluated on each instrument by comparing the peak areas of cytosine and 5-methylcytosine under the same UHPLC conditions (column, solvents, gradient and flow). The chromatograms were processed and integrated according to the mass analyzer, and each integral ratio was plotted for each injection (Figure 6).

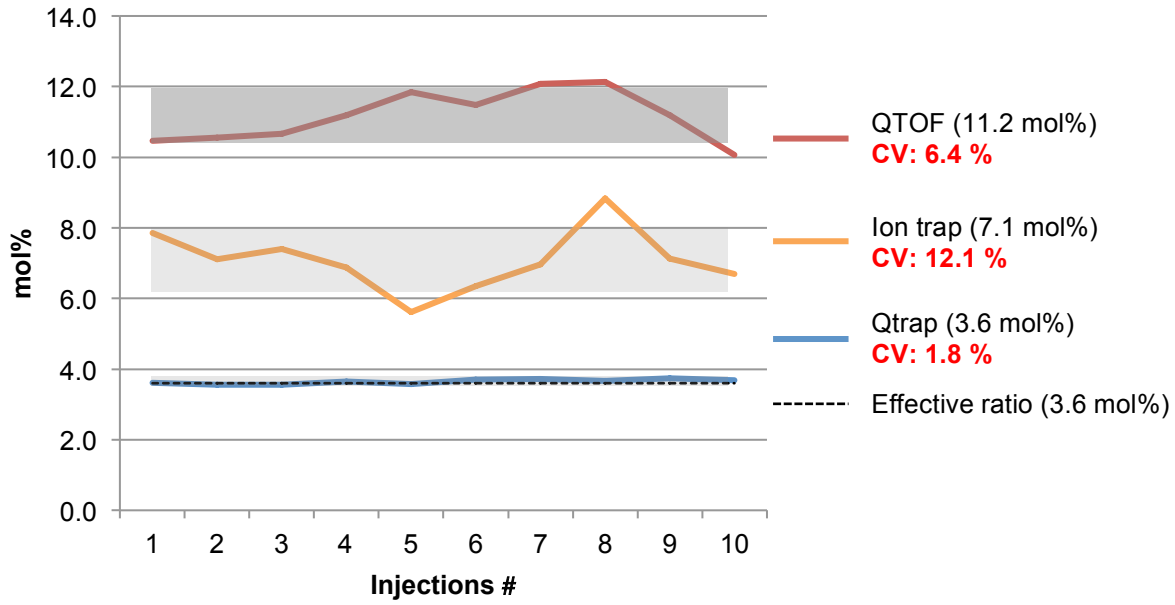

Figure 6: Reproducibility and precision of 10 injections of a solution containing cytosine/5-methylcytosine standards in a 3.6 mol% ratio (black dashed line) and measured with the maXis QTOF, HCT ion trap and 3200 Qtrap mass analyzers. Mean ratios are given in brackets, intra-assay CV in red, and std dev in grey.

Mass spectrometers are concentration sensitive detectors. Assuming uniform ion response for cytosine and 5-methylcytosine, an integral ratio of 3.6 mol%[4] should be obtained, the same as the effectively weighed molar ratio. Depending on the instrumentation used, these ratios varied obviously a lot between 3.6 and 11.2 mol%, which is not a surprise as the ion response of the analytes were not expected to be identical. However, the huge disparity of the CVs was unforeseen because in each case, a unique sample was measured 10 times consecutively under exactly the same conditions and the ratio of the two components expressed in relative values of both.

The measured ratios of integrals highlighted the excellent reproducibility of the Qtrap (CV of 1.8 %). Also the averaged integral ratio is matching perfectly (3.6 mol%), although MS/MS transitions were considered without ISTD corrections of the ion response. Furthermore, the precision of the QTOF can be rated as sufficient (6.4 %) and that of the ion trap as poor (12.1 %). These precisions obtained from QTOF and ion trap analyses are not proportional to the accuracy and worse than the precision achieved for the integration of cytosine and 5-methylcytosine separately (e.g. CVs of respectively 3.9 and 3.5 % for the QTOF, see Table 2). This is shocking because a better precision was expected for repeated determinations of the ratio of two

[4] The HR-EIC peak integrals for 5-methylcytosine and cytosine correspond to the nmol/mL of each analyte, since MS are concentration sensitive detectors. The ratio of both integrals give us the mol% of 5-methylcytosine in the sample.

components compared to absolute peak integrals, since the variability due to differences in injected amounts is not relevant when ratios are measured.

	Qtrap 3200	maXis QTOF	HCT ion trap
Cytosine	1.3	3.9	5.4
5-Methylcytosine	1.3	3.5	9.4

Table 2: Intra-assay coefficients of variation (%) obtained for integrating the signal of 10 injections of a standard solution containing 1000 ng/mL cytosine and 40 ng/mL 5-methylcytosine and measured by UHPLC-ESI-MS

There are several reasons that could explain the divergences in the ratio of absolute peak integrals shown in Table 2, including e.g. different ionization efficiencies, discrimination in transmission of ions below *m/z* 140 (particularly concerning the QTOF), and irregular matrix effects. The determination of absolute concentrations using appropriate labeled internal standards should therefore annihilate such discrepancies and clearly increase precision and accuracy.

b) Reproducibility of concentration ratios after ISTD correction

As next, signal responses of the mass analyzer have been transformed into absolute analyte concentrations. Differences between integrals in terms of ion response and matrix effects are compensated with signal intensities of the ISTDs that are themselves correlated to fix concentrations. The mol% ratio between two analytes was then obtained after conversion of the absolute amount (ng/mL) of cytosine and 5-methylcytosine in concentrations (nmol/mL).

In quantitative determination with MS, the use of labeled internal standards is the most appropriate way because analyte and ISTD have quasi identical ion responses (in full scan and MS/MS mode), same retention time, and undergo therefore same matrix effects (see chap. 1.2.3 c) for more details). For these reasons, known amounts of labeled internal standards, 2,4-[$^{13}C_2$,$^{15}N_3$]-cytosine and 5',5',5',6-[$^{2}H_4$]-5-methylcytosine (1000 and 50 ng/mL, respectively) were added to the sample used previously.

The QTOF, ion trap and Qtrap mass analyzers were tested 10 times again under the same chromatographic and MS conditions with this unique solution of standards and ISTDs. The peak integrals of cytosine and 5-methylcytosine were then converted to absolute concentrations using the signal of their corresponding labeled ISTD. The ratios were finally expressed in mol% (see Figure 7).

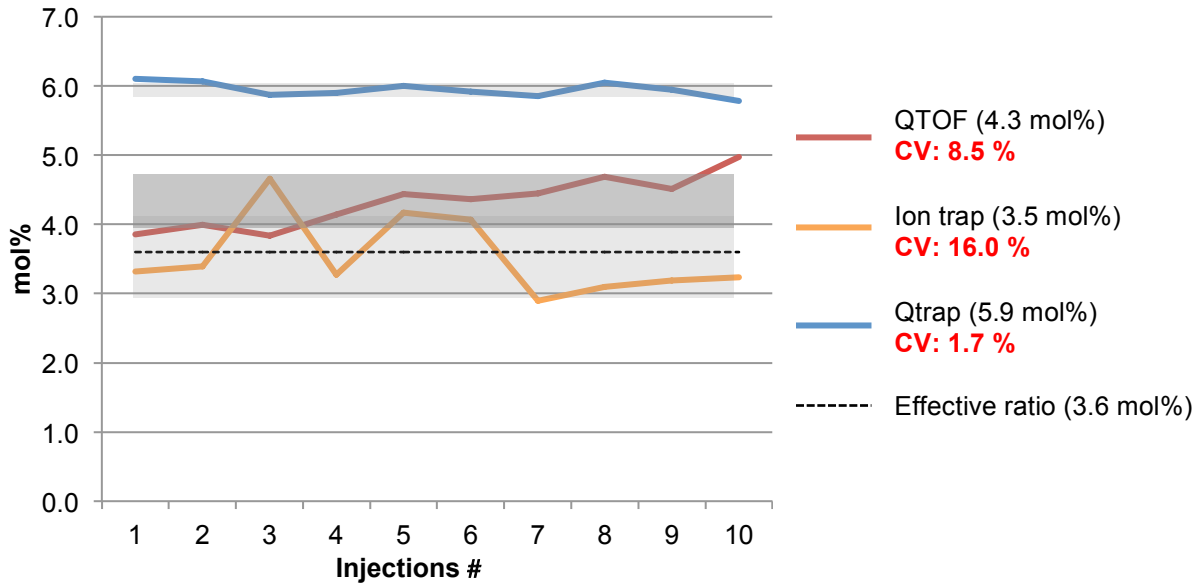

Figure 7: Reproducibility and precision of 10 injections of a single solution containing standards of cytosine and 5-methylcytosine prepared in a 3.6 mol% ratio (black dashed line) and their corresponding labeled ISTD. Analyses were performed using the maXis QTOF, HCT ion trap and 3200 Qtrap mass analyzers. Mean ratios are given in brackets, intra-assay CV in red, and std dev in grey.

ISTDs were added in the sample because they increase the precision of the results and allow an estimation of the absolute amounts of the analytes. One-point calibration methods make only sense since concentrations of analytes and ISTD are identical (cytosine and 2,4-[$^{13}C_2$,$^{15}N_3$]-cytosine, 1000 ng/mL) or comparable (40 ng/mL 5-methylcytosine and 50 ng/mL 5',5',5',6-[$^{2}H_4$]-5-methylcytosine). They cannot be used for real samples where the unknown amount is varying. In this case, standard procedure with a calibration has to be used.

The results obtained surprisingly diverge. On one hand, the Qtrap data is still excellent in terms of precision (CV of 1.7%), but the average ratio has been shifted from the effective 3.6 mol% to 5.9 mol%. On the other hand, the ion trap leads to an excellent ratio of 3.5 mol%, however with inacceptable precision (CV of 16 %), value that is even worse than without ISTD (12.1 %). Data qualities obtained from the QTOF were average, with 4.3 mol% instead of 11.2 % integral ratio. The CV of 8.5 % (6.4 %) was worse with an evident drift from the first to the 10th injection (see Figure 7).

Addition of ISTD leads to better values of methylation grade (ion trap and QTOF) but not for CV's. Qtrap shows still a very good CV but a poor accuracy. This is probably due to the one-point calibration procedure.

c) Selection of the mass analyzer

Criteria of accuracy and precision have to be considered for the selection of the most appropriate mass analyzer.

With a QTOF and an ion trap instrument, determination of the ratio of two integrated chromatographic peaks lead to imprecision beyond the tolerance whether a ISTD was used or not. This problem was revealed with the repeated analysis of a unique sample under identical chromatographic conditions. The use of an ISTD allowed correlation of the ion response to an absolute concentration and therefore improved the accuracy but, surprisingly, not the precision of the method (e.g. with the QTOF, CV of 6.4 and 8.5 % were obtained without and with ISTD, respectively, see Table 3). The poor reproducibility of integral ratios was confirmed by the analysis of the same sample on a second maXis QTOF instrument in the Bruker application's laboratory. Furthermore, on-flow ESI-MS analyses of two further analytes, caffeine and theobromine, detected in a higher masse range (*m/z* of 191 and 185, respectively) lead also to such unexpected and inexplicable mismatches.

A) **5-Methylcytosine/Cytosine integral ratio in mol% (1 vial, 10 injections)**

	Effective ratio	Qtrap 3200 (MRM)	maXis QTOF (FS)	HCT ion trap (FS)
5-Methylcytosine [mol%]	**3.6**	3.6	11.2	7.1
CV [%]		1.8	6.4	12.1

B) **5-Methylcytosine/Cytosine corrected in mol% (1 vial, 10 injections)**

	Effective ratio	Qtrap 3200 (MRM)	maXis QTOF (FS)	HCT ion trap (FS)
5-Methylcytosine [mol%]	**3.6**	5.9	4.3	3.5
CV [%]		1.7	8.5	16.0

Table 3: Accuracy and precision of the ratio between cytosine and 5-methylcytosine expressed in A) integral ratio and B) in mol% after ISTD correction

The Qtrap mass analyzer provided clearly the most precise data (CV of 1.8 without and 1.7 % with ISTD). The main distinction with the QTOF and ion trap method was the use of MRM instead of FS acquisition mode. This could explain the variability of the measurements. This hypothesis was refuted with the determination of integral ratios of two components measured with a TSQ mass. The results obtained on the Waters TQD were however even worse with a CV of 12.8 % after ISTD correction (1 sample at 7.1 mol% ratio of cytosine/5-methylcytosine, 10 injections).

From the results shown in Table 3, it is possible to conclude that variance is neither specific to the type of instruments (triple quadrupole, ion trap or QTOF), nor depending on the type of MS acquisition method (MRM or full scan).There was no way to tune the QTOF or the ion trap in order to obtain satisfying data, which was confirmed by the Bruker application laboratory. A possible explanation could be related to the detectors or to the analog to digital conversion that is different in AB Sciex compared to Bruker and Waters instruments.

Because the highest precision was achieved on an AB Sciex Qtrap 3200, the determination of the methylation grade of DNA was further validated on this instrument.

4.2.3 Validation

The method for determining the methylation grade of DNA based on UHPLC coupled to a Qtrap mass analyzer in the MRM mode was validated with samples containing 1 µg of CT DNA (prepared from a stock solution) and labeled cytosine and 5-methylcytosine ISTDs that were hydrolyzed with concentrated formic acid. The internal standardization is certainly the most appropriate procedure since loss of sample, decomposition, matrix effects, and ion suppression effects are compensated.

The analysis of a series of 10 samples was repeated nine times in order to calculate intra- and inter-assay coefficients of variation. For quantitative determinations, two calibration curves with 6 points were prepared in a range of 100 to 3000 ng/mL and 10 to 160 ng/mL for cytosine and 5-methylcytosine, respectively. Three series of samples were prepared simultaneously and analyzed in a joint sequence. The data recorded lead to excellent calibration curves with quadratic coefficients of correlation often close to 1 as presented in Figure 8. Quadratic calibrations curves are often used with MS detectors due to their non-linear ion responses over the concentration range.

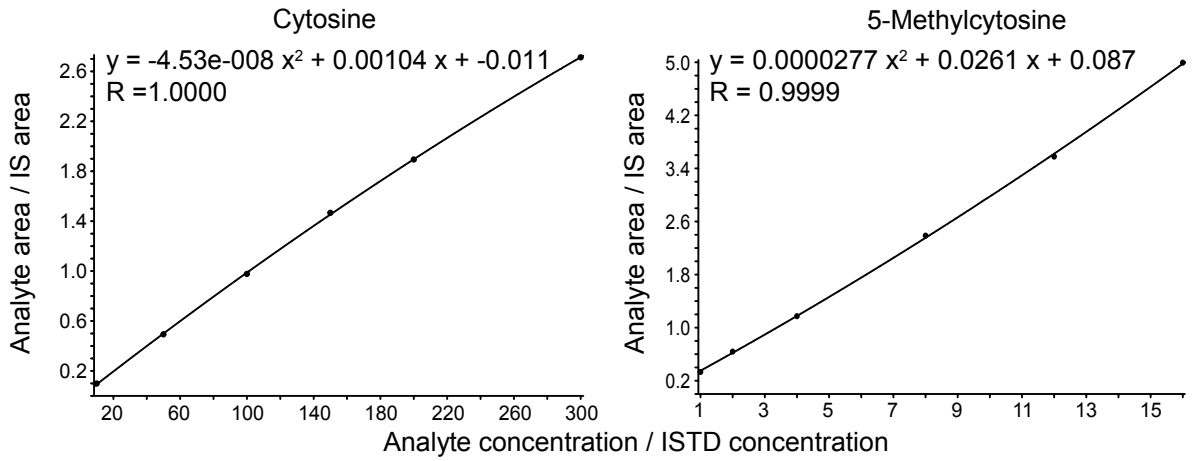

Figure 8: Quadratic internal calibration curves for the quantification of cytosine and 5-methylcytosine in CT DNA with the Qtrap mass analyzer

After calculating the absolute amount of cytosine and 5-methylcytosine in each sample, the masses were converted in mol and the degrees of methylation expressed in mol%. All nine series of quantitative determinations of the methylation grade of CT DNA are presented in Table 4.

	serie1	serie2	serie3	serie4	serie5	serie6	serie7	serie8	serie9
	6.573	6.658	7.042	6.804	6.767	6.421	6.929	7.018	6.883
	6.570	6.817	6.938	7.001	6.564	6.359	6.964	6.979	6.575
	6.585	6.928	7.284	6.792	6.652	6.649	7.139	6.701	6.788
	6.717	7.079	7.044	6.910	6.430	6.510	6.975	6.765	6.885
	6.498	6.684	6.821	6.738	6.858	6.706	6.919	6.799	7.036
	6.784	6.684	6.932	6.724	6.425	6.762	7.053	6.608	6.948
	6.749	6.762	7.220	7.146	6.549	6.639	7.087	7.016	6.880
	6.802	6.649	7.043	6.969	6.547	6.505	7.100	7.045	6.960
	6.681	6.873	6.649	6.702	6.568	6.647	6.929	6.923	7.045
	6.910	6.774	6.723	7.010	6.464	6.511	7.039	6.843	6.845
mean	6.687	6.791	6.970	6.880	6.582	6.571	7.013	6.870	6.885
std dev	0.129	0.138	0.202	0.149	0.141	0.129	0.080	0.150	0.135
CV [%]	1.930	2.032	2.892	2.171	2.144	1.966	1.143	2.182	1.967

Table 4: Determination of the methylation grade in nine series of ten CT DNA samples used for the calculation of intra- and inter-assay coefficients of variation

To assign the overall intra-assay precision of the method, the CV's of all nine series were plotted and the mean CV calculated. The average of 2.0 % obtained (see Figure 9) is close to the literature value of 1.7 % [23].

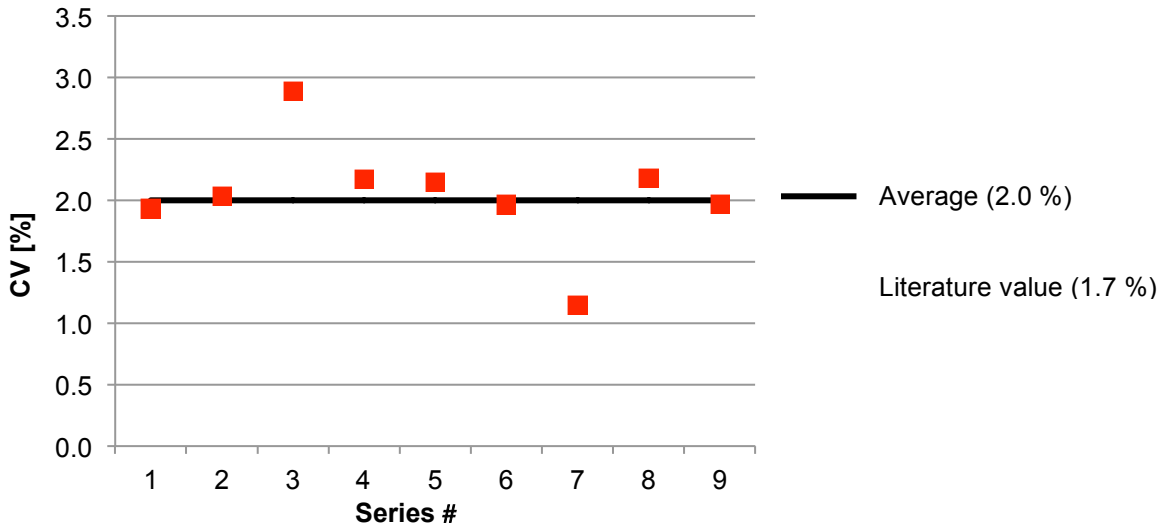

Figure 9: Intra-assay validation of the method for determination of the methylation grade of CT DNA (9 series of 10 samples)

Regarding the inter-assay stability, the average methylation values were plotted for all nine series including relative errors (see Figure 10). A mean methylation grade of 6.8 mol% (CV of 2.4 %) was obtained for the CT DNA reference. These values are close to the published values of 6.5 mol% (3.5 %) and 7.1 mol% (1.5 %) obtained from the same samples measured in Kok's group.

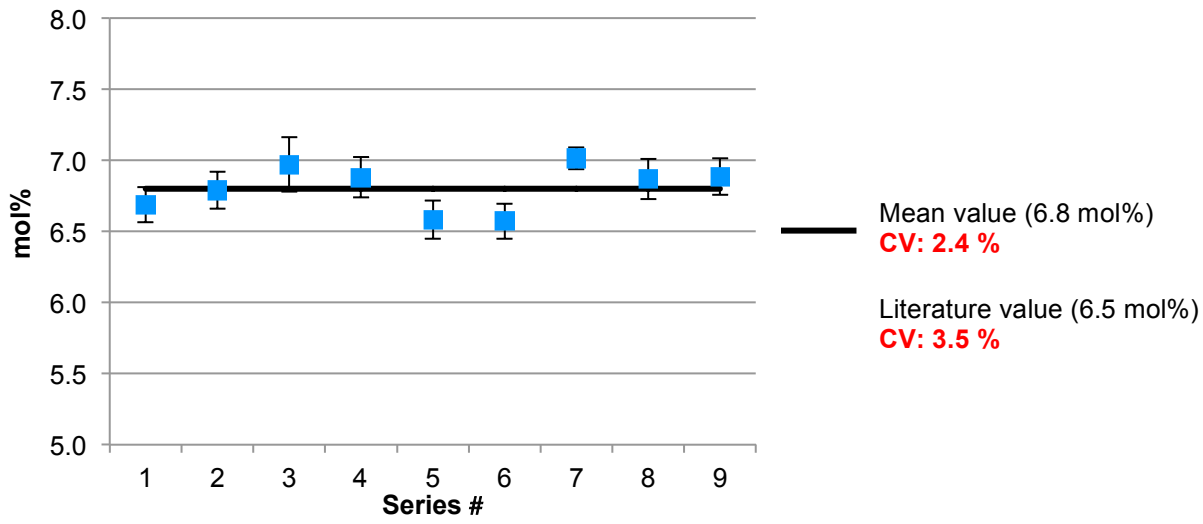

Figure 10: Inter-assay validation of the methylation grade of CT DNA with 9 series of 10 samples

The good results of the validation reflect the quality of the developed quantification method, in particular sample preparation procedure and instrument precision and stability. This method is therefore suitable for the determination of the DNA methylation grade of patients, and to trace the possible relation between methylation and infections or diseases.

4.3 Conclusion

During the method development, it has been demonstrated that the choice of the MS instrument is crucial in order to get accurate and reproducible data. Inexplicable results obtained from the first developed method on a QTOF mass analyzer revealed to be inaccurate. It has been shown that unstable ratios of peak integrals were obtained for repeated analyses of a unique sample containing two analytes. Neither precision, nor accuracy were enhanced by addition of an internal standard. Similar problems were also observed with ion trap or triple quadrupole mass analyzers from the same (Bruker) or from other manufacturer (Waters, ABSciex) operating in different acquisition modes (full scan or MS/MS). Therefore, it seems that the problems could arise from the detector and/or the analog to digital conversion.

A reliable method based on UHPLC-Qtrap-MS/MS has been developed to determine the methylation grade of DNA. This new method requires 1 µg of material and has a time analysis of 8 min per sample. This is at least 33% faster than the best published method developed by Kok and coworkers [23]. The accuracy of 6.8 mol% of methylation found in CT DNA is really close the published value of 6.5 mol% [23], with a better inter-assay precision of 2.4 % obtained for the analysis of 9 series of 10 CT DNA, compared to the published one (3.5 %). The 2 % intra-assay is also comparable to the literature value (1.7 %). This proves that our method can be chosen to check if infections or diseases like e.g. sepsis, cancer, and alcoholism influence the methylation grade of human DNA (see Chapt. 5 for application).

This method could also be further used for the quantification of other damages to DNA as oxidative or UV induced mutations. A major drawback could be the selection of an appropriate internal standard or related substance.

4.4 Experimental part

4.4.1 Chemical, standards and reagents

Chromasolv® LC-MS grade acetonitrile (MeCN) and methanol (MeOH), formic acid (HCOOH, MS grade) and ammonium formate (NH_4HCO_2, MS grade), cytosine (99%, puriss), 5-methylcytosine hydrochlorid (99%, puriss), 2,4-[$^{13}C_2$,$^{15}N_3$]-cytosine (99 at.% ^{13}C; 98 at.% ^{15}N), and calf thymus DNA (Type I, "Highly Polymerized"; 42 % GC content, sodium salt) were obtained from Sigma-Aldrich (Buchs, Switzerland). 5',5',5',6-[$^2H_4$]-5-methylcytosine (99.1 at.% ^2H) was purchased from Dr. Ehrenstorfer (Augsburg, Germany). LC-MS grade H_2O (< 3 ppb) was obtained by purification of deionized H_2O with a MilliQ gradient apparatus equipped with a BioPack® ultrafiltration module (Millipore, Milford, MA, USA).

4.4.2 Preparation of standard solutions

All standard (STD) and internal standard (ISTD) solutions were prepared from a stock solution (SS) at a concentration of 100'000 ng/mL (1 mg of substance weighted accurately in 10 mL MeCN/MeOH 75:25). Summarized in Table 5, the procedure and dilution steps for making the solutions used for evaluation and calibration.

Standard cytosine

Solution	Calc. conc. [ng/mL]	Eff. conc. [ng/mL]	Volume added	Final volume [mL]
SS(STD)	100'000	101'500		
WS1(STD)	10'000	10'150	1000 µl SS	10
WS2(STD)	1'000	1'015	1000 µl WS1	10
STD1	100.0	101.50	1000 µl WS2	10
STD2	500.0	507.50	500 µl WS1	10
STD3	1'000.0	1'015.00	1000 µl WS1	10
STD4	1'500.0	1'522.50	150 µl SS	10
STD5	2'000.0	2'030.00	200 µl SS	10
STD6	3'000.0	3'045.00	300 µl SS	10

Standard 5-methylcytosine

Solution	Calc. conc. [ng/mL]	Eff. conc. [ng/mL]	Volume added	Final volume [mL]
SS(STD)	100'000	100'200		
WS1(STD)	10'000	10'020	1000 µl SS	10
WS2(STD)	1'000	1'002	1000 µl WS1	10
WS3(STD)	100	100	1000 µl WS2	10
STD1	10.0	10.02	1000 µl WS3	10
STD2	20.0	20.04	2000 µl WS3	10
STD3	40.0	40.08	400 µl WS2	10
STD4	80.0	80.16	800 µl WS2	10
STD5	120.0	120.24	120 µl WS1	10
STD6	160.0	160.32	160 µl WS1	10

Internal standard 2,4-[$^{13}C_2$,$^{15}N_3$]-cytosine

Solution	Calc. conc. [ng/mL]	Eff. conc. [ng/mL]	Volume added	Final volume [mL]
SS(ISTD)	100'000	100'600		
ISTD	1'000	1'006	500 µl SS(ISTD)	50

Internal standard 5',5',5',6-[$^{2}H_4$]-5-methylcytosine

Solution	Calc. conc. [ng/mL]	Eff. conc. [ng/mL]	Volume added	Final volume [mL]
SS(ISTD)	100'000	100'000		
WS1(ISTD)	10'000	10'000	1000 µl SS(ISTD)	10
ISTD	50.0	50.00	250 µl WS1(ISTD)	50

Table 5: Solution preparation tables for both standards and internal standards including dilution steps

The ISTD solution was prepared by mixing 500 µL of SS(ISTD) cytosine and 250 µL of WS1(ISTD) 5-methylcytosine in a 50 mL volumetric flask and diluted with MeCN/MeOH 75:25, to obtain a final concentration of 1006 ng/mL and 50 ng/mL of 2,4-[$^{13}C_2$,$^{15}N_3$]-cytosine and 5',5',5',6-[$^{2}H_4$]-5-methylcytosine, respectively.

The standard solutions used for the calibration curves were built with one blank and six concentrations between 100 and 3'000 ng/mL for cytosine and 10 and 160 ng/mL for 5-methylcytosine. The first calibration point was prepared mixing 100 µL of STD1 cytosine, 100 µL of STD1 5-methylcytosine in a micro-vial. The next five calibration points (STD2-6) are prepared exactly in the same way. Then, 100 µL of ISTD solution is added before sample preparation to all calibration points and quality control samples (see Chapt. 4.4.5). After evaporation of the solvent with continuous N_2 gas flow in a heat block (Techne Dri-block DB-3D, Staffordshire, UK) at room temperature (RT), the samples were reconstituted in 100 µL of MeCN/MeOH 75:25.

The standard solution containing 3.6 mol% 5-methylcytosine without ISTD used for evaluation of the mass analyzers was prepared by mixing 900 µL of STD3 cytosine with 900 µL of STD3 5-methylcytosine. After solvent evaporation under N_2 at RT in a heat block, the samples were reconstituted in 900 µL MeCN/MeOH 75:25.

The standard solution with 3.6 mol% 5-methylcytosine containing both ISTDs was prepared by mixing 700 µL of STD3 cytosine with 700 µL of STD3 5-methylcytosine and 700 µL of ISTD solution. Finally, the solvent was evaporated with N_2 at RT in a heat block and the samples were reconstituted in 700 µL MeCN/MeOH 75:25.

4.4.3 Chromatography

The QTOF and the ion trap mass analyzers were coupled to an Acquity system (Waters, Milford, MA, USA) equipped with sample manager, solvent manager, column manager and PDA eλ detector.

The Qtrap instrument was connected to an Ultimate 3000 Binary Rapid Separation LC system (Dionex, Sunnyvale, CA, USA) equipped with an Ultimate 3000 autosampler, a binary pump, and a DAD-3000RS diode array detector.

Following conditions were used for the reversed phase conditions: Acquity UPLC BEH column (1.7 μm, 2.1 x 50 mm, Waters, Milford, MA, USA) and a mobile phase consisting of solvent A H_2O and B MeCN both buffered with 5 mM nonafluoro-pentanoic acid (NFPA). The compounds were eluted at 0.5 mL/min flow rate, first isocratically from 0 to 2 min at 5 % of B, followed with a first linear gradient from 5 % to 35 % of B within 3 min and a second linear gradient from 35 % to 70 % within 3 min. The column was then equilibrated with 5 % of B during 3 min until next injection. The autosampler needle of the Acquity system was washed with a strong needle wash solution of MeOH/H_2O 2:1 + 0.1% formic acid and a week needle wash solution of MeCN/H_2O 10:90. A volume of 5 µL sample solution was respectively injected.

For normal phase conditions, an Acquity UPLC BEH Amide column (1.7 μm, 2.1 x 100 mm, Waters, Milford, MA, USA) and a mobile phase consisting of solvent A (MeCN/H_2O 1:1) and B (MeCN/H_2O 95:5) both buffered with 10 mM $HCOONH_4$ and 0.125% HCOOH were chosen. The compounds were eluted at 0.5 mL/min flow rate with a linear gradient from 95% to 85% of B within 4 min. The wash step consisted in a non-linear gradient (curve 2) from 85% to 50% of B in 2 min. The column was finally equilibrated during 2 min until the next injection. The autosampler needle of the Dionex system was washed with a solution of MeCN/H_2O 9:1 and that of the Acquity with a strong needle wash solution of MeCN/MeOH 75:25 and a week needle wash solution of MeCN/H_2O 95:5. A volume of 5 µL sample solution was respectively injected.

4.4.4 Mass spectrometry

Mass spectrometer parameters were optimized with a continuous flow injection of a solution containing cytosine (concentration of 100 ng/mL), 5-methylcytosine (40ng/mL), 2,4-[$^{13}C_2$,$^{15}N_3$]-cytosine (100 ng/mL), and 5',5',6-[$^{2}H_4$]-5-methylcytosine (50 ng/mL) at a flow rate of 7 μL/min.

The maXis UHR-QTOF (Bruker Daltonics GmbH, Bremen, Germany) connected to the Acquity UPLC system (Waters) was equipped with an electrospray ion source. Condition for ESI: end plate offset (-500 V), Capillary (4000 V), nebulizer gas (N_2, 1.6 bar), dry gas (N_2, 10 L/min), and dry temperature (200 °C). MS-parameters: funnel RF (200 Vpp), ISCID energy (0 eV), multipole RF (200 Vpp), ion energy (2 eV), low mass (50 m/z), collision energy (10 eV, He gas), collision RF (400 Vpp), ion cooler (45 Vpp), transfer time (32 μs), and pre-puls storage (9 μs). MS acquisitions were performed in the positive ionization mode at 20'000 full width half maximum (FWHM) resolution. Spectra were acquired between *m/z* 50 and 500, in the full scan mode, and at 5 Hz scan rate. An external mass calibration below 2 ppm accuracy was performed between *m/z* 91 and 1450 just before starting a sequence with a 2 mM solution of sodium formate in H_2O/propan-2-ol 1:1. Signals corresponding to cytosine (*m/z* 112.050), 5-methylcytosine (126.066), 2,4-[$^{13}C_2$,$^{15}N_3$]-cytosine (117.048), and 5',5',6-[$^{2}H_4$]-5-methylcytosine (130.091) were integrated from high-resolution extracted ion chromatograms with a mass width of ± 0.05 *m/z* and using the Bruker QuantAnalysis® software.

The HCT ion trap mass spectrometer (Bruker Daltonics GmbH, Bremen, Germany) was connected to a Waters Acquity UPLC system from (Waters) and equipped with an electrospray ion source. Condition for ESI: nebulizer gas (N_2, 35 psi), dry gas (N_2, 8 L/min), and dry temperature (320 °C). MS-parameters: target mass (*m/z* 120), compound stability (100 %), trap drive level (90 %). MS acquisitions were performed in the positive ion mode at a normal resolution (0.6 u peak width) and under ion charge control conditions (ICC, target: 10'000). Full scan MS were averaged over 8 single spectra and acquired with a mass window between *m/z* 20 and 200. Data were processed with the Bruker DataAnalysis® software.

The Dionex UHPLC system was coupled to a 3200 QTRAP LC/MS/MS hybrid triple quadrupole/linear ion trap mass spectrometer (AB Sciex, Foster City, CA, USA) equipped with a TurboIonSpray source. Ionization was performed using positive

electrospray ionization. Collision-induced dissociation was done in the second quadrupole with N_2 as collision gas. Following optimized parameters were used: Curtain gas (CUR, 20 psi), collision gas (CAD, Medium), ion spray voltage (IS, 5000 V), temperature (TEM, 450 °C), ion source gas 1 (GS1, 50 psi), ion source gas 2 (GS2, 60 psi), interface heater (ihe, on), collision energy (CE, 21 V), and collision cell exit potential (CXP, 4 V). Compound specific parameters are summarized in Table 6.

	Declustering potential (DP)	Entrance potential (EP)	Collision cell entrance potential (CEP)
cytosine	46 V	12 V	14 V
2,4-[$^{13}C_2$,$^{15}N_3$]-cytosine	46 V	9.5 V	18 V
5-methylcytosine	46 V	12 V	16 V
5',5',5',6-[$^{2}H_4$]-5-methylcytosine	51 V	11.5 V	16 V

Table 6: Qtrap MS/MS specific parameters for cytosine, 2,4-[$^{13}C_2$,$^{15}N_3$]-cytosine, 5-methyl-cytosine, and 5',5',5',6-[$^{2}H_4$]-5-methylcytosine

For the detection of cytosine, 2,4-[$^{13}C_2$,$^{15}N_3$]-cytosine, 5-methylcytosine, and 5',5',5',6-[$^{2}H_4$]-5-methylcytosine, MS/MS transitions from *m/z* 112.0 to 95.0, 117.0 to 99.0, 126.0 to 108.9, and 130.1 to 113.0, respectively, were selected with 150 ms dwell time. Data were acquired at normal resolution (0.6 u peak width) and processed using the Analyst software (AB Sciex).

After integration of the corresponding HR-EIC (maXis) and EIC (ion trap, Qtrap) signals, a quadratic regression was finally used to calculate the absolute amount of cytosine and 5-methylcytosine in the hydrolyzed CT and human DNA samples. The percentage of methylated cytosine was calculated after conversion of ng/mL in nmol/mL and using following equation:

$$5-methylcytosine\left[mol\%\right]=\frac{5-methylcytosine\left[nmol\right]}{5-methylcytosine\left[nmol\right]+cytosine\left[nmol\right]}\times 100$$

4.4.5 DNA hydrolysis

Aqueous solutions containing 1 µg of CT DNA in 100 µL or approximately 2 µg of human DNA (volumes varying between 10 and 500 µL) were transferred into 250 µL micro-vials (Infochroma, Zug, Switzerland). 100 µL of the internal standard solution containing 1'006 and 50 ng/mL of 2,4-[$^{13}C_2$,$^{15}N_3$]-cytosine and 5',5',5',6-[$^{2}H_4$]-5-methylcytosine, respectively, dissolved in MeCN/MeOH 75:25 were added. After evaporation of the solvent with a continuous N_2 gas flow at 23°C in a sample

concentrator (Techne Dri-block DB-3D), the residue was dissolved in 50 µl formic acid (98%). The micro-vials were then sealed with alumina crimp caps and PTFE/silicone/PTFE septa (Infochroma), and DNA was hydrolyzed at 150 °C for 3 h. After been cooled down, the solution was completely dried under a continuous N_2 flow at room temperature and the residue reconstituted in 100 µL MeCN/MeOH 75:25. Samples were stored at -20°C for maximum one day prior UHPLC-MS analysis.

As quality control 100 µL of an aqueous CT DNA solution (10'000 ng/mL) was used sample during the determination of the methylation grade of human DNA.

4.5 Bibliography

[1] Feil, R., Fraga, M. F., *Nat. Rev. Genet.* **2011**, *13*, 97.
[2] Ito, Y., *Science & Technology Trends - Quarterly Review* - **2009**, *33*, 11.
[3] Santos, K. F., Mazzola, T. N., Carvalho, H. F., *Braz. J. Med. Bio. Res.* **2005**, *38*, 1531.
[4] Robertson, K. D., *Nat. Rev. Genet.* **2005**, *6*, 597.
[5] Baylin, S. B., Herman, J. G., *Trends Genet.* **2000**, *16*, 168.
[6] Egger, G., Liang, G., Aparicio, A., Jones, P. A., *Nature* **2004**, *429*, 457.
[7] Frigola, J., Sole, X., Paz, M. F., Moreno, V., Esteller, M., Capella, G., Peinado, M. A., *Hum. Mol. Genet.* **2005**, *14*, 319.
[8] Semmler, A., Smulders, Y., Struys, E., Smith, D., Moskau, S., Blom, H., Linnebank, M., *Clin. Chem. Lab. Med.* **2008**, *46*, 1398.
[9] Hillemacher, T., Frieling, H., Moskau, S., Muschler, M. A., Semmler, A., Kornhuber, J., Klockgether, T., Bleich, S., Linnebank, M., *Eur. Neuropsychopharmacol.* **2008**, *18*, 295.
[10] Razin, A., Sedat, J., *Anal. Biochem.* **1977**, *77*, 370.
[11] Fisher, D. H., Giese, R. W., *J. Chromatogr. A* **1988**, *452*, 51.
[12] Ehrlich, M., Gama-Sosa, M. A., Huang, L.-H., Midgett, R. M., Kuo, K. C., McCune, R. A., Gehrke, C., *Nucleic Acids Res.* **1982**, *10*, 2709.
[13] Catania, J., Keenan, B. C., Margison, G. P., Fairweather, D. S., *Anal. Biochem.* **1987**, *167*, 347.
[14] Yuki, H., Kawasaki, H., Kobayashi, T., Yamaji, A., *Chem. Pharm. Bull.* **1977**, *25*, 2827.
[15] Adams, R. L. P., Burdon, R. H., *Molecular Biology of DNA Methylation*, Springer-Verlag, **1985**.
[16] Kuo, K. C., McCune, R. A., Gehrke, C., Midgett, R. M., Ehrlich, M., *Nucleic Acids Res.* **1980**, *8*, 4763.
[17] Reddy, V. M., Gupta, R. C., Randerath, K., *Anal. Biochem.* **1981**, *117*, 271.
[18] Deutsch, J., Razin, A., Sedat, J., *Anal. Biochem.* **1976**, *72*, 586.
[19] Singer, J., Schnute, W. C. J., Shively, J. E., Todd, C. W., Riggs, A. D., *Anal. Biochem.* **1979**, *94*, 297.
[20] Crain, P. F., McCloskey, J. A., *Anal. Biochem.* **1983**, *132*, 124.
[21] Romerio, A. S., Fiorillo, G., Terruzzi, I., Senesi, P., Testolin, G., Battezzati, A., *Anal. Biochem.* **2005**, *336*, 158.
[22] Friso, S., Choi, S.-W., Dolnikowski, G. G., Selhub, J., *Anal. Chem.* **2002**, *74*, 4526.
[23] Kok, R. M., Smith, D. E., Barto, R., Spijkerman, A. M., Teerlink, T., Gellekink, H. J., Jakobs, C., Smulders, Y. M., *Clin. Chem. Lab. Med.* **2007**, *45*, 903.
[24] Shelnutt, K. P., Kauwell, G. P., Gregory, J. F., 3rd, Maneval, D. R., Quinlivan, E. P., Theriaque, D. W., Henderson, G. N., Bailey, L. B., *J. Nutr. Biochem.* **2004**, *15*, 554.
[25] *Deoxyribonucleic acid sodium salt from calf thymus – Product Information, Sigma-Aldrich* **MWM/SAG 9/02**.

CHAPTER 5

METHYLATION METABOLISM IN SEPSIS AND SYSTEMIC INFLAMMATORY RESPONSE SYNDROME[1]

5.1 Introduction

Despite an increase in knowledge on its pathogenesis, sepsis remains the most common non-cardiac cause of critical illness. The incidence of sepsis even increases, probably due to an increase in the number of immune-compromised patients, increase in anti- biotic resistance, and aging of the population [1].

The mortality of sepsis is around 30%, and many sepsis survivors suffer from sustained and severe long-term cognitive impairment and functional disability, which further intensifies the public health burden from this disease [2]. Almost all innovative treatment strategies have failed in the recent years, and clearly, there is a strong need for better insight in disease pathogenesis and subsequent emerging treatment strategies.

In a rodent model it has been recently shown that sepsis leads to alterations of methylation metabolism, especially increased plasma S-adenosyl methionine (SAM) levels [3]. S-adenosyl methionine (SAM) has a central position in methylation metabolism as a universal and unique methyl-donor to maintain normal methylation of DNA, RNA, proteins, phospholipids and variety of other molecules. The degradation product of SAM is S-adenosyl homocysteine (SAH). As SAM and SAH are the substrate and product of methylation reactions and SAH is a potent inhibitor

[1]Paper accepted: Methylation metabolism in sepsis and systemic inflammatory response syndrome, *Scandinavian Journal of Clinical and Laboratory Investigation,* **2013**, Alexander Semmler, Jean-Christophe Prost, Yvo Smulders, Desiree Smith, Henk Blom, Laurent Bigler, Michael Linnebank

of transmethylation reactions, the cellular SAM/SAH ratio is commonly regarded as reflecting methylation capacity. Alterations in methylation metabolism during sepsis may be clinically relevant because SAM has been demonstrated to have anti-inflammatory function in sepsis [4] and endotoxemia [5] and because alterations of methylation capacity potentially impair a huge variety of essential biochemical reactions and thereby may contribute to disease mortality. In this study we address possible alterations in methylation metabolism in human sepsis.

5.2 Method

5.2.1 Patient selection

Adult patients of Caucasian origin treated in one of the Intensive Care Units (ICU) at the University Hospital Bonn were included. Patients were classified as having sepsis or systemic inflammatory response syndrome (SIRS) diagnosed according to the diagnostic criteria defined by the American College of Chest Physicians/Society of Critical Care Medicine Consensus Conference [6] (n = 12). Patients who were treated due to traumatic brain injury, stroke (subarachnoid haemorrhage or ischaemic), and who did not met the diagnostic criteria for sepsis/SIS were included as comparison group (n = 22). Exclusion criteria included pre- existing metabolic diseases that might influence test results such as diabetes mellitus, alcohol abuse or patients with pre-existing renal or hepatic dysfunction. Patients with baseline vitamin B12 and folate plasma levels below the reference range were also excluded from the study. Patients who developed renal or hepatic dysfunction during the ICU treatment were not excluded from the study. Patients who developed renal impairment during ICU treatment received hemofiltration as considered necessary by the treating physician. The ICU treatment of all patients was carried out according to standard clinical procedures. Critically ill patients who could not eat received enteral nutrition sup- port if they did not have contraindications to enteral feeding (e.g. peritonitis, pancreatitis, ileus). Others received parenteral nutrition. Patients were included in the study within the first three days of ICU treatment. Blood samples were taken two times a week, until the ICU treatment was discontinued. Because sample collection was discontinued after discharge from ICU and sepsis patients stayed longer on the ICU than non-septic patients, there was a significant difference between groups in number of samples available after the 5th sample (third week of ICU treatment).

Therefore, all samples collected after the 5th one were excluded from statistical analyses. Medical data collected during ICU treatment included diagnosis, length of ICU stay, survival, age, and gender.

5.2.2 Ethics statement

All patients gave written informed consent. When patients were not able to consent, because they had analgosedation, ventilator support or a neurological deficit, their legal representatives were asked to consent. The study was approved by the local ethics committee of the University of Bonn.

5.2.3 Analytical methods

Blood samples were collected in EDTA-containing vials for the determination of plasma SAM and SAH, and DNA isolation. Vials containing heparinlithium as anticoagulant were used for later measurement of homocysteine levels. Vials were immediately placed on ice. To obtain plasma, the blood was first centrifuged for 15 min at 4000 *g* and 4°C, immediately after collection. The supernatant was deproteinized by perchloric acid 10%. All aliquots were stored at –80°C for 1–2 months before shipment on dry ice. Deproteinized plasma was used for simultaneous determination of SAM and SAH by using stable isotope dilution tandem mass spectrometry as previously published [7]. Inter-assay coefficients of variation were 6.8% for SAM and 6.9% for SAH.

Homocysteine was determined by fully automated particle-enhanced immunonephelometry with a BN II System (Dade Behring) by enzymatic conversion to S-adenosyl homocysteine (SAH). The intra-assay coefficient of variation of the homocysteine assay was 3.4 % (mean: 11 µmol/L, n = 20), while the inter-assay coefficient was 5.6 % (mean: 11 mg/dL, n = 20). Serum concentrations of vitamin B12 and folate were measured by means of a competitive chemiluminescent immunoassay with an Access™ Immunoassay System (Beckman Coulter, Krefeld, Germany) according to manufacturer's instructions.

5.2.3 Global DNA-methylation

Global DNA-methylation was measured by liquid chromatography tandem mass spectrometry according the method developed and validated (see Chap. 4 and literature [8]). In short, 1 µg of DNA was hydrolyzed using formic acid. Cytosine and

5-methylcytosine were separated using gradient elution normal phase chromatography and electrospray ionization (ESI) tandem mass spectrometry, operating in the multiple reaction monitoring (MRM) mode and quantified using labeled internal standards. The level of DNA methylation is expressed as the 5-methylcytosine/total-cytosine ratio. The intra- and inter-assay coefficient of variation (CV) for the 5-methylcytosine/total-cytosine was 2.0 % (*n* = 9) and 2.4 % (*n* = 9) for calf thymus DNA (mean 5-methylcytosine/total-cytosine ratio 6.8 %) respectively. For human control (n = 50) and patients (n = 60) samples the 5-methylcytosine/total-cytosine ratio varied from 2.3 % to 5.8 % (median 4.3 %) and from 2.6 % to 6.3 % (median 4.4 %), respectively

5.2.4 Statistics

Biochemical parameters are presented as median (range) and analyzed using ANOVA for repeated measures for samples 1–5. IBM SPSS Statistics 20 (SPSS Inc., Chicago, IL, USA) was used. To address clustering of measurements within patients, linear regression with robust standard errors was used to compute differences between values of patients with and without sepsis. Stata 11 (StataCorp, College Station, TX, USA) was used.

5.3. Results

5.3.1 Clinical Characteristics

The clinical characteristics of the patients included are summarized in Table I. Septic patients were older, stayed longer on the ICU, had higher APACHE 2 scores, more often renal failure, and received more often parenteral nutrition during ICU treatment.

5.3.2 Biochemical Parameters

The results of all measured biochemical parameters are shown are shown in Figures 1–4. Plasma SAM levels were increased in septic patients by 127 nmol/L (95% CI 81–172; $p < 0.001$). Plasma SAH levels were increased in septic patients by 48 nmol/L (95% CI 24–71; $p < 0.001$). The ratio of SAM/SAH was decreased in septic patients by 1.67 (95% CI 2.70–0.64; $p > 0.002$). There was no difference in plasma homocysteine levels (reduction of 0.63 µmol/L in septic patients, 95% CI reduction of 2.56 to an increase of 1.29; p = 0.32) and no difference in global DNA methylation

between septic and non-septic patients (reduction of 0.064 in septic patients, 95% CI reduction of 0.039 to an increase of 0.17; p = 0.21). Folate and vitamin B12 levels were within the reference range for all patients and not different between septic and non-septic patients at all measured time points (data not shown).

	Sepsis/SIRS	**Non-septic patients**
Age (years)	65.5 (24–76)	49 (33–80)
Gender (female/male), *n*	5/7	8/14
Apache 2 score	21.5 (17–28)	12 (3–26)
ICU length of stay (days)	22.5 (15–81)	10 (5–32)
Survival (%)	75%	95%
Multiple trauma (%)	33%	5%
Head trauma (%)	8%	18%
Stroke (%)	0%	82%
Surgery (%)	91%	59%
Peritonitis/pancreatitis (%)	33%	0%
Sepsis/SIRS (%)	50%/50%	-
Parenteral nutrition (%)	50%	27%
Hemofiltration (%)	58%	9%
Vitamin B12 baseline pmol/L (n 130–680)	559 (203–739)	498 (128–1107)
Folic acid baseline nmol/L (n 6.8–39)	19.0 (10.9–29.2)	12.9 (7.0–35.6)

Table 1: Clinical characteristics of sepsis and non-septic ICU patients. Continuous variables are presented as median (range). SIRS, systemic inflammatory response syndrome.

The results of all measured biochemical parameters are shown are shown in Figures 1–4. Plasma SAM and SAH levels were higher in septic patients. The ratio of SAM/SAH was lower in septic patients. There was no difference in plasma homocysteine levels and no difference in global DNA methylation between septic and non-septic patients. Folate and vitamin B12 levels were within the reference range for all patients and not different between septic and non-septic patients at all measured time points (data not shown).

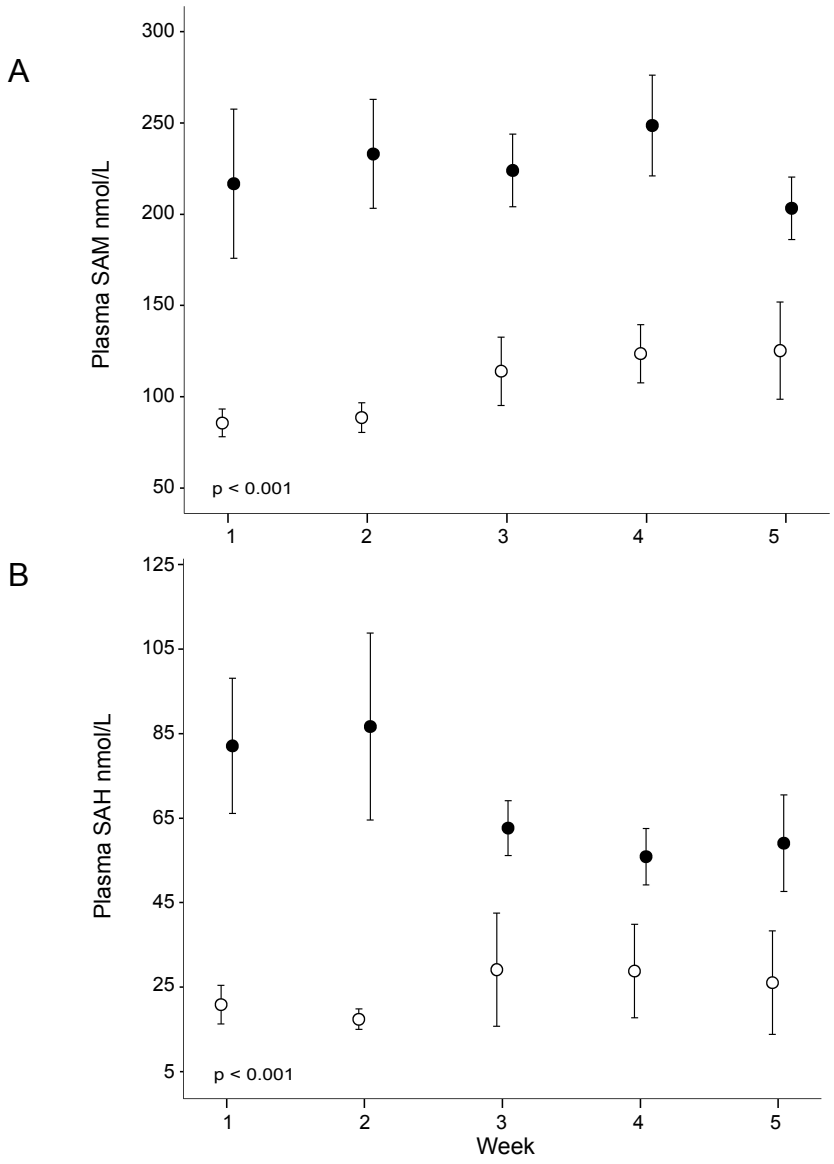

Figure 1: Plasma SAM (A) and SAH (B) levels. X-axis depicts the week when the sample was taken. Filled circels represent sepsis patients, empty circles depict non-septic ICU patients. Error bars represent SEM. *p*-values are significance levels of ANOVA for repeated measures. Bar plots are not exactly placed on the five different time points to avoid overlap of error bars.

5.4. Discussion

This study shows that human methylation metabolism may be altered during sepsis. Plasma SAM and SAH levels of sepsis and control patients did not approximate throughout the observation period. This demonstrates that the alterations of methylation metabolism during sepsis are sustained and do not normalize during ICU treatment.

In septic patients, plasma SAM and SAH levels are increased. As intracellular SAM and SAH levels re physiologically several times higher than their plasma levels [9], the increase of plasma SAM and SAH levels may be explained by sepsis-induced intravascular hemolysis and lysis of other cells, such as liver cells and therefore release of cell SAM and SAH into the plasma. However, the present data do only allow speculations on the underlying mechanisms of SAM and SAH level changes. Patients diagnosed with sepsis in general had a more severe disease than non-septic patients documented by higher APACHE2 scores, more renal failure, longer ICU treatment, more use of parental nutrition. Therefore, it is possible that the changes seen in the methylation metabolism are, in part, not specific for sepsis/SIRS, but an expression of disease severity and its treatment.

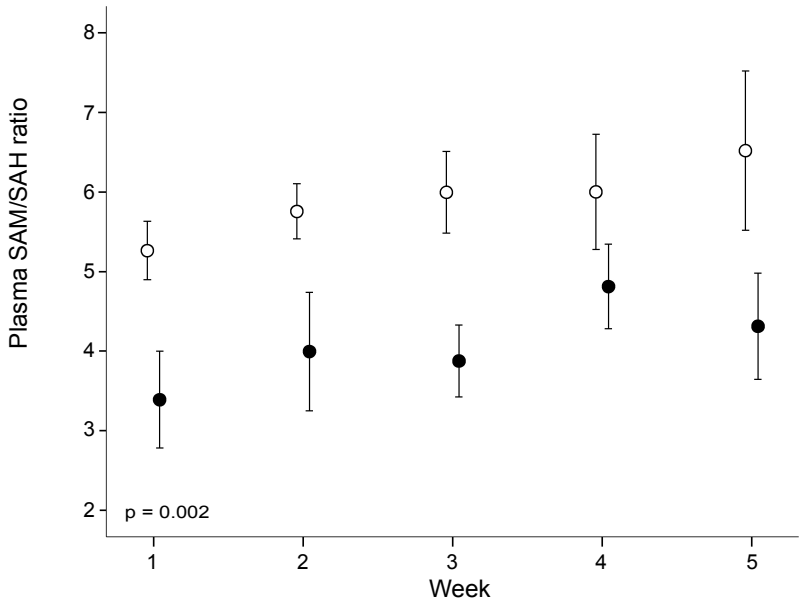

Figure 2: Error bar plots of plasma SAM and SAH ratios. X-axis depicts the week when the sample was taken. Filled circels represent sepsis patients, empty circles depict non-septic ICU patients. Error bars represent SEM. *p*-values are significance levels of ANOVA for repeated measures. Bar plots are not exactly placed on the five different time points to avoid overlap of error bars.

In a rodent model of sepsis, we observed increased plasma SAM levels 24 hours after sepsis-induction, but the plasma SAH levels remained unchanged [3]. However, the animal data are not readily comparable with the present study, as they only demonstrate a one-time measurement of plasma SAM and SAH levels 24 h after sepsis induction, and do not show the progression of SAM/SAH levels during more than two weeks of sepsis as the current study. In septic patients, SAH levels approximated to the levels observed in disease controls during the clinical course.

Thus, the normal SAH level observed in rodents might well have been a question of the time- point of measurement.

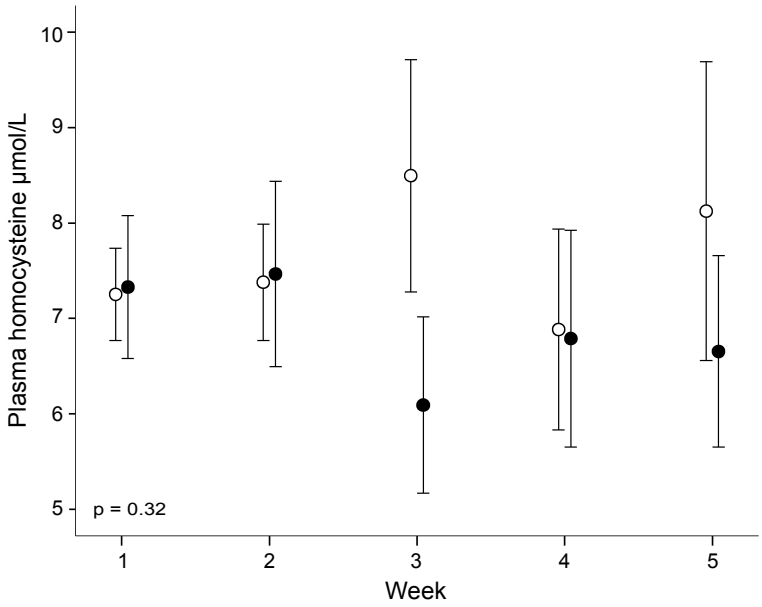

Figure 3: Error bar plots of plasma homocysteine levels. X-axis depicts the week when the sample was taken. Filled circels represent sepsis patients, empty circles depict non-septic ICU patients. Error bars represent SEM. *p*-values are significance levels of ANOVA for repeated measures. Bar plots are not exactly placed on the five different time points to avoid overlap of error bars.

Plasma homocysteine levels have been reported to correlate with plasma SAH levels and also with lymphocyte DNA methylation [10]. We did not observe an association of SAH and homocysteine plasma levels, as the plasma homocysteine levels remained unaltered during the whole observation period. The sepsis-induced changes of SAM and SAH levels result in a reduced SAM/SAH ratio and thus in a significantly reduced methylation capacity during sepsis. However, this was not associated with changes of homocysteine plasma levels or global methylation of leukocyte DNA. The distribution of data differed between groups as in the group of non-septic ICU patients we included more patients but with less measurements per patient, because non-septic patients had on average a shorter ICU stay. We therefore additionally calculated linear regression with robust standard errors to address clustering of measurements within patients. These calculations show a wide 95% confidence interval for homocysteine and for DNA-methylation indicating that small effect sizes may have been over- looked and possibly could be detected in a larger sample. It is also possible that the sepsis-induced changes of methylation capacity do affect other SAM methyl transfer reactions such as histone or RNA

methylation, methylation of proteins, neurotransmitters and phospholipids, but this has not been examined in the present study. Thus, further studies may explore the clinical relevance of those observed changes.

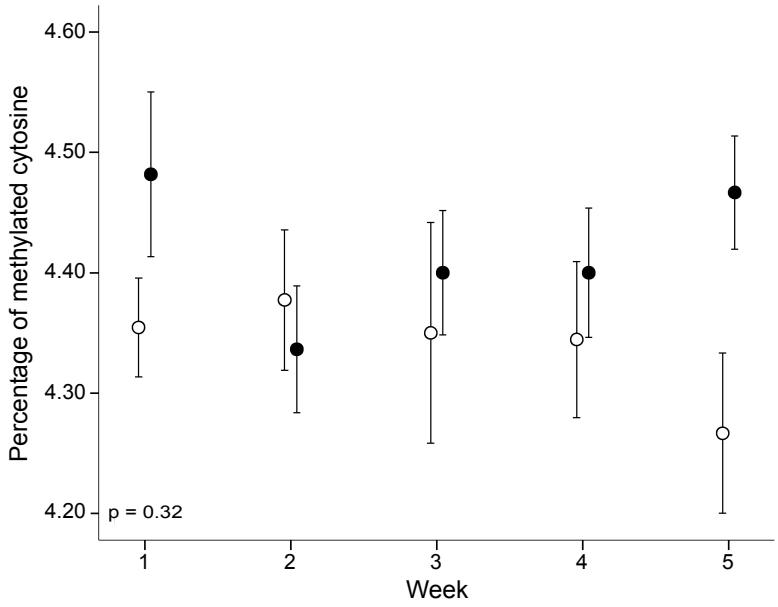

Figure 4: Error bar plots of percentage of methylated cytosine (%mCyt). X-axis depicts the week when the sample was taken. Filled circels represent sepsis patients, empty circles depict non- septic ICU patients. Error bars represent SEM. *p*-values are significance levels of ANOVA for repeated measures. Bar plots are not exactly placed on the five different time points to avoid overlap of error bars.

5.5 Bibliography

[1] G. S. Martin, D. M. Mannino, S. Eaton, M. Moss, *N. Engl. J. Med.* **2003**, *348*, 1546.
[2] T. J. Iwashyna, E. W. Ely, D. M. Smith, K. M. Langa, *JAMA* **2010**, *304*, 1787.
[3] A. Semmler, Y. Smulders, E. Struys, D. Smith, S. Moskau, H. Blom, M. Linnebank, *Clin. Chem. Lab. Med.* **2008**, *46*, 1398.
[4] F. Garcia-Alvarez, M. Navarro-Zorraquino, L. Larrad, J. C. Salinas, R. Sousa, C. Pastor, R. Lozano, *Int. J. Surg. Investig.* **2000**, *2*, 9.
[5] K. Ko, H. Yang, M. Noureddin, A. Iglesia-Ara, M. Xia, C. Wagner, Z. Luka, J. M. Mato, S. C. Lu, *Lab Invest* **2008**, *88*, 1121.
[6] M. M. Levy, M. P. Fink, J. C. Marshall, E. Abraham, D. Angus, D. Cook, J. Cohen, S. M. Opal, J. L. Vincent, G. Ramsay, Sccm/Esicm/Accp/Ats/Sis, *Crit. Care Med.* **2003**, *31*, 1250.
[7] E. A. Struys, E. E. Jansen, K. de Meer, C. Jakobs, *Clin. Chem.* **2000**, *46*, 1650.
[8] R. M. Kok, D. E. Smith, R. Barto, A. M. Spijkerman, T. Teerlink, H. J. Gellekink, C. Jakobs, Y. M. Smulders, *Clin. Chem. Lab. Med.* **2007**, *45*, 903.
[9] S. Melnyk, M. Pogribna, I. P. Pogribny, P. Yi, S. J. James, *Clin Chem* **2000**, *46*, 265.
[10] P. Yi, S. Melnyk, M. Pogribna, I. P. Pogribny, R. J. Hine, S. J. James, *J. Biol. Chem.* **2000**, *275*, 29318.

SUMMARY — ZUSAMMENFASSUNG

1. English version

Epigenetic modifications, as e.g. methylation of histones and DNA, regulate gene expression. However, misregulation of this methylation can lead to very dangerous diseases as cancers, neurological disorders or autoimmune diseases. DNA also undergoes simply changes in the genomic sequence called mutations. They can be classified in advantageous, neutral and lethal processes. Advantageous mutations can contribute to evolutionary changes due to environmental influences. In contrast, lethal damages of the genomic sequence in cellular processes arising from DNA methylation, replication errors, ionizing radiation, or UV-irradiations, frequently result in cancers.

These important concepts necessary for the macromolecular machinery of life are presented in the first part of *Chapter 1*. They include also the flow of genetic information in a cell, primary, secondary, and tertiary structures of DNA, as well as packaging of DNA in a cell by proteins called histones.

As the rate of DNA mutation and relative binding affinities of small molecules to DNA will be considered in this thesis, the second part of *Chapter 1* deals with quantitative determinations. Aspects of calibration, systematic and random errors, limit of detection, limit of quantification, dynamic range, and linearity are discussed. Combination of chromatography with mass spectrometry is often the method of choice used in quantification. Regarding the sample properties, criteria for selecting the most appropriate analytical method are developed, including chromatography, ionization modes, and mass analyzers.

In *Chapter 2*, a method has been optimized in order to detect double stranded DNA with maximal intensity and minimal adducts formation using an ESI-HR-QTOF mass spectrometer. With this method, non-covalent interactions between short 14-mers ds DNA and small organic molecules were investigated, including polyamine derivatives, flavonoids (Figure 1), or DNA stains (DAPI and EthBr).

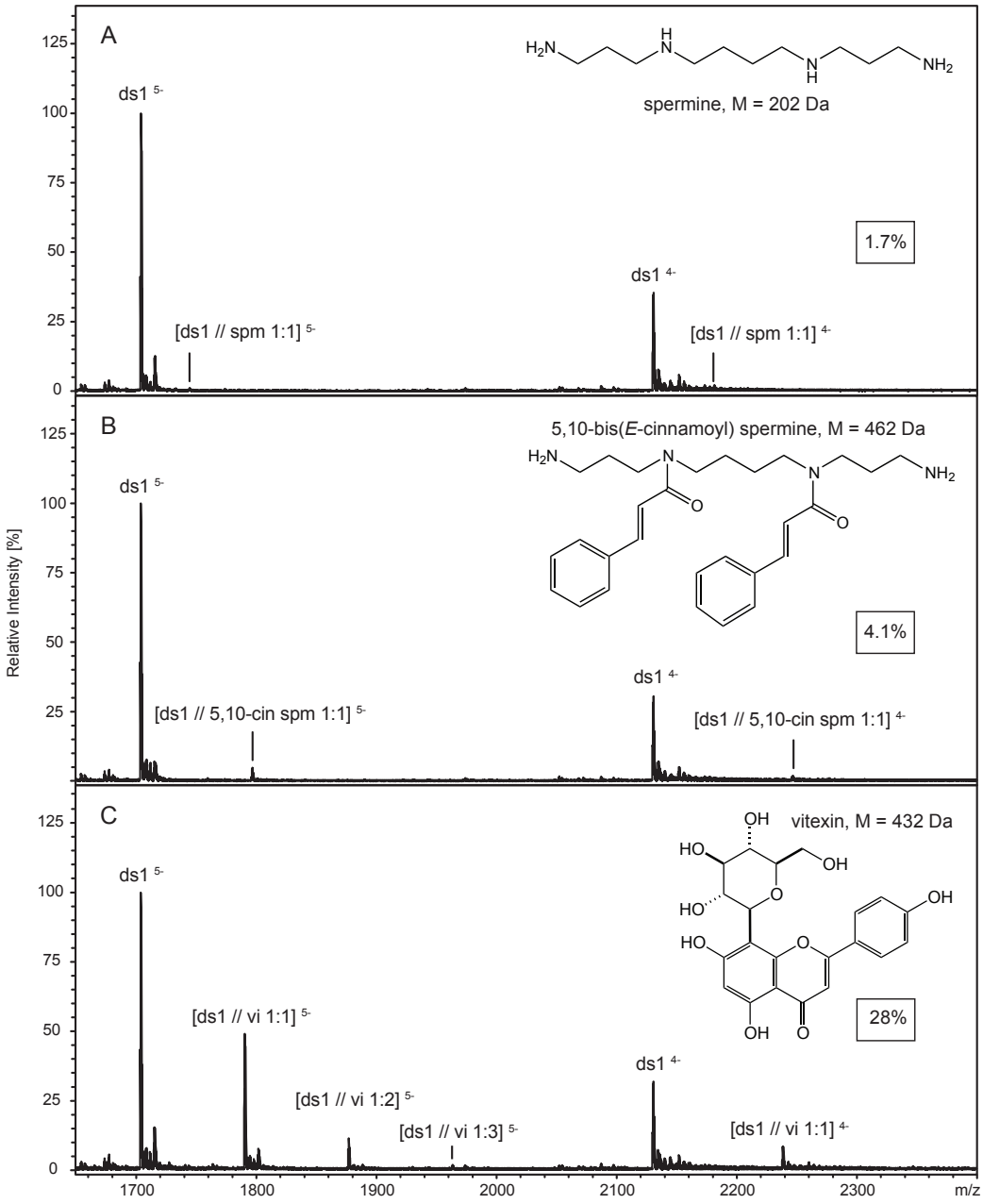

Figure 1: ESI-MS spectra of ds1 d(**AA**CTCCCGGCACAC/GTGTGCCGGGAG**TT**) mixed with (A) spermine, (B) 5,10-bis(*E*-cinnamoyl) spermine and (C) vitexin in a 1:4 ratio. Calculated fraction of bound DNA (in mol%) is framed.

The new ESI-HR-QTOF method was validated with the measure of relative binding affinities between flavonoids and synthetic ds DNA strands. The results obtained were comparable to published data, although the absolute values were lower. Experiments with the ligands DAPI and EthBr demonstrated that the method could also be used to investigate the selectivity of the non-covalent interactions with regard to the GC- and AT-content of the DNA sequences. Finally, polyamines derivatives were found to interact with DNA under MS conditions, whereby acyl-polyamines

presented twice so high binding affinities than free polyamines (ca 4 compared to 2 %, respectively). However, these values are much lower as those observed for the flavonoids derivatives (6 – 28 %).

In *Chapter 3*, a method was developed for quantifying the photoprotection effect of secondary metabolites in relation to UV irradiation of ds DNA. Therefore, a procedure was developed consisting of a self-made UV-irradiation box, photolysis of TpT solutions in presence of UV filters dissolved in separated or in the same cuvette, and UHPLC-ESI-MS quantification. Best chromatographic properties were obtained with normal phase conditions. Best selectivity of the MS-detection was obtained with a method based on MS/MS and best sensitivity with acquisition in the high-resolution full-scan mode. It appears that signals corresponding to photoproducts were of low intensities, probably because of the very low quantum yields of only 2% for the major product.

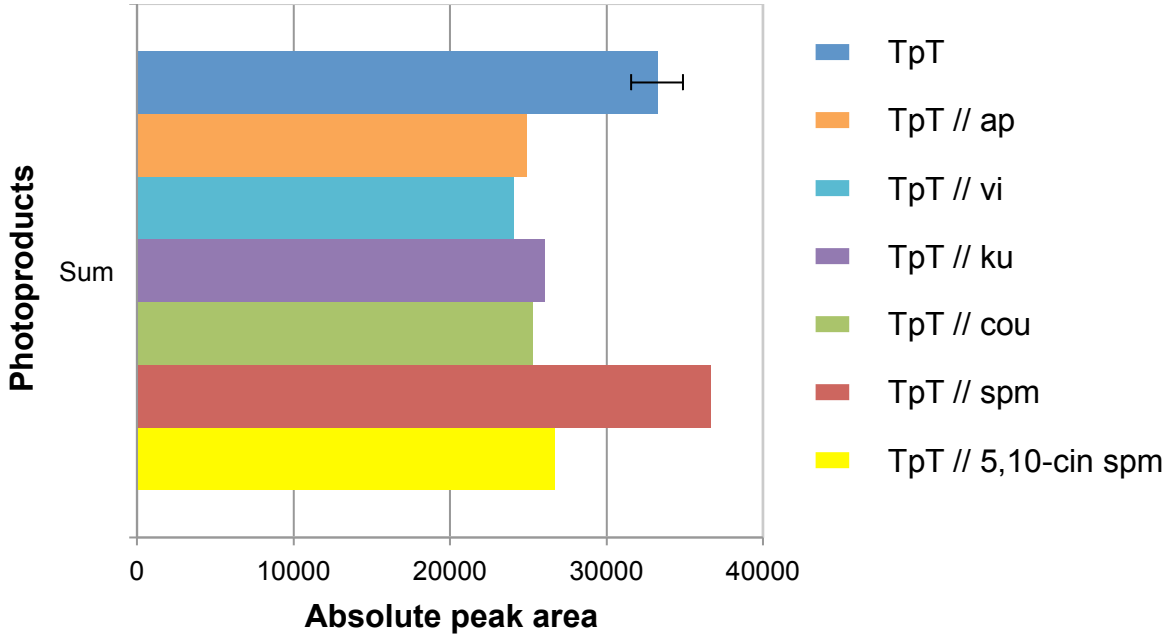

Figure 2: Sum of the formation of all four photoproducts after irradiating an aqueous solution of 10 µM TpT at 312 nm during 56 min without and in the presence of 50 µM UV filter solutions of apigenin, vitexin, kuromanin, *p*-coumaric acid, spermine, and 5,10-bis(*E*-cinnamoyl) spermine prepared in separated cuvettes

The inhibition rate of TpT photoproduct formation was measured in presence of specific natural products (polyamines and their derivatives, flavonoids, anthocyan and hydroxycinnamic acid) in two quartz micro-cuvettes (see Figure 2). A decrease of photoproduct formation is observed after irradiation of TpT at 312 nm in presence of these UV-filters. Only spermine did not inhibit photoproduct formation. This is due

to the lack of chromophore absorbing in the irradiation wavelength. Similar effects have been observed at 254 nm, but to a lesser extent. Preliminary experiences of photoprotection were also performed with oligomers (TpT and ds DNA) using single cuvette. Unfortunately the signals obtained were just above the limit of detection.

Chapter 4 discusses the development of an analytical method for the quantitative determination of the methylation grade of DNA. High-resolution and tandem mass spectrometric techniques were used in combination with the addition of isotopically labeled internal standards to the samples. UHPLC-ESI-MS/MS showed the best reproducibility and was also more precise than other tested mass analyzers as QTOF or ion trap operated in full scan acquisition mode (Figure 3). The method was finally validated using calf thymus DNA samples.

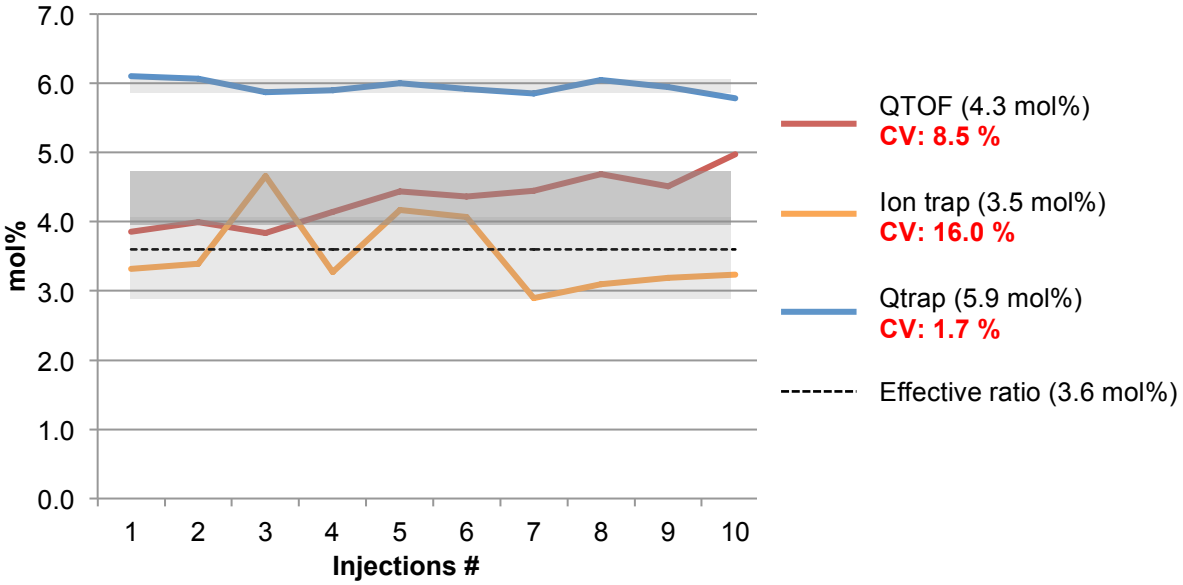

Figure 3: Reproducibility and precision of 10 injections of a single solution containing standards of cytosine and 5-methylcytosine prepared in a 3.6 mol% ratio (black dashed line) and their corresponding labeled ISTD. Analyses were performed using the maXis QTOF, HCT ion trap and 3200 Qtrap mass analyzers. Mean ratios are given in brackets, intra-assay CV in red, and standard deviation in grey.

Compared to the best-published method, an analysis time reduction of 33 % could be achieved with the method developed here. A mean methylation grade of 6.8% was obtained with intra- and inter-assay CVs of 2.0 and 2.4%, respectively. These values indicate that the new method is precise and reproducible enough to be used for the quantification of 5-methylcytosine in patient samples.

Chapter 5 involves an application of the method for determination of the DNA methylation grade developed in Chapter 4. A biological study was completed to verify

if methylation metabolism and DNA methylation are correlated in human sepsis systemic inflammatory response syndrome. The global DNA-methylation was measured by means of extracting DNA from blood samples and quantifying cytosine and 5-methylcytosine with the new UHPLC-ESI-MS/MS method. It appears that sepsis and systemic inflammatory response syndrome induce considerable changes of methylation metabolism without apparent functional consequences on homocysteine plasma levels or DNA methylation.

1. Deutsche Version

Epigenetische Änderungen wie zB die Methylierung von Histonen und und der DNA regeln den Ausdruck der Gene. Gleichwohl können Fehlregelungen dieser Methylierung jedoch zu sehr gefährlichen Krankheiten wie Krebs, neurologischen Störungen oder autoimmunen Krankheiten führen. Die DNA unterliegt auch einfachen Änderungen in der genomischen Sequenz, den sogenannten Mutationen. Sie können eingeteilt werden in vorteilhafte, neutrale und tödliche Prozesse. Die vorteilhaften Mutationen können zu evolutionären Änderungen bedingt durch Umwelteinflüsse beitragen. Im Gegensatz haben tödlichen Beschädigungen der genomischen Sequenz in Zellprozessen herrührend von einer DNA Methylierung, Replikationsfehlern, ionisierenden Strahlen oder UV-Bestrahlung oft Krebs zur Folge.

Diese für die makromolekularen Mechanismen des Lebens wichtigen Begriffe werden im ersten Teil von *Kapitel 1* vorgestellt. Sie enthalten auch den Fluss der genetischen Information in der Zelle, die primären, sekundären und tertiären Strukturen der DNA sowie das Einbetten der DNA in einer Zelle durch Proteine, den sogenannten Histonen.

Da die Geschwindigkeit der DNA Mutation und die relative Bindungsaffinität von kleinen Molekülen zur DNA in dieser Arbeit betrachtet werden, behandelt der zweite Teil von *Kapitel 1* die quantitative Bestimmung. Gesichtspunkte zur Kalibrierung, der systematischen und zufälligen Fehler, der Detektionsgrenzen, der Quantifizierungsgrenzen, des dynamischen Bereiches und der Linearität werden diskutiert. Chromatographie kombiniert mit Massenspektrometrie ist eine oft benützte Methodenwahl für die Quantifizierung. Bezüglich der Probeneigenschaften werden Auswahlkriterien für die geeignetste Methode entwickelt, einschliesslich Chromatographie, Ionisierungsmodus und Massenanalysator.

In *Kapitel* 2 wird eine Methode optimiert um eine doppel-strängige DNA mit maximaler Intensität und einer minimalen Bildung von Nebenprodukten zu detektieren mittels eines ESI-HR-QTOF Massenspektrometers. Mit dieser Methode wurden nicht-kovalente Wechselwirkungen zwischen kurzen 14-mers ds DNA und kleinen organischen Molekülen untersucht, einschliesslich Polyamin-Derivate, Flavonoide (Figur 1) oder DNA Flecken (DAPI und EthBr).

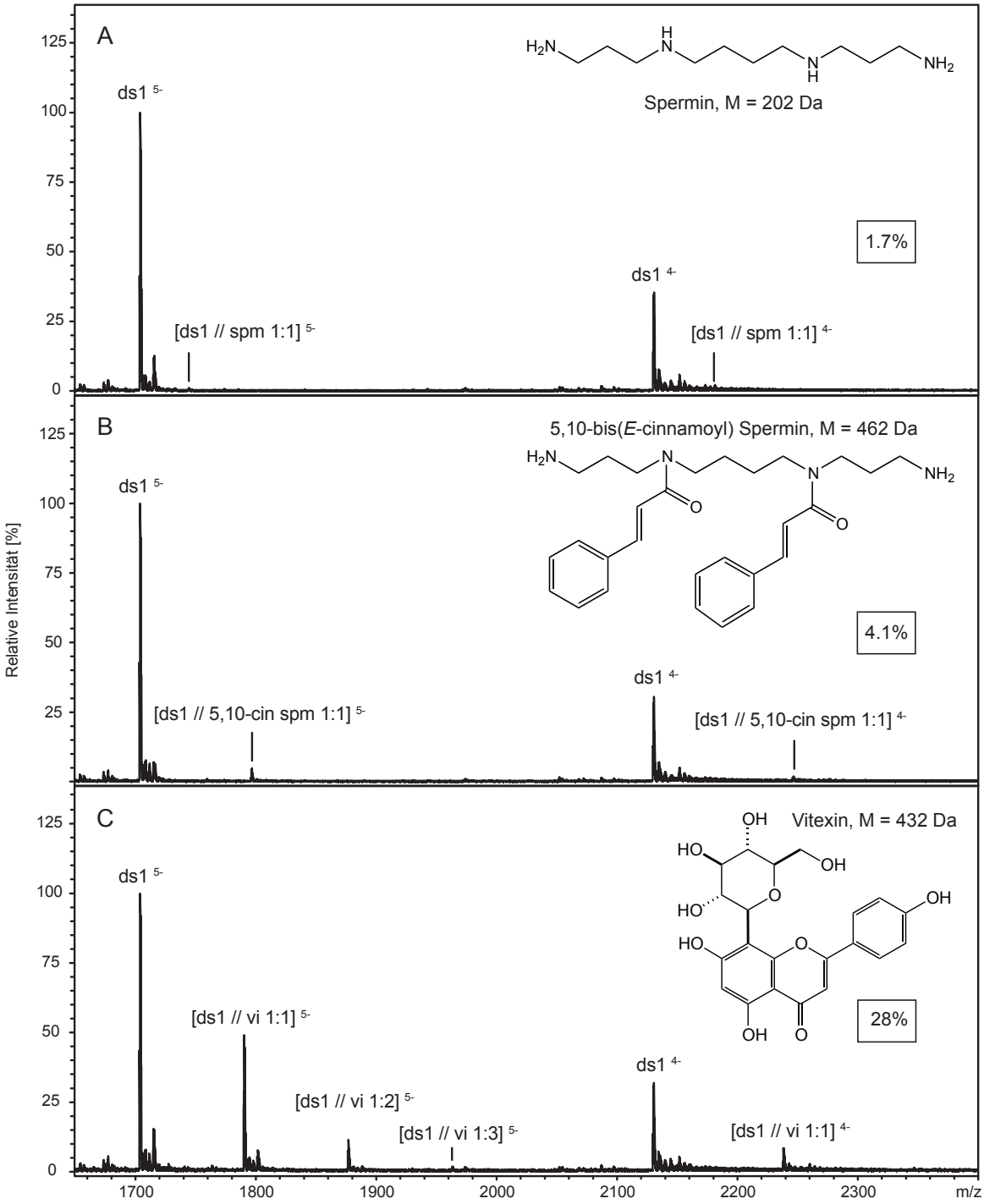

Figur 1: ESI-MS Spektra von ds1 d(**AA**CTCCCGCACAC/GTGTGCCGGGAG**TT**) gemischt mit (A) Spermin, (B) 5, 10-bis(*E*-cinnamoyl) Spermin und (C) Vitexin in einem 1:4 Verhältnis. Der berechnete Anteil von gebundener DNA (in mol%) ist eingerahmt.

Die neue ESI-HR-QTOF Methode wurde validiert durch die Messung der relativen Bindungsaffinität zwischen Flavonoiden und synthetischen ds DNA Strängen. Die erhaltenen Resultate waren vergleichbar mit publizierten Daten, auch wenn die absoluten Werte tiefer lagen. Versuche mit den Liganden DAPI und EthBr bewiesen,

dass die Methode auch benützt werden kann um die Selektivität von nicht-kovalenten Wechselwirkungen bezüglich des GC- und AT-Gehaltes der DNA-Sequenzen zu untersuchen. Schliesslich wurde bemerkt, dass Polyaminderivate mit der DNA unter MS-Bedingungen in Wechselwirkung treten, wobei Acyl-Polyamine eine zweifach höhere Bindungsaffinität aufwiesen als freie Polyamine (ca 4 verglichen mit 2% respective). Hingegen sind diese Werte viel tiefer als jene die für Flavonoid-Derivate beobachtet wurden (6 – 28 %).

In *Kapitel 3* wurde eine Methode entwickelt um den Photoschutzeffekt von Sekundärmetaboliten im Zusammenhang mit der UV-Bestrahlung von ds DNA zu quantifizieren. Hierzu wurde ein Verfahren entwickelt bestehend aus einem hier gefertigten UV-Bestrahlungskasten, Photolyse von TpT-Lösungen im Beisein von UV-Filter gelöst in einer separaten oder der gleichen Küvette, und einer UHPL-ESI-MS Quantifizierung. Die besten chromatographischen Eigenschaften wurden unter normalen Phasenbedingungen erreicht. Die beste Selektivität der MS-Detektierung wurde erreicht mit einer Methode basierend auf MS/MS und beste Empfindlichkeit mit der Aufnahme im hoch-auflösenden Full-Scan Modus

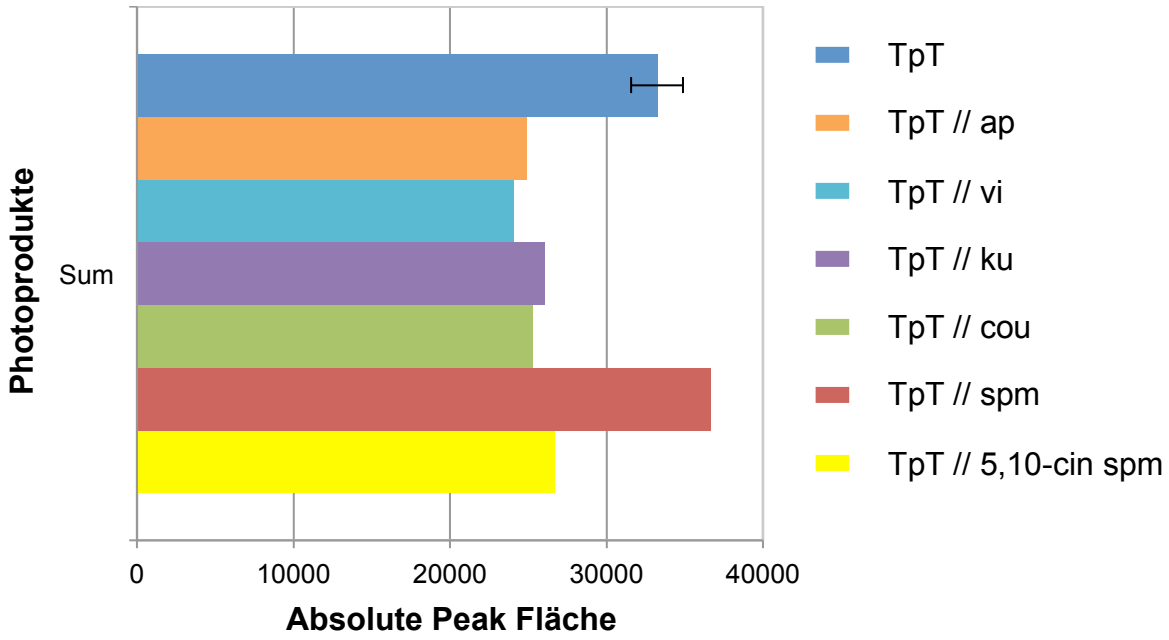

Figure 2: Summe der Bildung aller vier Photoprodukte nach nach Bestrahlung einer wässerigen Lösung von µM TpT bei 312 nm während 56 min ohne und im Beisein einer 50 µM UV Filter Lösung von Apigenin, Vitexin, Kuromanin, *p*-coumarichen Säure, Spermin, and 5,10-bis(*E*-cinnamoyl) Spermin hergestellt in separaten Küvetten

Man sieht, dass Signale welche Photoprodukten entsprechen von tiefer Intensität sind, dies wahrscheinlich wegen einer tiefen Quantenausbeute von nur 2% für das Hauptprodukt.

Die Inhibitonsrate der Bildung von TpT Photoprodukten wurde gemessen im Beisein von spezifischen natürlichen Produkten (Polyamine und ihre Derivate, Flavonoide, Anthocyan und hydroxycinnamicher Säure) in zwei Quarz-Mikroküvetten (siehe Figur 2) Eine Abnahme der Bildung von Photoprodukten wurde nach der Bestrahlung von TpT bei 312 nm im Beisein von diesen UV-Filter beobachtet. Nur Spermin inhibierte die Bildung von Photoprodukten nicht. Dies ist bedingt durch die Abwesenheit von Chromophoren die in diesem Strahlungswellenbereich absobieren. Aehnliche Effekte wurden bei 254 nm beobachtet, wenn auch weniger stark. Vorläufige Versuche von Photoschutz wurden auch ausgeführt mit Oligomeren (TpT und ds DNA) unter Benützung einer einzelnen Küvette. Leider waren die erhaltenen Resultate unterhalb der Detektionsgrenze.

Kapitel 4 diskutiert die Entwicklung einer analytischen Methode für die quantitative Bestimmung des Methylierungsgrades der DNA. Hoch auflösende und tandem massenspektrometrische Techniken wurden benützt in Verbindung mit der Zugabe von isotopisch markierten internen Normalen zu den Proben. UHPLC-ESI-MS/MS zeigte die beste Reproduzierbarkeit und war auch genauer als andere getesteten Massanalysatoren wie QTOF oder eine Ionen-Falle im „Full Scan Acquisition“ Modus (Figur 3). Die Methode wurde schliesslich validiert unter Benützung von Kalbsthymus DNA Proben.

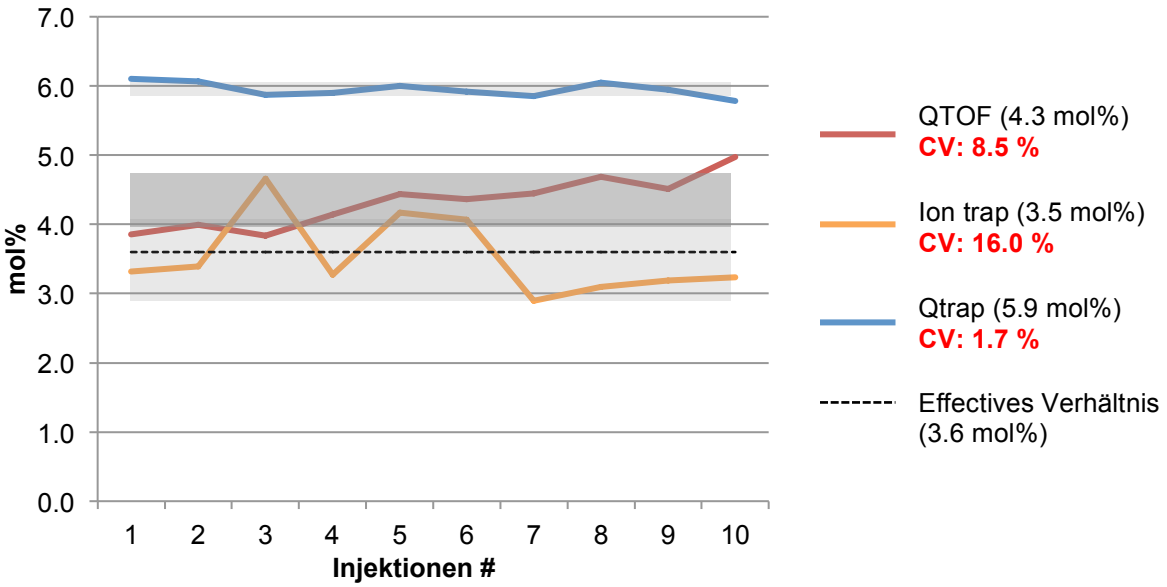

Figur 3: Reproduzierbarkeit und Genauigkeit von 10 Injektionen in einer einzelnen Lösung enthaltend Standards von Cytosine und 5-Methylcytosine zubereitet in einem 3.6 mol% Verhältnis (schwarz gestrichelte Linie) und ihre entsprechend markierte ISTD. Es wurden Analysen ausgeführt unter Benützung von maXis QTOF, einer HCT Ionenfalle und einem 3200 Qtrap Massenanalysator. Mittlere Verhältnisse sind in Klammern angegeben und die Intraproben CV in rot, und die Standardabweichung in grau.

Verglichen mit der besten publizierten Methode wurde mit der hier entwickelten Methode eine Reduzierung der Analysenzeit von 33% erreicht. Ein mittlerer Methylierungsgrad von 6.8 % wurde erreicht mit intra- und inter-Proben CVs von 2 % respektive von 2.4 %. Diese Werte zeigen auf, dass die neue Methode genügend genau und reproduzierbar um für die Quantifizierung von 5-methylcytosine in Patientenproben benützt zu werden.

Kapitel 5 beinhaltet die Anwendung der in Kapitel 4 entwickelten Methode für die Bestimmung des Methylierungsgrades der DNA. Eine biologische Studie wurde ausgeführt um nach zu prüfen ob der Methylierungsstoffwechsel und die DNA Methylierung korreliert sind bei einem menschlichen septisch systemischen entzündlichem Reaktionssyndrom. Die globale DNA-Methylierung wurde gemessen mit Hilfe der Extrahierung von DNA aus Blutproben und der Quantifizierung von Cytosin und 5-Methylcytosin mit der neuen UHPLC-ESI-MS/MS Methode. Es scheint, dass septische und systemische entzündliche Reaktionssyndrome beachtliche Aenderungen des Methylierungsstoffwechsels herbeiführen ohne sichtbare funktionale Konsequenzen auf die Homocystein-Plasmaniveaus oder die DNA-Methylierung.

LIST OF ABBREVIATION

ap	apigenin
APCI	atmospheric pressure chemical ionization
BEH	Bridged Ethylene Hybrid
CE	capillary electrophoresis
CI	chemical ionization
CID	collision-induced dissociation
cou	*p*-coumaric acid
c-s T<>T	*cis-syn* I cyclobutane thymine
CT	calf thymus
CV	coeffiecient of variation
Da	dalton
DAPI	4',6-diamidino-2-phenylindole
ds	double stranded
DMSO	dimethyl sulfoxide
EI	electron ionization
EIC	extracted ion chromatogram
ESI	electrospray ionization
EthBr	ethidium bromide
Eth	ethidium
$fb_{(DNA)}$	fraction of bound DNA
FT-ICR	Fourier-transform ion cyclotron resonance
FS	full scan
glu	glucose

GC	gaz chromatography
HPLC	high performance liquid chromatography
HR	high-resolution
ICU	Intensive Care Units
ISTD	internal standard
ku	kuromanin
LOD	limit of detection
LOQ	limit of quantification
MALDI	matrix-assisted laser desorption ionization
min	minutes
mol%	mole percent
M_R	molecular mass
MRM	multiple reaction-monitoring
MS	mass spectrometry
MS/MS	tandem mass spectrometry
m/z	mass to charge
NEC	non-endcapped
NH_4OAc	ammonium acetate
NH_4HCO_2	ammonium formate
RP	reversed-phase
SAH	S-adenosyl homocysteine
SAM	S-adenosyl methionine
SAR	structure-activity relationship
SIL	stable-isotope-labeled
SIM	single ion monitoring
SIRS	systemic inflammatory response syndrome
spd	spermidine

spm	spermine
S/N	signal to noise ratio
SRM	selectecte reaction-monitoring
STD	standard
Q	quadrupole
QIT	quadrupole ion trap
QC	quality control
QqQ	triple quadrupole
T_m	melting temperature
TOF	time-of-flight
TpT	thymidylyl(3'-5')thymidine
t-s T<>T	*trans-syn* I cyclobutane thymine
UHPLC	ultra high perfomance liquid chromatography
vi	vitexin
1,14-cin spm	1,14-bis(*E*-cinnamoyl) spermine
5,10-cin spm	5,10-bis(*E*-cinnamoyl) spermine
6-4 TT	pyrimidine (6-4) pyrimidone

CURRICULUM VITAE

Personal Data

Name:	Jean-Christophe Prost
Date and Place of Birth:	18th January 1982 in Neuchâtel (NE)
Origin:	Corcelles-Cormondrèche

Education

1998-2001	Lycée Denis-de-Rougemont Neuchâtel, 2001, Baccalauréat type G
2001-2007	University of Neuchâtel, Institute of Inorganic Chemistry, Master of Science (M sc).
	Diploma Thesis in Inorganic Chemistry. (6 months) under the supervision of Prof. Dr. T. Ward ”Asymmetric dihydroxylation with the biotin-(strept)avidin system”.
Since 2008	Ph. D. student at the University of Zurich, Institut of Organic Chemistry under the supervision of Prof. Dr. Stefan Bienz and PD Dr. Laurent Bigler

Experiences

2007-2008	LONZA AG, Visp, Quality Control Large Molecule (QC-LM), 6 months internship in Analytical Chemistry
Since 2008	Research assistant position in the Mass Spectrometry Laboratory

LIST OF PUBLICATION AND SCIENTIFIC PRESENTATION

Methylation Metabolism in Sepsis and Systemic Inflammatory Response Syndrome, *Scandinavian Journal of Clinical and Laboratory Investigation,* **2013.** Semmler, A.; Prost, J.-C.; Smulders, Y.; Smith, D.; Blom, H.; Bigler, L.; Linnebank, M., in preparation

Jean-Christophe Prost, Laurent Bigler, and Stefan Bienz. Determination of the degree of methylation in DNA, Swiss Group for Mass spectrometry, 2011, Beatenberg, Oral presentation

Jean-Christophe Prost, Laurent Bigler, and Stefan Bienz. How do plants protect their DNA from UV Damage?, Retreat of the Graduate School of University of Zurich, 2010, Andermatt, Oral presentation

Jean-Christophe Prost, Laurent Bigler, and Stefan Bienz. Protection of plant DNA from UV Damage, CUSO PhD Summer School “Frontiers in Mass Spectrometry”, 2009, Villars, Oral presentation

ACKNOWLEDGMENTS

I would like to express my gratitude to many people for their contribution to this work:

Prof. Dr. Stefan Bienz, for his cordial acceptance in his research group, for the supervision of this work, his help during the group meetings, availability and his precision.

Prof. Dr. Roland Sigel, for acting as a co-referent and of course to be a wonderful Head of the Graduate School of Chemical and Molecular Sciences Zurich.

PD. Dr. Laurent Bigler, pour m'avoir ouvert au monde complètement fascinant qu'est la spectrométrie de masse. Pour m'avoir aidé à trouver des idées et des réponses à quelques problèmes analytiques récalcitrants durant ce projet. Merci pour tous ces très bons moments dans et en-dehors du labo. Mais surtout un grand merci de m'avoir donné assez de temps, pendant les corrections, pour m'occuper de ma fille Wanda.

Peter Schürmann, my godfather, for the time he took to correct my thesis.

All the members of the Bienz's Group for the great moments we had together, the former team, Silvan Eichenberger, Michaël Méret, Maurizio Campagna, Manuel Tzouros, Pascal Bisegger, Renate Brokamp, Martin Meyer and Simon Dünki, the actual crew, Luisa Topf, Daniel Marti, Rahel Bucher, but a special thanks to Denise Pauli and Basil Lörtscher for their great support and the nice discussions during the not always so easy time I encounter during my PhD. The Luedtke Group for lunch sparring-partnership, and Martin Seyfried for his perfect organization of the riflery contest. Jawad for helping me finding my PhD thesis title and having many nice scientific discussions.

PD Dr. med. Alexander Semmler for this nice collaboration.

The people from the "Institut für Rechtsmedizin", especially Prof. Dr. rer. nat. Thomas Krämer, allowing me to measure on their instruments. Milena, Annika und Michi, who helped me, with patience, to understand how to handle them.

Bien sûr, mes chers Francophones, Julien, Anaëlle, Michaël, Pierre, Cédric, Gilles, Vivian, Ludovic et le petit dernier Guillaume pour, certainement, mes plus beaux moments et discussions pendant ces cinq ans, que ce soit sur la terrasse, dans l'appart, au Letten, à Münich, à Berlin (avec ou sans copine), à la fête des vendanges, aux 10km de Lausanne, dans le Züriberg, au Sächsilüüte ou au concert des Guns N'Roses. Merci beaucoup.

All the members of the Graduate school, Fivos, Ana, Joachim, David, Tanja and many other for the epic aperos and retreats we had together.

The Graduate school for its financial help to print my thesis.

Urs Stalder for his great and unbidden helps anytime when strange problems occurred during my projects, and for introducing me into the world of quantification.

Mr. Armin Guggisberg for the interesting scientific discussions.

Salomé Faessler who always helped me for all the administrative annoyance.

All my friends from Neuchâtel (unihockey, music and studies)

My family, my mum, my father (he translated my summary in German), my sister and my brother for all their support, that helped me in my life and scholar achievements.

Mais le plus grand MERCI revient à ma femme, Joëlle, et à ma fille Wanda sans qui, jamais je n'aurais réussi à tenir le coup pendant toute ma thèse.